"Investigation of medication-related osteonecrosis of the jaw by real-time *in vitro* assays, histologic examination, and radiographic evaluation"

Thesis submitted as requirement to fulfill the degree
“Doctor of Philosophy” (Ph.D.)

at the
Faculty of Medicine
Eberhard Karls University
Tübingen

by
Anna Yuan, DMD

from
Shenzhen, China

2018

Dean:	Professor Dr. I. B. Autenrieth
1. Reviewer:	Professor Dr. Dr. S. Reinert
2. Reviewer:	Professor Dr. A. Nüssler

Dedication

I dedicate this with gratitude to my Labor Mutter Heidi and my Doktor Vater Sebastian, who became my German family.

All praise goes to Christ Jesus:
The fear of the LORD is the beginning of knowledge. [Proverbs 1:7]

Table of Contents

List of abbreviations

A. actinomycetemcomitans = *Actinobacillus actinomycetemcomitans*
AAOMS = American Association of Oral and Maxillofacial Surgery
ANOVA = analysis of variance
BMP-2 = bone morphogenetic protein 2
BPs = bisphosphonates
BP-exposed = bone exposed to bisphosphonate
BPDN-exposed = bone exposed to bisphosphonate and denosumab
BRONJ = bisphosphonate-related osteonecrosis of the jaw
CBCT = cone beam computed tomography
CD = cluster of differentiation
CI = Cell Index
COX-2 = cycloxygenase-2
CT = computed tomography
DRONJ = denosumab-related osteonecrosis of the jaw
ELISA = enzyme-linked immunosorbent assay
F. nucleatum = *Fusobacterium nucleatum*
FCS = fetal calf serum
FOH = farnesol
γδ = gamma delta
GAPDH = glyceraldehyde-3-phosphate dehydrogenase
GGOH = geranylgeraniol
H&E = hematoxylin and eosin
HGF = human gingival fibroblast
IAN = inferior alveolar nerve
IFN-γ = interferon gamma
IL = interleukin
IL-1β = interleukin 1 beta
IPP = isopentenyl pyrophosphate

KGF = keratinocyte growth factor

LPS = lipopolysaccharide

MMPs = matrix metalloproteinases

MRI = magnetic resonance imaging

MRONJ = medication-related osteonecrosis of the jaw

mRNA = messenger RNA

mTOR = mechanistic target of rapamycin

N-BPs = nitrogen-containing bisphosphonates

OM = secondary chronic osteomyelitis

ONJ = osteonecrosis of the jaw

OPG = osteoprotegerin

ORN = osteoradionecrosis of the jaw

P. gingivalis = *Porphyromonas gingivalis*

PBS = phosphate-buffered saline

qRT-PCR = quantitative real-time polymerase chain reaction

RANK = receptor activator of nuclear factor kappa-B

RANKL = receptor activator of nuclear factor kappa-B ligand

TGF-β = transforming growth factor beta

TKIs = tyrosine kinase inhibitors

TNF-α = tumor necrosis factor alpha

TRAP = tartrate-resistant acid phosphatase

VEGF = vascular endothelial growth factor

VEGFR2 = vascular endothelial growth factor receptor 2

1 Introduction

1.1 Antiresorptives

Antiresorptive agents have revolutionized cancer and osteoporosis therapy.[1] Following the introduction of non-nitrogen-containing etidronate and clodronate into clinical practice, nitrogen-containing bisphosphonates (BPs) pamidronate, alendronate, ibandronate, risedronate, and zoledronate soon followed.[2] Nitrogen-containing BPs possess a higher clinical potency, better binding affinities to bone, and different mechanisms of action in the target cell compared with their non-nitrogen-containing predecessors.[3, 4] BPs are inorganic pyrophosphates which incorporate into bone to deactivate osteoclasts located on bone surfaces.[5] Denosumab, a fully human monoclonal antibody, was approved by the Food and Drug Administration in 2010 with the ability to inhibit the binding of receptor activator of nuclear factor kappa-B ligand (RANKL) to receptor activator of nuclear factor kappa-B (RANK).[5, 6] It was recognized that densoumab did not present with evidence of sustained binding to bone surfaces, a benefit for patients concerned with the long half-life of BPs.[5]

1.2 Medication-related osteonecrosis of the jaw

Antiresorptive medications such as BPs and the RANKL-inhibitor denosumab are used for the treatment of osteoporosis, Paget's disease, hypercalcemia of malignancy, multiple myeloma, and metastatic bone disease from oncologic tumors.[7] Medication-related osteonecrosis of the jaw (MRONJ) is a serious complication of these frequently prescribed medications which has profound implications for the fields of oral and maxillofacial surgery, oral medicine, dentistry, oncology, pharmacology, and oral biology. A diagnosis of MRONJ, according to the American Association of Oral and Maxillofacial Surgeons (AAOMS), includes current or previous treatment with antiresorptives or anti-angiogenic agents, visible exposed bone or bone that can be probed through an intraoral or extraoral fistula in the maxillofacial region persisting for more than 8 weeks, and no history of

radiation therapy or obvious metastatic disease to the jaws.[7] Treatment of MRONJ is difficult and costly, and disease sequela can include pain, infection, inability to eat, extraoral fistula, and pathologic fracture, all of which significantly impact the quality of life for patients (Figure 1).[8, 9]

Although the first case of bisphosphonate-related osteonecrosis of the jaw (BRONJ) was reported over a decade ago[10], the pathogenesis of the disease remains unclear. Consequently, there is no unified recommended prevention or treatment protocol. Denosumab-related osteonecrosis of the jaw (DRONJ) was more recently reported with the RANKL-inhibiting fully human monoclonal antibody (Figure 2).[5, 11] The prevalence of BRONJ ranges from 3% to as high as 27.5%[12] in patients receiving nitrogen-containing BPs for metastatic bone malignancy and multiple myeloma, with a mean incidence of 7%[13] depending on cumulative dose.[14, 15] The risk for DRONJ among cancer patients has been considered by the AAOMS to be comparable to the risk for BRONJ in patients exposed to zoledronate[7], while others estimate a higher occurrence rate for DRONJ compared to BRONJ.[16, 17] Over 2800 articles can be currently found on the Pubmed database investigating this phenomenon. Newer cases are being reported with other medication classes including tyrosine kinase inhibitors (TKIs), vascular endothelial growth factor (VEGF) inhibitors, and mechanistic target of rapamycin (mTOR) inhibitors[18-21], so clinicians and researchers may expect to see an increase in the incidence of MRONJ.

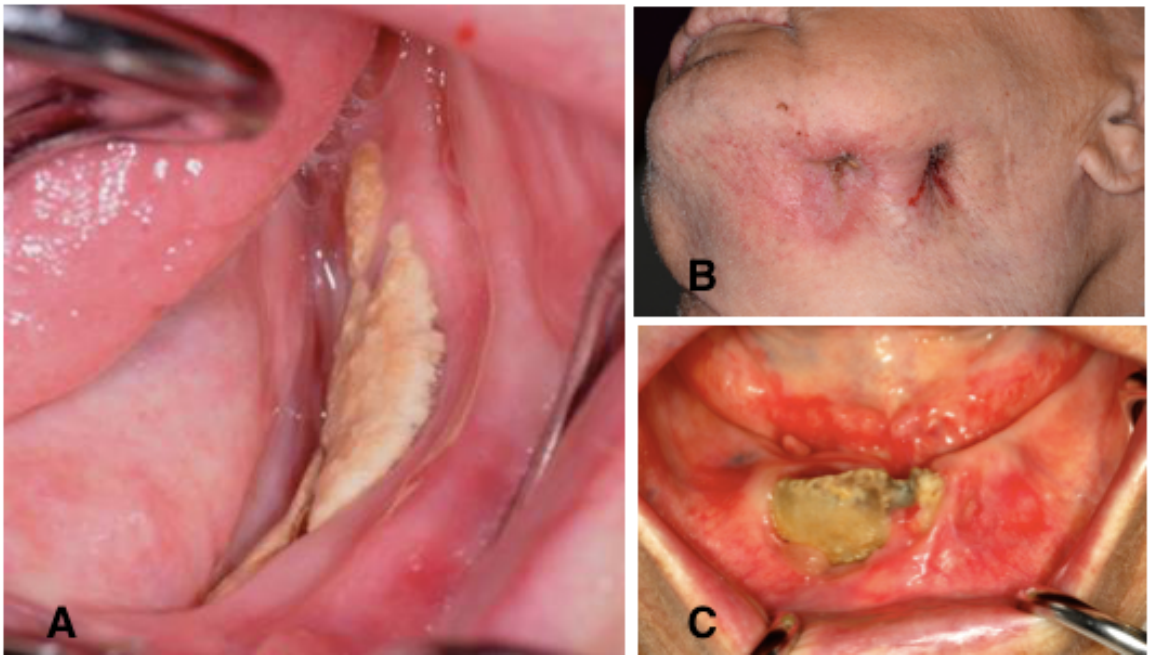

Figure 1. Intraoral bone exposure and extroral fistula in patients with medication-related osteonecrosis of the jaw. A: Stage 2; B and C: Stage 3.

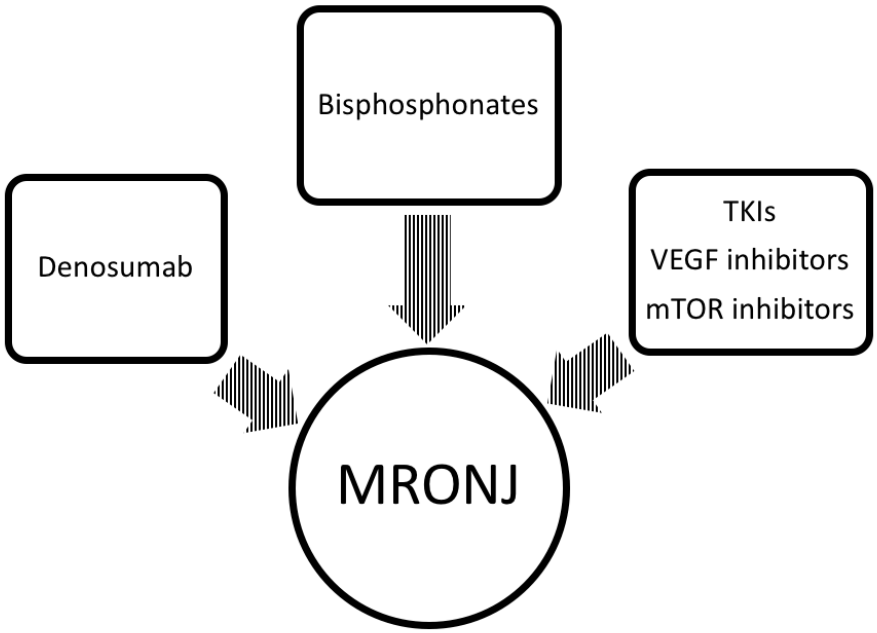

Figure 2. Therapies associated with medication-related osteonecrosis of the jaw according to the American Association of Oral and Maxillofacial Surgeons 2014 Update.[7] TKIs = tyrosine kinase inhibitors; VEGF = vascular endothelial growth factor; mTOR = mechanistic target of rapamycin; MRONJ = medication-related osteonecrosis of the jaw.

1.3 Etiology

Various mechanisms have been proposed for how antiresorptives may cause such a site-specific osteonecrosis. The jaw bone may be particularly sensitive to BPs since it demonstrates up to a 20-fold higher turnover rate compared to other skeletal sites.[22-24] If high BP content resulted in generalized bone necrosis, then evidence of toxicity throughout the skeleton would be expected in proportion to bone turnover.[25] Site-dependent differences in matrix composition, biomechanical properties, osteoclastic bone resorption, and skeletal pathobiology may also contribute to the unique localisation of MRONJ exclusively to the jaws.[26, 27] Proposed hypotheses that attempt to explain the pathogenesis of MRONJ include altered bone remodelling or over-suppression of bone resorption[28-30], angiogenesis inhibition[31], sustained microtrauma[32], suppression of innate or acquired immunity[33], suppression of local immunity[34-36], vitamin D deficiency[37], soft tissue toxicity[25], and inflammation and infection.[38-40] These models for the etiology of MRONJ have been discussed theoretically, however confirming the exact process is still in progress.

1.4 Extrinsic and intrinsic pathways of necrosis

As the name implies, osteonecrosis of the jaw (ONJ) is assumed to be primarily a bone condition. How precisely ONJ is initiated remains controversial. It is unknown whether the lesion originates within the bone or from the mucosa; historically, speculation has been focused on the bone.[41] The main hypothesis is that ONJ is caused by an over-suppression of bone turnover by BPs.[29, 30] Yet, this theory

does not explain why ONJ occurs almost exclusively in the maxillofacial region, and it is also unclear why it should present with loss of the soft tissue covering of the jaw bones as the primary clinical feature.[25] Several definitions for ONJ have been proposed, and with the exception of the stage 0 non-exposed bone variant, stage 1, 2, and 3 MRONJ all involve a breach in the oral mucosa leading to the exposure of maxillary or mandibular bone.[7] Although the bulk of research thus far has involved the effect of BPs on bone—an “inside-out” theory—it is also compelling to investigate how the adverse effects of BPs in circulation and/or released from the bone could influence the viability of the soft tissues to play a critical role in the initiation of MRONJ—an “outside-in” hypothesis.[41] Some authors propose that soft tissues exposed to BPs could trigger osteolysis, which could be combined with or exacerabated by the effects of BPs released from the bone on the soft tissues.[42]

1.5 Research aims

The main goal of this doctoral project was to provide a more profound picture of how BPs and denosumab could influence the expression patterns of human gingival fibroblasts (HGFs) and participating cells in MRONJ. Retrospective histologic and radiographic examinations provide the possibility to correlate the altered bone structure with different disease variants and degree of antiresorptive exposure.

1.6 Real-time in vitro assays of HGFs

One of the proposed mechanisms of MRONJ involves the soft tissue toxicity of HGF cells, leading to delayed wound healing after epithelial damage and secondary infection.[43] However, the role of soft tissue in the pathogenesis of MRONJ is particularly not well defined. Gingival cells have been previously analysed *in vitro* at selected fixed time points[44, 45], but so far no real-time analysis has been performed to observe how the cells are affected in growth and

wound repair. Furthermore, the effects of denosumab on this cell type have not yet been published at present.

This project attempted to clarify the pathogenesis of MRONJ due to the medication-related damage of the surrounding soft tissue by investigating the role of antiresorptives to induce or inhibit cell death and inflammation in HGFs that may influence angiogenesis and wound healing in response to BP and denosumab therapy (Figure 3). We investigated whether this effect was medication dose-dependent, and whether it could be augmented by a bacterial challenge simulated by lipopolysaccharide (LPS) and/or a co-culture with a mononuclear cell line.

The investigation was carried out on an *in vitro* HGF cell culture model. Four different BPs of varying potencies (alendronate, ibandronate, zoledronate, and clodronate) and denosumab at low, middle, and high concentrations were used to determine the Effective Concentration. The readout was cell adhesion, proliferation, and cell death of HGFs as well as in response to infection and a co-culture with monocytes via the xCELLigence Real-Time Cell Analyzer (ACEA Biosciences Inc., San Diego, USA; Figure 4). This system provided a non-invasive approach to assess cellular growth, morphologic changes, viability, migration, cytotoxicity, and cell death on a cell culture level via electrical impedance measurements in real-time.[46] Depending on the proliferation curves of HGFs, optimal examination times were defined for analyses to be performed. A further co-culture of peripheral blood mononuclear cells with HGFs helped to clarify the interaction between cells in the presence of BPs, denosumab, and LPS to allow for observation of additional immunologic reactions. The THP-1 human monocytic cell line was chosen as a historically reliable monocyte/macrophage model due to similar morphologic and functional properties, including differentiation markers.[47, 48]

Additionally, gingival fibroblasts have been demonstrated to interact with immunologic and tissue repair functions by reacting to and secreting mediators or vascular and tissue growth factors. Most of these findings were linked to research on periodontitis.[49, 50] A quantitative real-time polymerase chain reaction (qRT-PCR) assay was performed for pro-inflammatory, angiogenic, and osteogenic/osteoclastogenic gene expression. An enzyme-linked immunosorbent assay (ELISA) of the co-culture medium in the presence and absence of BPs, denosumab, and LPS was performed for further inflammatory and angiogenic markers. Experimental findings could be compared to findings in periodontal research.

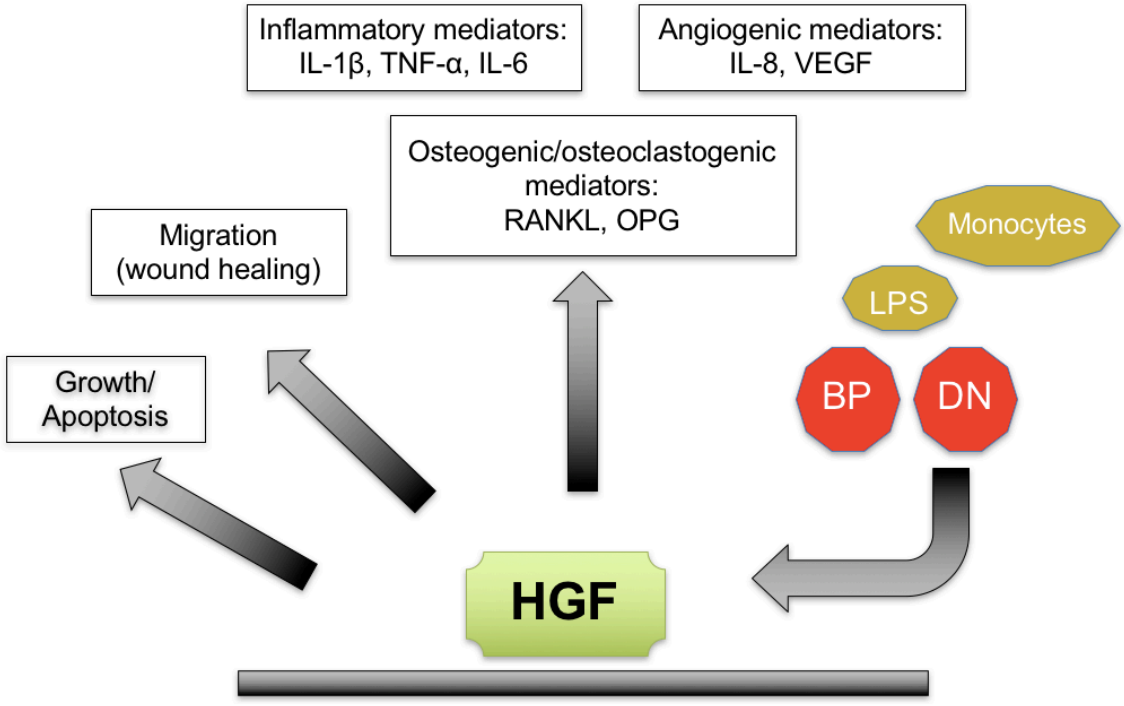

Figure 3. Real-time *in vitro* assays of human gingival fibroblasts exposed to antiresorptives with and without the addition of LPS and THP-1 mononuclear cells in co-culture. LPS = lipopolysaccharide; BP =

bisphosphonate; DN = denosumab; HGF = human gingival fibroblasts; IL = interleukin; TNF-α = tumor necrosis factor alpha; VEGF = vascular endothelial growth factor; RANKL = Receptor activator of nuclear factor kappa-B ligand; OPG = osteoprotegerin.

RANKL is a surface-associated ligand expressed on hematopoietic bone marrow stromal cells, osteoblasts, and B and T lymphocytes[51, 52], which is responsible for activating its corresponding receptor RANK on mononucleated osteoclast precursor cells of the monocyte/macrophage lineage.[53] This consequently leads to their differentiation into multinucleated bone-resorbing osteoclasts.[54] Osteoprotegerin (OPG) is a soluble decoy receptor for RANKL that inhibits its interaction with RANK, thereby preventing osteoclastogenesis.[55] These three molecules are important regulators of bone modeling, and alteration of the RANKL/OPG expression ratio has been demonstrated clinically in periodontal disease.[56, 57]

Cytokines such as tumor necrosis factor alpha (TNF-α), interleukin 1 beta (IL-1β), and interleukin (IL)-6 are closely linked to the occurrence of inflammation due to their regulation of cycloxygenase-2 (COX-2) expression, resulting in the production of key inflammatory mediators.[58] TNF-α is produced by many cell types and works synergistically with IL-1 to stimulate the production of chemokines and mediators which sustain the inflammatory response, including prostaglandins and lytic enzymes.[59, 60] The loss of fibroblasts that occurs during infection with periodontal pathogens is also mediated in part by TNF.[61] IL-1β is an important element of the inflammatory response which directly regulates several genes expressed during inflammation and also has been demonstrated to play a role in osteoclastic bone resorption.[62-64] One of the major functions of IL-6 is in B cell differentiation in the adaptive immune response.[65] B cells are activated and transformed into plasma cells, which produce antibodies against bacterial

antigens. IL-8 is produced by epithelial cells, and is responsible for chemotaxis and angiogenesis by recruiting neutrophil migration and increasing monocyte adhesion in the blood vessels.[66] VEGF is a signal protein produced by many cell types that stimulates the formation of blood vessels.[50]

Figure 4. xCELLigence Real-Time Cell Analyzer system (ACEA Biosciences), a non-invasive approach to assess cellular growth, morphologic changes, viability, migration, cytotoxicity, and cell death on a cell culture level via electrical impedance measurements in real-time.

1.7 Histologic examination

In addition to *in vitro* studies on soft tissue damage, the examination of bone affected by and exposed to antiresorptive medications is essential to identifying the pathophysiology of the MRONJ disease process. This project characterized histopathologic features of MRONJ by examining and comparing bone biopsies of BRONJ, DRONJ, and Mixed ONJ (necrosis with both BP and denosumab) with bone exposed to antiresorptive medications (BP and both BP and denosumab) and other bone samples of inflammatory (primary osteoporosis), infectious

(secondary chronic osteomyelitis), and necrotic jaw diseases (osteoradionecrosis), as well as bone from healthy patients (removed during dental extractions).

This project aimed to contribute the following information currently missing from the literature: the comparison of histologic changes including bone histomorphometrics in tissue composition, the composition of immune competent cells and cytokine profiles in infectious environments, and evidence of the remodeling of bone exposed to antiresorptive therapy with no clinical signs of MRONJ. Micro-computed tomography (CT) was utilitized to analyze the relation of bone and medullary space in response to antiresorptive treatments. DRONJ patients in previous studies were often initially exposed to other antiresorptives, perhaps confounding the influence of any distinct agent. With this patient cohort we were able to identify features of denosumab-specific osteonecrosis without influence from previous BP therapy.

1.8 Radiographic evaluation

MRONJ demonstrates a mixed pattern of necrosis and infection clinically. The clinical examination does not usually show the full extent and severity of necrotic sites beneath the mucosa. In principle, the diagnosis is made based on both the clinical and radiographic examination. However, diagnostic radiographic findings are not universally agreed upon since imaging findings are non-specific and can also be found in other conditions such as osteomyelitis, osteoradionecrosis, cancer metastasis, and Paget´s disease. Thus far, imaging findings have not been incorporated into the diagnostic criteria, nor have radiographic features been included for the classification of disease stage. Their findings corroborate the evaluation of the course, extent, and progression of the disease. Panoramic radiography, CT, magnetic resonance imaging (MRI), and scintigraphy are valuable imaging modalities that confirm and augment clinical findings by revealing different aspects of bone involvement.

The goal of this project was to characterize radiographic signs of necrosis in BRONJ, DRONJ, and Mixed ONJ using various imaging techniques and to evaluate the correlation of the clinical presentation with imaging findings. Diagnostic radiographic files of MRONJ patients were analysed retrospectively for radiographic signs before and after disease management, including surgical operation when needed. Imaging findings were compared with histologic results to confirm the analysis of the effect on bone tissues. Radiographic changes such as increased bone density/sclerosis could be an indirect indication of bone remodeling, allowing for the corroboration of the macroscopic appearance to microscopic activity in histologic samples. Radiologic findings were also evaluated for possible predictive parameters that may be prognostic for disease development and clinical course.

2 Materials and Methods

Part I Real-time *in vitro* assays of HGFs

2.1 Cell culture with HGFs and THP-1 cells

Commercially available HGF cells (Provitro, Berlin, Germany) were cultured in HGF medium (Provitro, Berlin, Germany) containing 10% heat-inactivated fetal calf serum (FCS, Provitro, Berlin, Germany), 50.00 ng/mL amphotericin B (Provitro, Berlin, Germany), and 50 µg/mL gentamicin (Provitro, Berlin, Germany). Cells were cultured in 75 cm^2 flasks at 37°C in a humidified incubator at 5% CO_2. Subculturing was performed when cell confluence exceeded 75%. Human gingival fibroblast cells were plated at a density of 3.0 x 10^5 per 75 cm^2 culture flask, and culture medium was changed every 48 to 72 hours.

THP-1 cells (ATCC, Manassas, VA, USA) were cultured in RPMI-1640 culture medium (GIBCO, Darmstadt, Germany) containing 0.05 mM 2-mercaptoethanol, 10% heat-inactivated FCS (Sigma-Aldrich, Munich, Germany), 100 U/mL penicillin/

streptomycin (Lonza, Cologne, Germany), and 50 mg/ mL fungicide (Biochrom AG, Berlin, Germany). Cells were cultured in 75 cm^2 flasks at 37°C in a humidified incubator at 5% CO_2. Subculturing was performed when cell density exceeded 5 to 7 x 10^6. THP-1 cells were plated at a density of 1.2 x 10^6 per 75 cm^2 culture flask, and culture medium was added or replaced in a new passage every 96 to 120 hours.

2.2 Live monitoring with the xCELLigence system

The xCELLigence DP system (ACEA Biosciences Inc., San Diego, USA) was used for continuous monitoring of cell adherence. Using xCELLigence E-plates 16 and E-plates 16 VIEW (ACEA Biosciences Inc., San Diego, USA), changes of impedance for cells attached to the detector plates were measured at 20 mV every 15 minutes and calculated as the dimensionless parameter Cell Index (CI):

$$CI = [Z_i - Z_0]/15$$

[Z_i: impedance at an individual experimental point; Z_0: background measurement at the beginning of the experiment]

Background measurements were performed twice with 50 mL HGF medium. Figures were displayed with the Delta Cell Index (DCI_{ti}), a standardized calculation of Cell Index (CI_{ti}) using a constant (delta value) over time with standard deviation. The measured value was proportional to the attached number of cells to the detector plate and also reflected the morphology of cells and quality of cell attachment.

2.3 Normal HGF cell growth

Normal HGF cell growth was measured with the xCELLigence system using various seeding densities (1500-6000 cells per cm^2) to determine the optimal growth curve. A cell suspension of 100 µl with 4000 cells was added in each E-plate well. Growth was monitored until natural cell death, and the appropriate live-

monitoring period was established. Culture medium was changed after 48 hours at the optimum time of confluence as confirmed visually by the E-plate 16 VIEW and simultaneous 24-well plate experiments.

2.4 Antiresorptives

Zoledronate (Sequoia Research Products, Pangbourne, UK), ibandronate (Sigma-Aldrich, Taufkirchen, Germany), and alendronate (Sequoia Research Products, Pangbourne, UK) in concentrations of 0.5 μM, 5 μM, and 50 μM[25, 41, 67-71]; clodronate (Sigma-Aldrich, Taufkirchen, Germany) in concentrations of 50 μM, 125 μM, and 500 μM[72]; denosumab in concentrations of 3 μg/mL, 10 μg/mL, and 40 μg/mL[6]; or a combination of zoledronate and denosumab in concentrations of 0.5 μM + 40 μg/mL, 5 μM + 10 μg/mL, and 5 μM + 40 μg/mL were then added to each E-plate well containing HGF cells for experimentation (Table 1).[73] These concentrations were determined by established experimental concentrations in the literature and reported tissue concentrations as referenced above.[45, 74]

Antiresorptive	**Low concentration**	**Middle concentration**	**High concentration**
Alendronate	0.5 μM	5 μM	50μM
Ibandronate	0.5 μM	5 μM	50μM
Zoledronate	0.5 μM	5 μM	50μM
Clodronate	50 μM	125 μM	500 μM
Denosumab	3 μg/mL	10 μg/mL	40 μg/mL
Zoledronate + Denosumab	0.5 μM + 40 μg/mL	5 μM + 10 μg/mL	5 μM + 40 μg/mL

Table 1. Tested concentrations of bisphosphonates and denosumab in the xCELLigence system.

Of note, BP concentrations are conventionally reported as molar units of μM, while the newer medication denosumab is recommended to be reported as mass units of μg/mL.[75] Equivalent concentrations of these medications can be calculated using the following formula:

μg/mL x 1,000 mL/L x 1 μmole/([molar mass] μg) = μmol/L = μM

2.5 LPS experiments

For experiments with LPS, various concentrations of *Porphyromonas gingivalis* (*P. gingivalis)* LPS (InvivoGen, San Diego, USA) were tested according to concentrations established in the literature.[76, 77] LPS was added at a concentration of 3 μg/mL or 10 μg/mL to each E-plate well with the applicable BP, which accompanied the medium change at 48 hours. LPS 10 μg/mL was determined to be the optimal concentration.

2.6 Co-culture experiments with THP-1 cells

Viability of a co-culture was established by initially confirming the successful growth of HGFs in RPMI medium. BPs and LPS 10 μg/mL in 100 μl RPMI medium were added at 48 hours as described above. Concurrently, 50 μl of THP-1 cell suspension optimized at a density of 40,000 cells[78, 79] and LPS 10 μg/mL were added to each well of an E-plate insert (ACEA Biosciences Inc., San Diego, USA) and loaded onto the E-plate. The E-plate insert allowed for the two different cell populations to be separated by a 0.4 μm pore size membrane. This pore size was tested to confirm the absence of cell migration, enabling the measurement of indirect cell-to-cell interactions in the co-culture.

2.7 Real-time monitoring of cell adherence

Live monitoring of adherence/differentiation was performed for a mimimum of 216 hours. In each experiment, the inflexion point of cell adherence/cell death was measured, indicating the beginning of cell death predominance over cell adherence. The mean of the inflexion point of each antiresorptive concentration and control was calculated from live-monitoring data. Intraindividual differences of inflexion points of cell adherence/death to the maximum control value in each experiment set were also calculated to exclude bias in individual experiments.

Each experiment was performed in duplicates and repeated at least twice to confirm reproducibility of results.

2.8 24-well plate confirmation experiments

Experiments performed on the xCELLigence system were confirmed by simultaneous experiments in 24-well plates (Costar, Kaiserslautern, Germany) using established concentrations (Figure 5). Three sets of experiments were performed analogous to the xCELLigence experiments: antiresorptives only, antiresorptives and LPS, and a co-culture with antiresorptives, LPS, and THP-1 cells. Two plates (one with a scratch assay and one without) were used for each experiment set to assess the effect on wound healing. Once normal growth and optimal cell densities were confirmed in preliminary experiments, 1 mL of HGF cell suspension at an experimentally established density of 25,000 cells were added to each well of the 24-well plate.

When the cell layer was fully confluent at 48 hours, the scratch assay wells were scraped with a 200 µl pipette tip, and antiresorptives were added to each well in both the scratch and non-scratch plates accompanying a medium change. In LPS experiments, *P. gingivalis* LPS 10 µg/mL was added with antiresorptives during the medium change at 48 hours. For co-culture experiments, a 200 µl THP-1 cell suspension with an experimentally established density of 250,000 cells and *P. gingivalis* LPS 10 µg/mL were added into a Greiner ThinCert™ (Greiner Bio-One, Frickenhausen, Germany), which was placed individually into each well. The Greiner insert allowed for the two different cell populations to be separated by a 0.4 µm pore size membrane, enabling the measurement of indirect cell-to-cell interactions in the co-culture and collection of the supernatant for protein analysis. Experiments were run for 9 days for the antiresorptive and LPS experiments, and 6 days for the co-culture with no further medium change. Each experiment was performed in duplicates and repeated at least twice to confirm reproducibility of results.

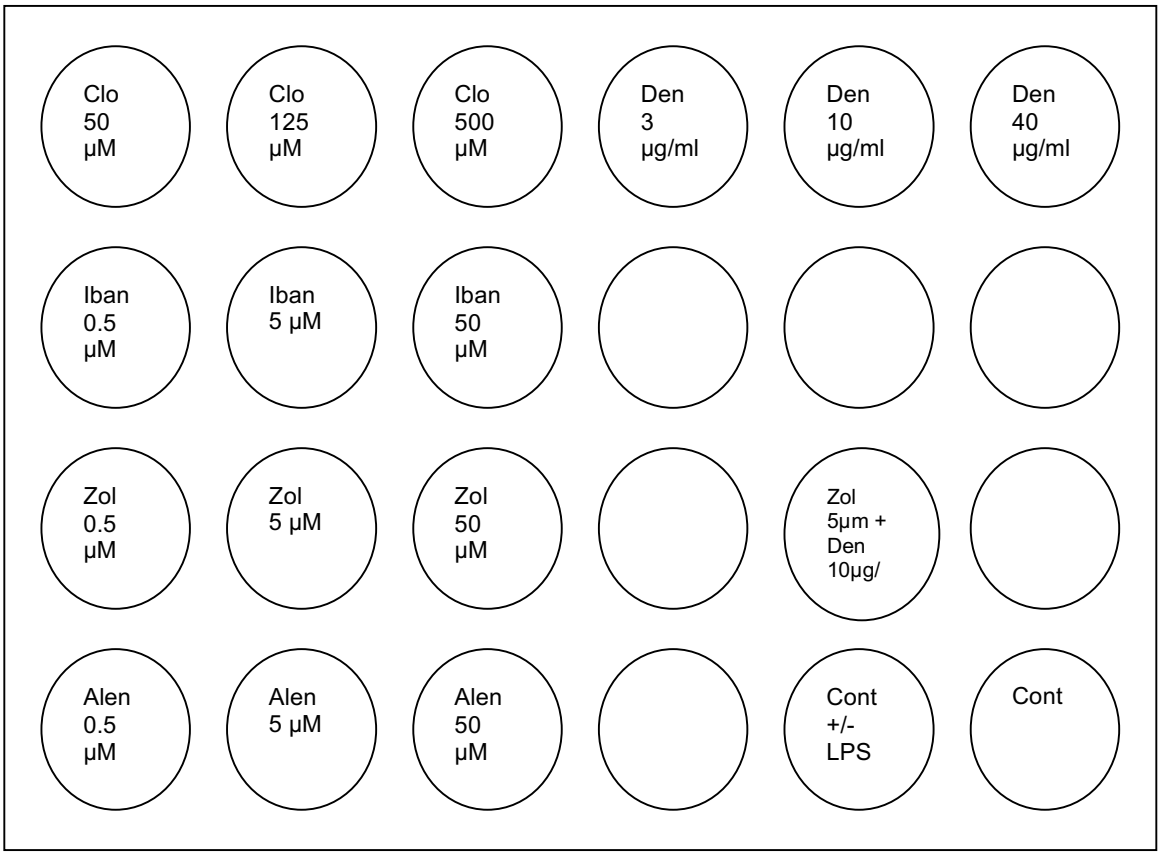

Figure 5. Layout of antiresorptive concentrations in 24-well plate experiments. Clo = clodronate; Iban = ibandronate; Zol = zoledronate; Alen = alendronate; Den = denosumab; LPS = lipopolysaccharide; Cont = control.

2.9 Morphologic analysis by light microscopy

Cells were monitored and visualized by inverted light microscopy (Leica Microsystems, Wetzlar, Germany) every 12-24 hours, and digital images of the cells were collected for the documentation of cell growth, scratch healing, and cell death. Greiner co-culture inserts were stained with hematoxylin after both 24 and 96 hours and visualized by light microscopy and photographed.

2.10 Analysis of cell viability/death with fluorescence staining

To confirm and visualize live-monitored effects of antiresorptives on HGF viability, a time-dependent Live/Dead staining (Life Technologies, Eugene, USA) was performed after 96 hours of incubation. Membrane-permeant calcein (2 mM) cleaved by esterase in living cells yielded cytoplasmic green fluorescence, and membrane-impermeant ethidium homodimer-1 (4 mM) labeled nucleic acids of membrane-compromised cells with red fluorescence. Cells were washed twice in phosphate-buffered saline (PBS) and incubated with 100 µL staining solution for 15 minutes at room temperature. Labeled cells were visualized using an Observer Z1 fluorescence microscope (Zeiss, Oberkochen, Germany) and AxioVs40 V4.8.2.0 software, and digital images were collected.

2.11 Scanning electron microscopy

Cell adherence was confirmed by scanning electron microscopy (DSM 982 Gemini by Zeiss, Oberkochem, Germany). Cells (initially seeded at a density of 50,000) in 12-well plates (Costar, Kaiserslautern, Germany) were fixated with glutaraldehyde (2.5%) and washed with ethanol (30%-100% for 2 minutes). Plates were then CO_2 dried (critical point dryer BAL-TEC CPD 030, Balzers, Lichtenstein), fixed onto Thermanox slices (Plano, Wetzlar, Germany) using Leit-Tabs (Plano, Wetzlar, Germany), and coated with gold (40 nm, Sputter Coater S150 B, Edwards, North Walsham, UK).

2.12 Gene expression analysis

HGF cells were collected from a separate run of 24-well plate experiments after 24 hours of antiresorptive treatment with and without LPS. Wells were washed with PBS, incubated with 80 µL trypsin for 5 minutes, and centrifuged. The supernatant was removed and 100 µL RA1 Buffer with 2 µL TCEP (NucleoSpin RNA XS, Macherey-Nagel, Düren, Germany) was added to each sample, which was frozen at -80°C until assayed. Highly pure RNA was eluted from the samples using the NucleoSpin RNA XS (Macherey-Nagel, Düren, Germany) and measured with a Qubit 3.0 Fluorometer (Thermo Fisher Scientific, Waltham, USA). First-stranded

cDNA for a PCR template was synthesized using 70-116 ng/μL (over 1μg total) of total RNA using an oligo-dT primer under conditions indicated by the manufacturer (Advantage RT-for-PCR Kit; Clontech, Heidelberg, Germany). Specific primers for TNF-α, OPG, RANKL, IL-8, and glyceraldehyde-3-phosphate dehydrogenase (GAPDH) were obtained from the LightCycler Primer Set (Search LC, Heidelberg, Germany). Each cDNA was amplified in the presence of SYBR Green Master Mix. The quantification of GAPDH encoding messenger RNA (mRNA) by qRT-PCR served as an internal control for each cDNA sample. The conditions for PCR were 1 x (95°C, 10 min) denaturation, 40 x (95°C, 10 sec; 68°C, 10 sec; 72°C, 16 sec) amplification, 1 x (95°C, 1 sec; 58°C, 10 sec; 95°C, 1 sec) melting curve, and 1 x (40°C, 30 sec) cooling. Gene expression analysis using was performed by qRT-PCR using the Light Cycler 2.0 System (Roche, Basel, Switzerland).

2.13 Protein expression analysis

Cell culture medium was collected from the 24-well plate co-culture experiments at 24 and 96 hours and frozen at -80°C until assayed. The production of IL-1β, VEGF, and IL-6 was measured in the cell culture supernatants using the Human IL-1β Quantikine ELISA Immunoassay (R&D Systems, Minneapolis, USA) at 24 hours, the Human VEGF Quantikine ELISA Immunoassay (R&D Systems, Minneapolis, USA) at 24 hours, and a Human IL-6 Quantikine ELISA Immunoassay (R&D Systems, Minneapolis, USA) at 96 hours following manufacturer instructions. The absorbance values of IL-1β, VEGF, and IL-6 secretion were measured at wavelengths of 450 nm, with corrections of 540 nm or 570 nm. Protein expression analysis was performed by the ELISA reader (BioTek, Winooski, USA).

2.14 Statistical analysis

Statistical analyses were performed using RTCA Software 1.2.1 (ACEA Biosciences Inc., San Diego, USA), and the standard deviation was stated in curve progression. Additional data analysis was performed with JMP 10.0.2 (SAS

Institute, Cary, NC, USA). The primary outcomes were the inflexion points of cell adherence/death in the xCELLigence experiments and calculated concentrations and relative gene expression in the ELISA and qRT-PCR analyses, respectively. Intraindividual differences of inflexion points to the individual experiment control were also calculated to account for individual experiment bias. A paired Student's t-test was performed, and the Tukey-Kramer method was used to confirm results and account for experiment-wise error. A p value $< .05$ was considered significant.

Part II Histologic examination

2.15 Patient population/histologic bone samples

Following informed consent and approval from the institutional ethical committee, surgical biopsies were obtained from the following patient groups:

1. BRONJ
2. DRONJ
3. Mixed ONJ (osteonecrosis due to both BP and denosumab)
4. Healthy bone exposed to BP (BP-exposed)
5. Healthy bone exposed to BP and denosumab (BP-DN exposed)
6. Osteoradionecrosis of the jaw (ORN)
7. Secondary chronic osteomyelitis (OM)
8. Osteoporosis
9. Healthy bone of the jaw
10. Necrotic bone secondary to other chemotherapies
11. Transplanted bone

Bone samples were analyzed in a retrospective histologic study and medical record review and compared to both the Healthy and Osteoporosis group. The osteoporosis groups also served as a reliable control since both cancer patients

(breast and prostate) and osteoporosis patients frequently begin antiresorptive therapy in an osteopenic state. The study population was composed of all patients presenting for evaluation and management of the above-mentioned jaw diseases between October 2010 and January 2016. To be included in the study, patients had to have at least one follow-up visit evaluated and managed in the Department of Oral and Maxillofacial Surgery, University Hospital Tuebingen, Germany, and were excluded if the total observation period was less than two months. According to the recommendation of the AAOMS, the diagnosis of MRONJ was confirmed if all the following criteria were satisfied: 1. current or previous treatment with a BP or denosumab; 2. exposed necrotic bone in the maxillofacial region that has persisted for more than 8 weeks; 3. no history of radiation therapy or metastasis to the jaws.[7] Patient characteristics collected included patient demographics, primary disease diagnosis, antiresorptive regimen and schedule, duration of therapy, concurrent primary disease therapy, time to onset of MRONJ, association of onset with dental procedure, AAOMS stage, presence of pain, treatment type, follow-up course, and management outcomes (healed versus not healed). Complete healing was defined as no exposed or probeable bone with no pain.

Bone biopsies were washed in saline solution, and immediately fixed in 10% buffered formalin. Bone samples were decalcified with Usedecalc (MEDITE, Orlando, USA), embedded in paraffin, and microsectioned at 3 µm thickness. The microsections were then stained with hematoxylin and eosin (H&E) to examine for signs of infection and cellular composition, RANKL and OPG for bone remodelling activity, tartrate-resistant acid phosphatase (TRAP) for osteoclast activation, toluidine blue for bony structural composition and architecture, and CD14 and CD68 for the presence of monocytes and macrophagic cells. Selected bone samples were additionally analyzed by micro-CT scanning (Siemens Inveon MicroCT System, Siemens, Germany). Images were reconstructed at a 27 µm voxel size and visualized using the Inveon Research Workplace Software by Siemens.

2.16 Data collection

Histochemical stains were visualized under an inverted light microscope (Leica Microsystems, Wetzlar, Germany). The following data were collected for H&E stain: presence of infection (0-1), pseudoepithelial changes (0-1), granulation tissue (0-1), fibrous tissue (0-1), and scallopped resorption (0-1); RANKL: RANKL stain positivity (0-8); TRAP: TRAP stain positivity (0-8), the number of TRAP-positive multinucleated cells with over three nuclei per cell; OPG: OPG stain positivity (0-8); Toluidine blue: number of osteocyte lacunae per area, organization level (0-2), presence of reversal lines (0-2), and presence of Haversian canals (0-2); CD14: CD14 positivity (0-8); CD68: CD68 positivity (0-8). Positivity of stains were assessed by the 9 point (0-8) Allred Score.[80, 81] Five different fields were analyzed at 20x magnification for each individual stain, and the mean was calculated. Individual cells per area were quantified manually for each specimen with Image J software (National Institutes of Health, Bethesda, USA). Digital images of the stained sections were collected using an inverted light microscope (Leica Microsystems, Wetzlar, Germany). Necrotic bone samples from BRONJ, DRONJ, and Mixed ONJ biopsies were further categorized into sequestrum, border bone, and newly formed bone and separately analyzed to account for location bias. Samples labeled as sequestrum were omitted from the immunohistochemical evaluation of living cells including RANKL, OPG, TRAP, CD14, and CD68. Analysis of micro-CTs was completed in 69 bone samples, and the percent of medullary space to bone was measured in addition to the width of bone trabeculae using Ginkgo CADx Dicom Viewer (MetaEmotion Healthcare, Valladolid, Spain). Histologic and histomorphometric analyses were performed blind by the reviewer, without knowledge of the clinical features of the patients corresponding to individual biopsies.

2.17 Statistical analysis

Descriptive statistics were used to report patient characteristics. Groups were compared using analysis of variance (ANOVA) with $p < .05$ indicating significance. All statistical analyses were performed with STATA version 14.0 (Statacorp LLC, College Station, USA).

Part III Radiographic evaluation

2.18 Radiographic evaluation

Electronic medical records of adult cancer and osteoporosis patients with at least two diagnostic panoramic radiographs/clinic visits diagnosed with BRONJ, DRONJ, or Mixed ONJ were reviewed. Patient characteristics collected included patient demographics, primary disease diagnosis, antiresorptive regimen and schedule, duration of therapy, concurrent primary disease therapy, time to onset of MRONJ, association of onset with dental procedure, AAOMS stage, presence of pain, treatment type (operative versus non-operative), follow-up course, and management outcomes (healed versus not healed). Complete healing was defined as no exposed or probeable bone with no pain.

Radiographs were obtained for each patient based on clinical need, and findings were confirmed by two oral specialists (oral and maxillofacial surgeon and oral medicine specialist) and one radiologist in consensus. Panoramic radiograph, cone beam computed tomography (CBCT), CT, scintigraphy, and MRI were evaluated for common radiographic signs of osteonecrosis including sequestrum, bony fistula, bone fracture, persistent extraction sockets, erosion of cortical bone, sclerosis of cortical bone, sclerosis of cancellous bone, periosteal sclerosis, inferior alveolar nerve (IAN) canal involvement, thickened lamina dura, maxillary sinus involvement, activity of scintigraphy, and cervical lymph node involvement (Table 2).[82-84]

	Imaging modality				
Radiographic sign	Panoramic radiograph	CBCT	CT	MRI	Scintigraphy
Sequestrum	X	X	X		
Bony fistula	X	X	X		
Bone fracture	X	X	X		
Persistent extraction sockets	X	X	X		
Erosion of cortical bone	X	X	X		
Sclerosis of cortical bone	X	X	X		
Sclerosis of cancellous bone	X	X	X		
Periosteal sclerosis	X	X	X		
IAN canal involvement	X	X			
Thickened lamina dura	X				
Maxillary sinus involvement		X	X		
Positive scintigraphy activity					X
Cervical lymph node involvement			X	X	

Table 2. Commonly reported radiographic signs of medication-related osteonecrosis of the jaw and their optimal imaging modality. CBCT = cone beam computed tomography; CT = computed tomography; MRI = magnetic resonance imaging; IAN = inferior alveolar nerve.

The detectability of MRONJ findings using the various imaging techniques was calculated according to a modified formula proposed by Stockmann et al. [85]:

$$\% \text{ detectability} = \frac{\text{number of positive findings with a particular imaging method}}{\text{number of total detected findings}}$$

(This excluded imaging modality-specific findings such as thickened lamina dura, scintigraphy activity, lymph node involvement, etc.)

Descriptive statistics were used to report patient characteristics. Radiographic changes over time were analyzed with linear regression, with $p < .05$ indicating significance. All statistical analyses were performed with STATA version 14.0 (Statacorp LLC, College Station, USA).

3 Results

Part I Real-time *in vitro* assays

3.1 Real-time analyses of cell adherence

Live monitoring indicated a similar initial differentiation of antiresorptive-treated and untreated HGF cells for approximately 60 hours (Figure 6), followed by an individual inflexion point of adherence/cell death. The inflexion point for the control group was observed after 90.4 ± 90.4 hours. Nitrogen-containing BPs at 50 µM concentrations exhibited early inflexion points at 64.0 (alendronate) to 66.0 hours (zoledronate), with later inflexion points for denosumab (69.5 hours), the combination of zoledronate and denosumab (70.0 hours), and the non-nitrogen-containing BP clodronate (78.0 hours; Table 3). Differences to control were significant with 50 µM alendronate (64.0 ± 1.0 hours). Intraindividual differences to the control in each experiment set also exhibited a significance to the individual experiment control at concentrations of 50 µM for zoledronate (-22.5 ± 31.8 hours), alendronate (-27.7 ± 28.3 hours), and ibandronate (-22.0 ± 31.1 hours), as well for the combination of 5 µM zoledronate + 10 µg/mL denosumab (20.3 ± 17.6 hours).

A

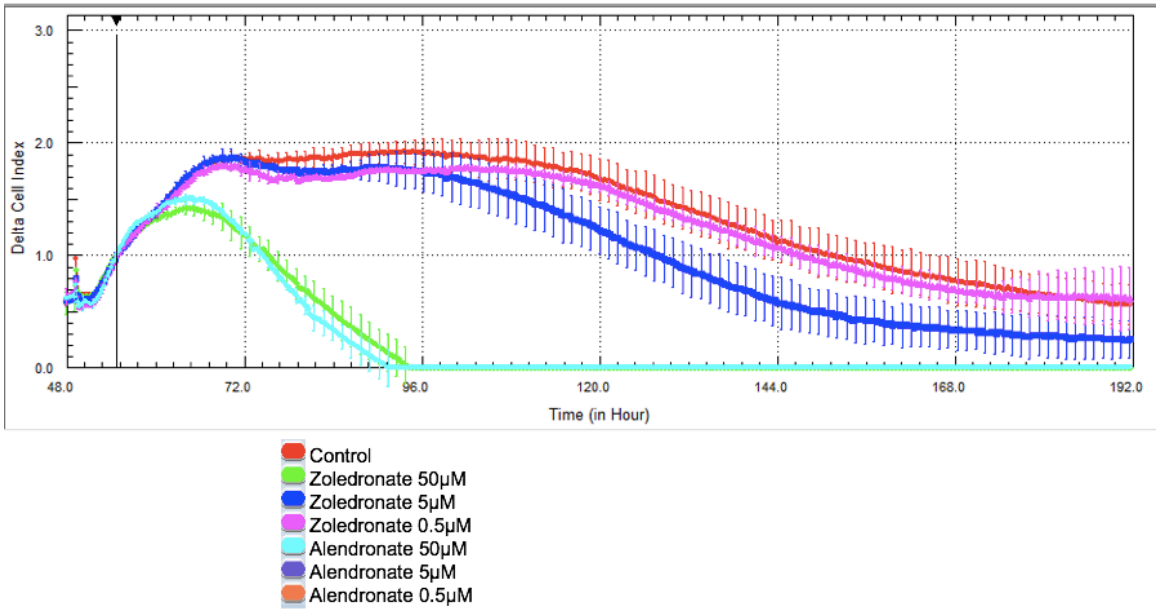
Delta Cell Index
3.0
2.0
1.0
0.0
48.0
72.0
96.0
120.0
144.0
168.0
192.0
Time (in Hour)
Control
Zoledronate 50μM
Zoledronate 5μM
Zoledronate 0.5μM
Alendronate 50μM
Alendronate 5μM
Alendronate 0.5μM

B

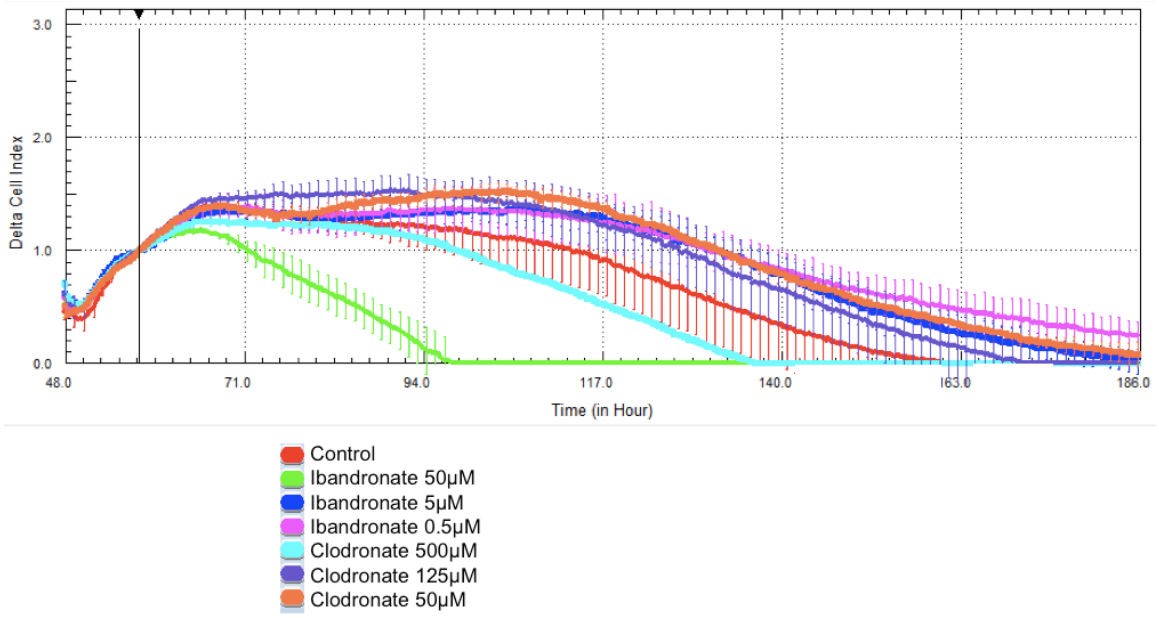
Delta Cell Index
3.0
2.0
1.0
0.0
48.0
71.0
94.0
117.0
140.0
163.0
186.0
Time (in Hour)
Control
Ibandronate 50μM
Ibandronate 5μM
Ibandronate 0.5μM
Clodronate 500μM
Clodronate 125μM
Clodronate 50μM

C

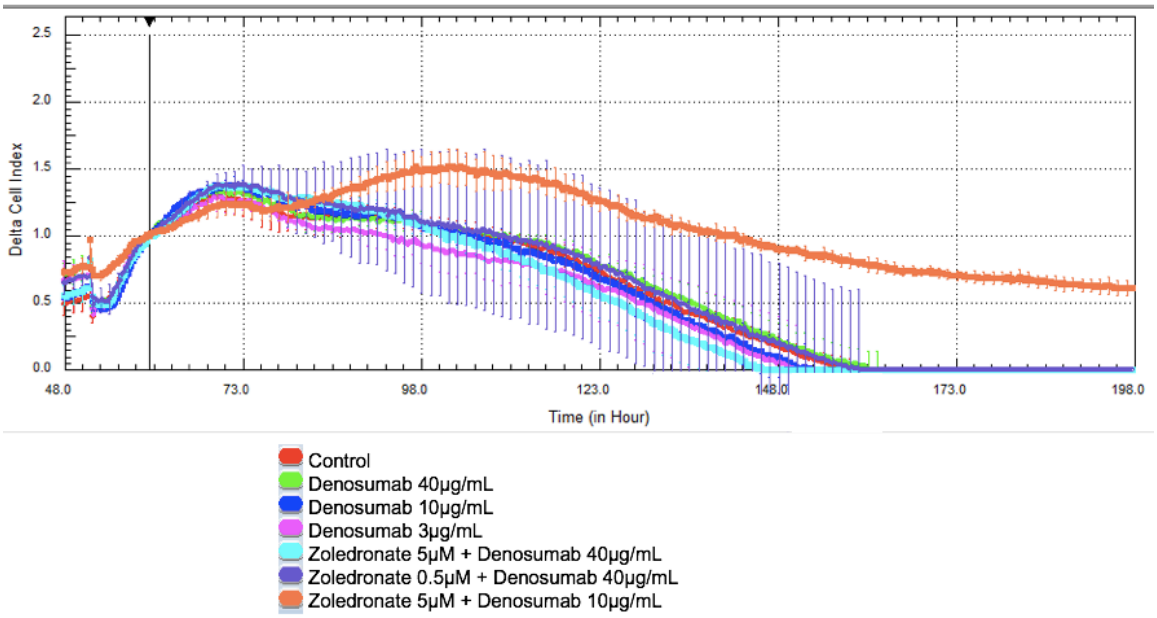

Figure 6. Real-time monitoring of human gingival fibroblast cell adherence after confluence and exposure to antiresorptive medications at various concentrations. Cell curve describes the mean values of cell impedance and standard deviation up to 190 hours of observation for the adherence curves of controls and (A) zoledronate and alendronate at concentrations of 0.5 µM, 5 µM, and 50 µM (B) clondronate at concentrations of 50 µM, 125 µM, and 500 µM and ibandronate at concentrations of 0.5 µM, 5 µM, and 50 µM, (C) denosumab at concentrations of 3 µg/mL, 10 µg/mL, and 40 µg/mL and combination of zoledronate and denosumab at concentrations of zoledronate 5 µM + denosumab 40 µg/mL, zoledronate 0.5 µM + denosumab 40 µg/mL, and zoledronate 5 µM + denosumab 10 µg/mL. Curve interruption is caused by medium renewal.

Antiresorptive concentration	Mean and standard deviation of inflexion points of cell	*p*-value	Mean and standard deviation of intraindividual differences of inflexion points of cell	*p*-value

	adherence/death (hours)		adherence/death to control (hours)	
Zoledronate				
50 µM	66.0 ± 4.2		-22.5 ± 31.8	< .05
5 µM	81.5 ± 21.9		-2.0 ± 14.1	
0.5 µM	87.5 ± 30.4		4.0 ± 5.6 h	
Alendronate				
50 µM	64.0 ± 1.0	< .05	-27.7 ± 28.3	< .05
5 µM	87.0 ± 29.7		4.0 ± 5.6	
0.5 µM	87.0 ± 29.7		4.0 ± 5.6	
Ibandronate				
50 µM	66.0 ± 0.0		-22.0 ± 31.1	< .05
5 µM	88.0 ± 31.1		0.0 ± 0.0	
0.5 µM	88.0 ± 31.1		0.0 ± 0.0	
Clodronate				
500 µM	78.0 ± 6.9		-10.0 ± 14.1	
125 µM	88.0 ± 31.1		0.0 ± 0.0	
50 µM	88.0 ± 31.1		0.0 ± 0.0	
Denosumab				
40 µg/ml	69.5 ± 0.7		0.0 ± 0.0	
10 µg/ml	69.5 ± 0.7		0.0 ± 0.0	
3 µg/ml	69.5 ± 0.7		0.0 ± 0.0	
Zoledronate + Denosumab				
5 µM + 40 µg/mL	70.0 ± 1.0		-12.33 ± 21.3	
0.5 µM + 40 µg/mL	82.3 ± 22.3		0.0 ± 0.0	
5 µM + 10 µg/mL	102.7 ± 4.7		20.3 ± 17.6	< .05
Control	90.4 ± 90.4			

Table 3. Inflexion points of cell adherence/cell death and intraindividual differences to the control for antiresorptive-treated human gingival fibroblast cells.

3.2 HGFs exposed to LPS

For HGFs treated with both antiresorptive medications and *P. gingivalis* LPS, a similar initial differentiation of antiresorptive-treated and untreated HGF cells was observed for approximately 60 hours (Figure 7), followed by an individual inflexion point of adherence/cell death. The inflexion point for the control group was observed after 125.3 ± 44.2 hours, and the control group with LPS at 105.2 ± 12.0 hours. Nitrogen-containing BPs at 50 µM concentrations exhibited early inflexion points at 63.0 (zoledronate) to 78.0 hours (ibandronate), with later inflexion points for the non-nitrogen BP clodronate (89.0 hours) and both denosumab and the combination of zoledronate and denosumab (both 117.0 hours; Table 4). Differences to control were significant with 50 µM zoledronate (63.0 ± 4.4 hours) and ibandronate (78.0 ± 18.3 hours), as well as all concentrations of alendronate dose-dependently. Intraindividual differences of the inflexion points of cell adherence/death in each experiment set exhibited a significance to the individual experiment control value at concentrations of 50 µM for zoledronate (-93.5 ± 78.4 hours) and all concentrations of alendronate dose-dependently.

A

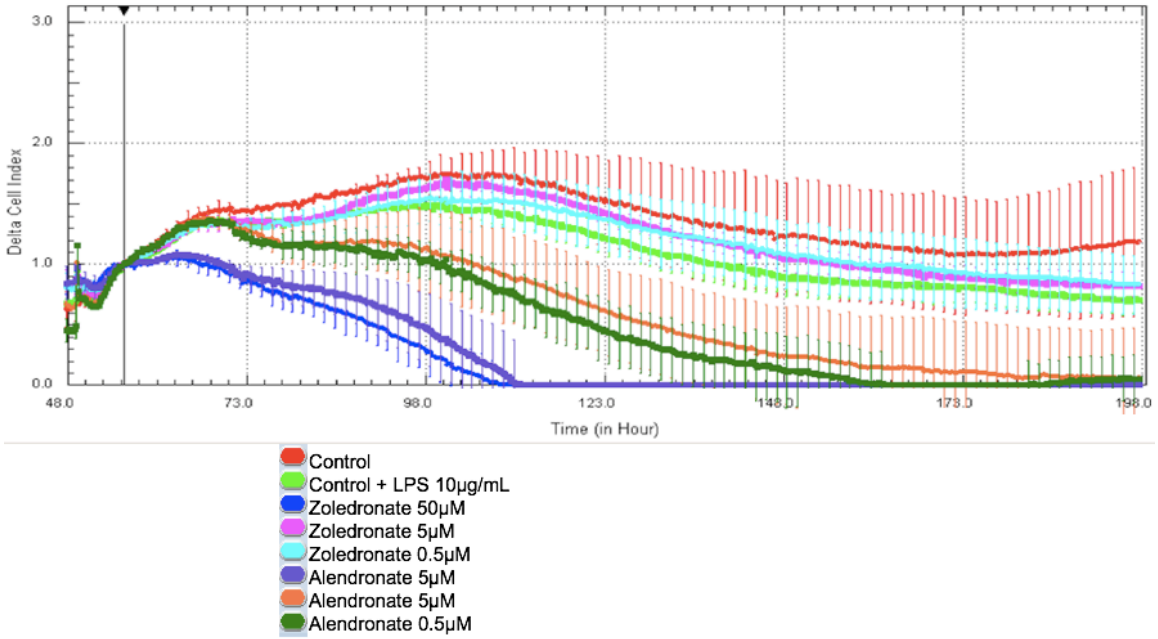

B

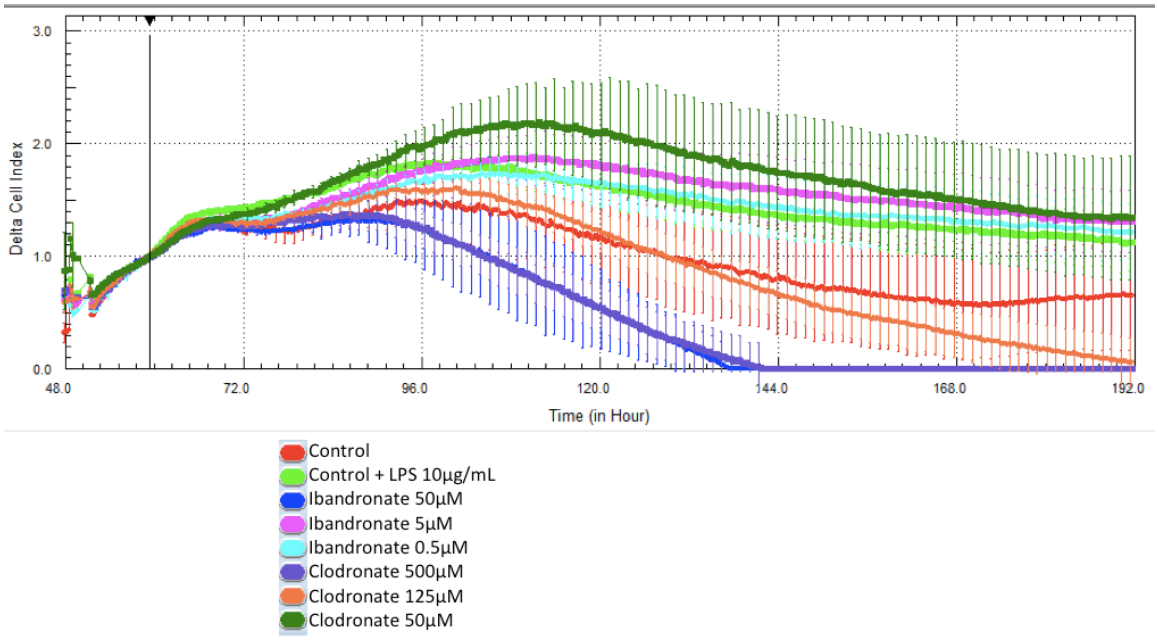

C

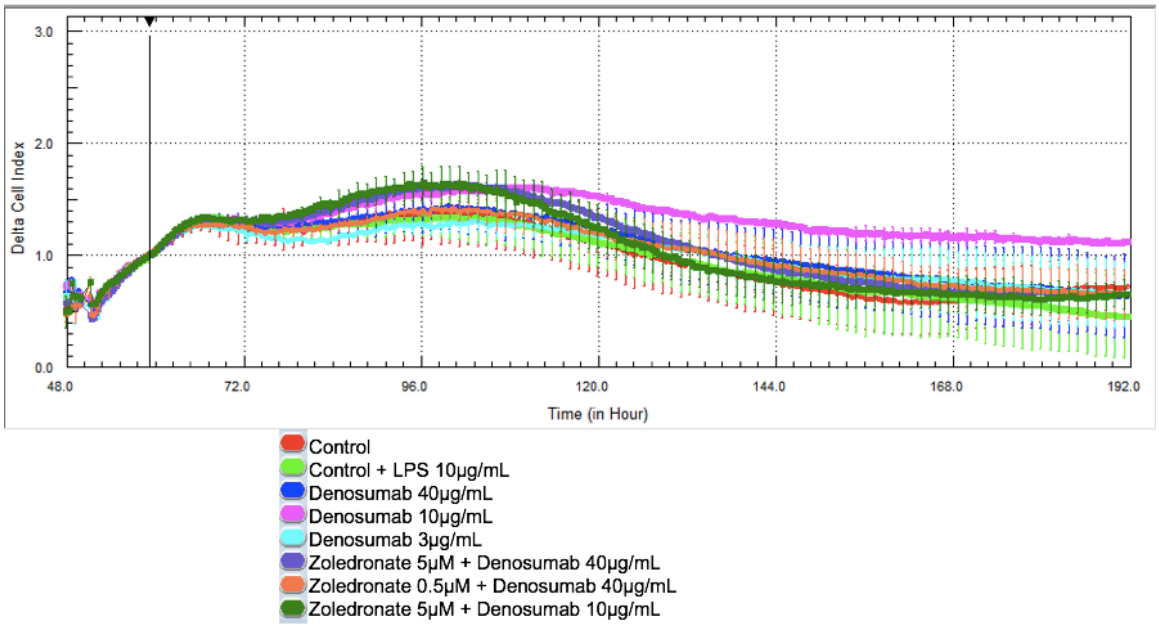

Figure 7. Real-time monitoring of human gingival fibroblast cell adherence after confluence and exposure to *Porphyromonas gingivalis*

lipopolysaccharide 10 µg/mL and antiresorptive medications at various concentrations. Cell curve describes the mean values of cell impedance and standard deviation up to 190 hours of observation for the adherence curves of controls and (A) zoledronate and alendronate at concentrations of 0.5 µM, 5 µM, and 50 µM (B) clodronate at concentrations of 50 µM, 125 µM, and 500 µM and ibandronate at concentrations of 0.5 µM, 5 µM, and 50 µM, (C) denosumab at concentrations of 3 µg/mL, 10 µg/mL, and 40 µg/mL and combination of zoledronate and denosumab at concentrations of zoledronate 5 µM + denosumab 40 µg/mL, zoledronate 0.5 µM + denosumab 40 µg/mL, and zoledronate 5 µM + denosumab 10 µg/mL. Curve interruption is caused by medium renewal.

Antiresorptive concentration	**Mean and standard deviation of inflexion points of cell adherence/death (hours)**	***p*-value**	**Mean and standard deviation of intraindividual differences of inflexion points of cell adherence/death to control (hours)**	***p*-value**
Zoledronate				
50 µM	63.0 ± 4.4	< .05	-93.5 ± 78.4	< .05
5 µM	103.0 ± 4.2		-53.5 ± 75.6	
0.5 µM	103.5 ± 4.9		-53.0 ± 74.9	
Alendronate				
50 µM	64.0 ± 0.0	< .05	-92.5 ± 79.9	< .05
5 µM	81.5 ± 17.6	< .05	-75.0 ± 97.5	< .05
0.5 µM	80.0 ± 15.5	< .05	-76.5 ± 95.4	< .05
Ibandronate				
50 µM	78.0 ± 18.3	< .05	-24.5 ± 16.2	
5 µM	113.0 ± 2.8		10.5 ± 0.7	
0.5 µM	108.5 ± 9.1		6.0 ± 7.0	
Clodronate				
500 µM	89.0 ± 2.8		-13.5 ± 0.7	
125 µM	102.5 ± 2.1		0.0 ± 0.0	

50 µM	103.0 ± 11.3		0.5 ± 9.1	
Denosumab				
40 µg/ml	117.0 ± 16.9		0.0 ± 0.0	
10 µg/ml	120.5 ± 12.0		3.5 ± 4.9	
3 µg/ml	117.0 ± 16.9		0.0 ± 0.0	
Zoledronate + Denosumab				
5 µM + 40 µg/mL	117.0 ± 16.9		0.0 ± 0.0	
0.5 µM + 40 µg/mL	117.0 ± 16.9		0.0 ± 0.0	
5 µM + 10 µg/mL	115.0 ± 19.8		-2.0 ± 2.8	
Control with LPS	105.2 ± 12.0			
Control	125.3 ± 44.2			

Table 4. Inflexion points of cell adherence/cell death and intraindividual differences to the control for antiresorptive- and lipopolysaccharide-treated human gingival fibroblast cells.

3.3 HGFs in co-culture

For HGFs treated with antiresorptive medications and *P. gingivalis* LPS in a co-culture with THP-1 cells, an initial differentiation of antiresorptive-treated and untreated HGF cells was observed for approximately 50 hours (Figure 8), followed by an individual inflexion point of adherence/cell death. The inflexion point for the control group was observed after 149.6 ± 8.6 hours. Nitrogen-containing BPs at 50 µM concentrations exhibited early inflexion points at 57.6 (zoledronate) to 68.0 hours (ibandronate), with later inflexion points for the combination of zoledronate and denosumab (101.0 hours), denosumab (152.0 hours), and the non-nitrogen BP clodronate (155.0 hours; Table 5). Differences to control were significant with 50 µM alendronate (57.7 ± 9.8 hours), 50 µM ibandronate (68.0 ± 4.2 hours), the combination of 5 µM zoledronate + 40 µg/mL denosumab (101.0 ± 67.8 hours), and zoledronate at concentrations of 50 µM and 5 µM dose-dependently.

Intraindividual differences of the inflexion points of cell adherence/death in each experiment set exhibited a significance to the individual experiment control value at concentrations of 50 µM for alendronate (-90.0 ± 1.7 hours), ibandronate (-82.5 ± 13.4 hours), the combination of 5 µM zoledronate + 40 µg/mL denosumab (-44.0 ± 62.2 hours), and zoledronate at concentrations of 50 µM and 5 µM dose-dependently. Lowest bisphosphonate concentrations of 0.5 µM alendronate, 40 µg/mL denosumab, the combination of 5 µM zoledronate + 10 µg/mL denosumab, and all concentrations (dose-dependently) of clodronate continued to display a prolonged peak until inflexion points of 152.0 to 166.0 hours, though none were statistically significant.

A

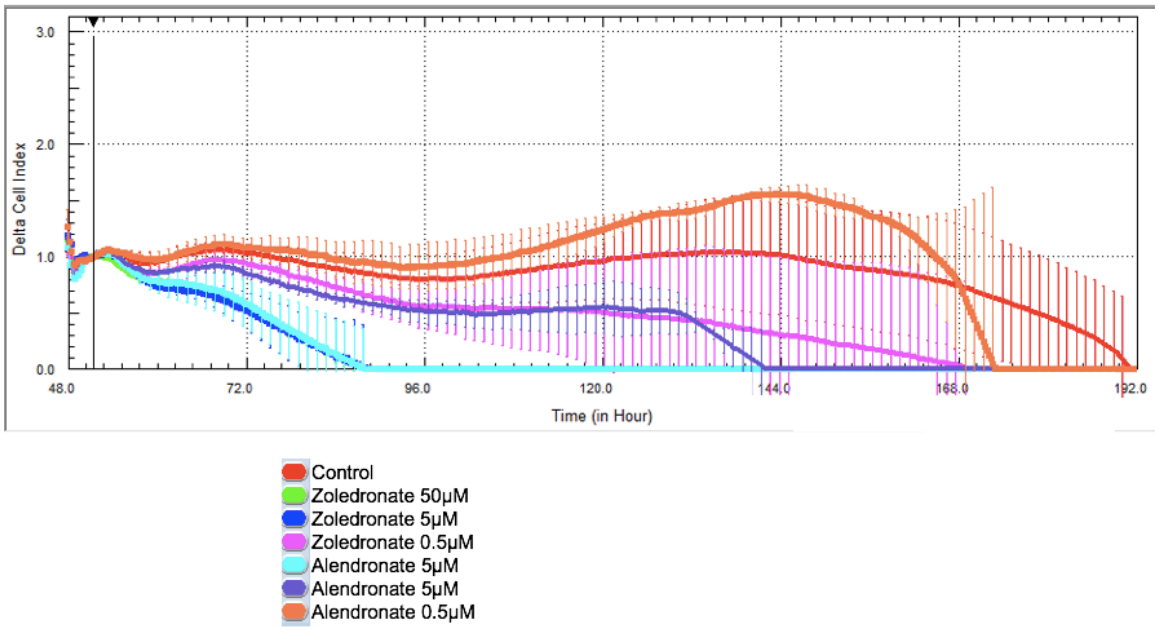

B

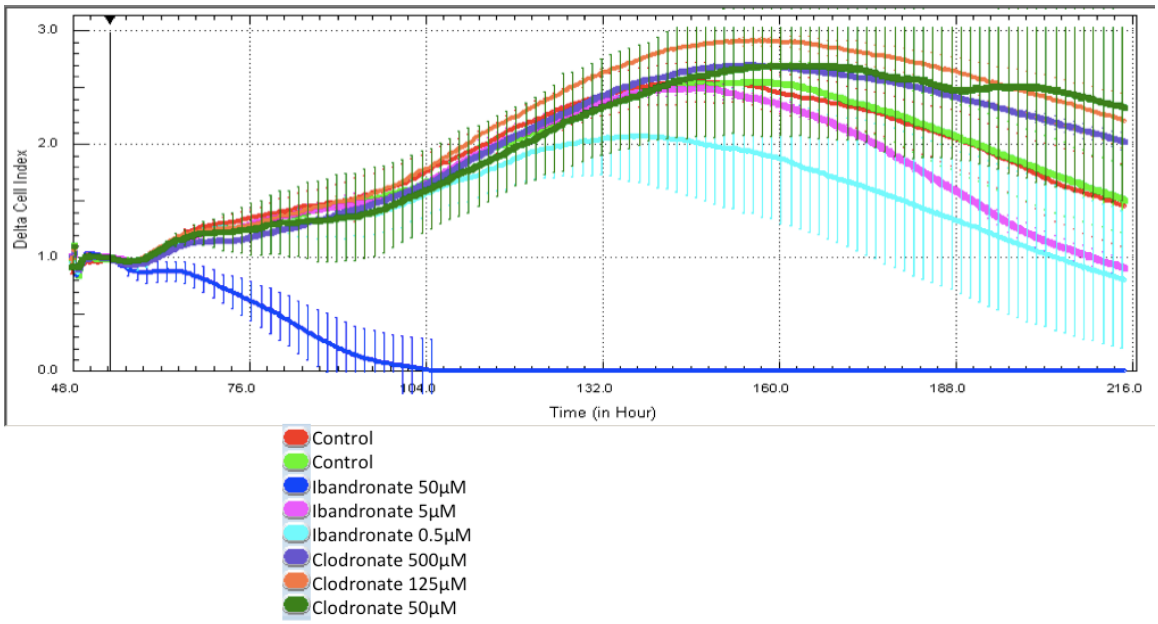
3.0
2.0
1.0
0.0
Delta Cell Index
48.0
76.0
104.0
132.0
160.0
188.0
216.0
Time (in Hour)
Control
Control
Ibandronate 50μM
Ibandronate 5μM
Ibandronate 0.5μM
Clodronate 500μM
Clodronate 125μM
Clodronate 50μM

C

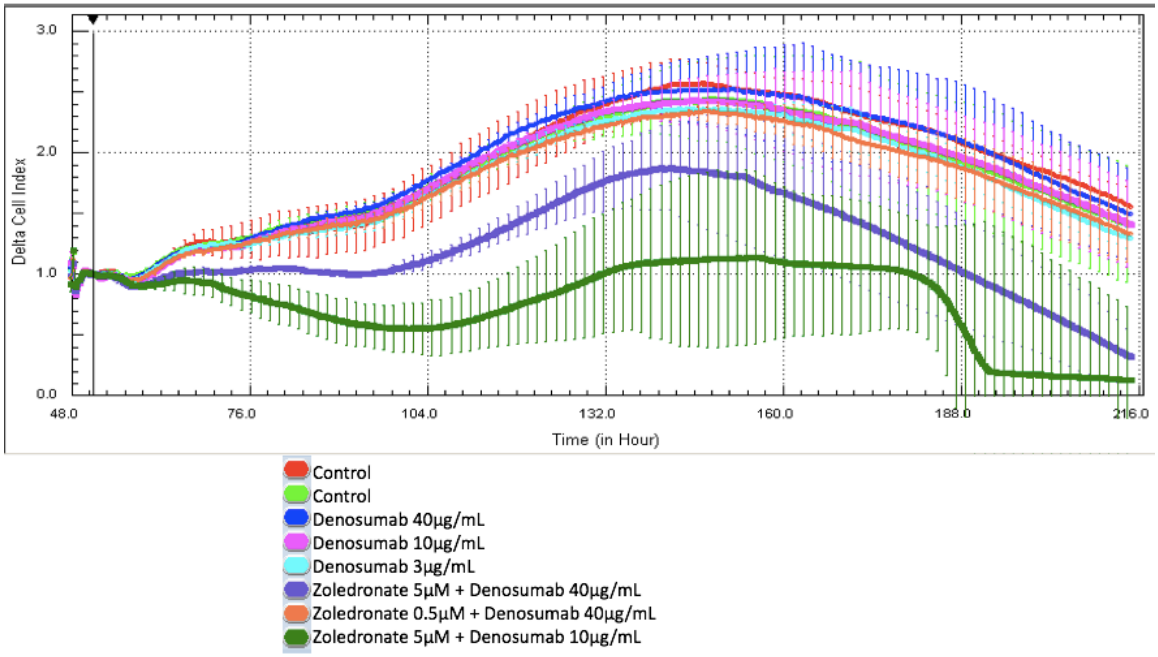

Figure 8. Real-time monitoring of human gingival fibroblast cell adherence after confluence and exposure to *Porphyromonas gingivalis* lipopolysaccharide 10 µg/mL and antiresorptive medications at various concentrations in co-culture with THP-1 cells in an xCELLigence 0.4 µM porous ThinCert™. Cell curve describes the mean values of cell impedance and standard deviation up to 190 hours of observation for the adherence curves of controls and (A) zoledronate and alendronate at concentrations of 0.5 µM, 5 µM, and 50 µM (B) clodronate at concentrations of 50 µM, 125 µM, and 500 µM and ibandronate at concentrations of 0.5 µM, 5 µM, and 50 µM, (C) denosumab at concentrations of 3 µg/mL, 10 µg/mL, and 40 µg/mL and combination of zoledronate and denosumab at concentrations of zoledronate 5 µM + denosumab 40 µg/mL, zoledronate 0.5 µM + denosumab 40 µg/mL, and zoledronate 5 µM + denosumab 10 µg/mL. Curve interruption is caused by medium renewal.

Antiresorptive concentration	**Mean and standard deviation of inflexion points of cell adherence/death (hours)**	***p*-value**	**Mean and standard deviation of intraindividual differences of inflexion points of cell adherence/death to control (hours)**	***p*-value**
Zoledronate				
50 µM	57.6 ± 9.8	< .05	-90.0 ± 1.7	< .05
5 µM	89.3 ± 53.6	< .05	-58.3 ± 57.5	< .05
0.5 µM	131.0 ± 68.4		-16.7 ± 62.7	
Alendronate				
50 µM	57.7 ± 9.8	< .05	-90.0 ± 1.7	< .05
5 µM	126.7 ± 65.0		-21.0 ± 59.1	
0.5 µM	152.0 ± 7.8		4.3 ± 8.5	
Ibandronate				
50 µM	68.0 ± 4.2	< .05	-82.5 ± 13.4	< .05
5 µM	146.0 ± 2.8		-4.5 ± 6.3	
0.5 µM	142.5 ± 2.1		-8.0 ± 11.3	
Clodronate				
500 µM	155.0 ± 9.9		4.5 ± 0.7	
125 µM	157.0 ± 5.6		6.5 ± 3.5	
50 µM	166.0 ± 48.0		15.5 ± 38.8	
Denosumab				
40 µg/ml	152.0 ± 4.2		7.0 ± 9.9	
10 µg/ml	147.5 ± 2.1		2.5 ± 3.5	
3 µg/ml	144.5 ± 6.3		-0.5 ± 0.7	
Zoledronate + Denosumab				
5 µM + 40 µg/mL	101.0 ± 67.8	< .05	-44.0 ± 62.2	< .05
0.5 µM + 40 µg/mL	145.0 ± 5.6		0.0 ± 0.0	
5 µM + 10 µg/mL	159.0 ± 25.4		14.0 ± 19.8	
Control	149.6 ± 8.6			

Table 5. Inflexion points of cell adherence/cell death and intraindividual differences to the control for antiresorptive- and lipopolysaccharide-treated human gingival fibroblast cells in co-culture with THP-1 cells.

3.4 Scratch assay in 24-well plates

HGFs cultured in 24-well plates were scratched and exposed to antiresorptives at the time point after confluence (48 hours). Delayed wound healing was observed between 72 to 96 hours in clodronate 500 μM, ibandronate 5 μM and 50 μM, alendronate 50 μM, zoledronate 5 μM + denosumab 10 μg/mL, and zoledronate 5 μM, with obvious severe fibroblast cell death in zoledronate 50 μM (Figure 9). By 168 hours, ibandronate 50 μM, zoledronate 50 μM, zoledronate 5 μM + denosumab 10 μg/mL, alendronate 50 μM all demonstrated obvious severe cell death, while clodronate 500 μM showed mild signs of cell death compared to the intact cell layer of healthy-appearing confluent controls.

Fibroblasts exposed to *P. gingivalis* LPS in addition to antiresorptives also demonstrated further delayed wound healing. Zoledronate 50 μM exhibited signs of cell death as early as 24 hours. By 48 hours, wound healing was affected in clodronate 500 μM, denosumab 40 μg/mL, ibandronate 5 μM and 50 μM, zoledronate 0.5 μM and 5 μM, zoledronate 5 μM + denosumab 10 μg/mL, alendronate 50 μM, with zoledronate 50 μM having already progressed to severe cell death. By 96 hours, both alendronate 50 μM and zoledronate 50 μM exhibited severe cell death.

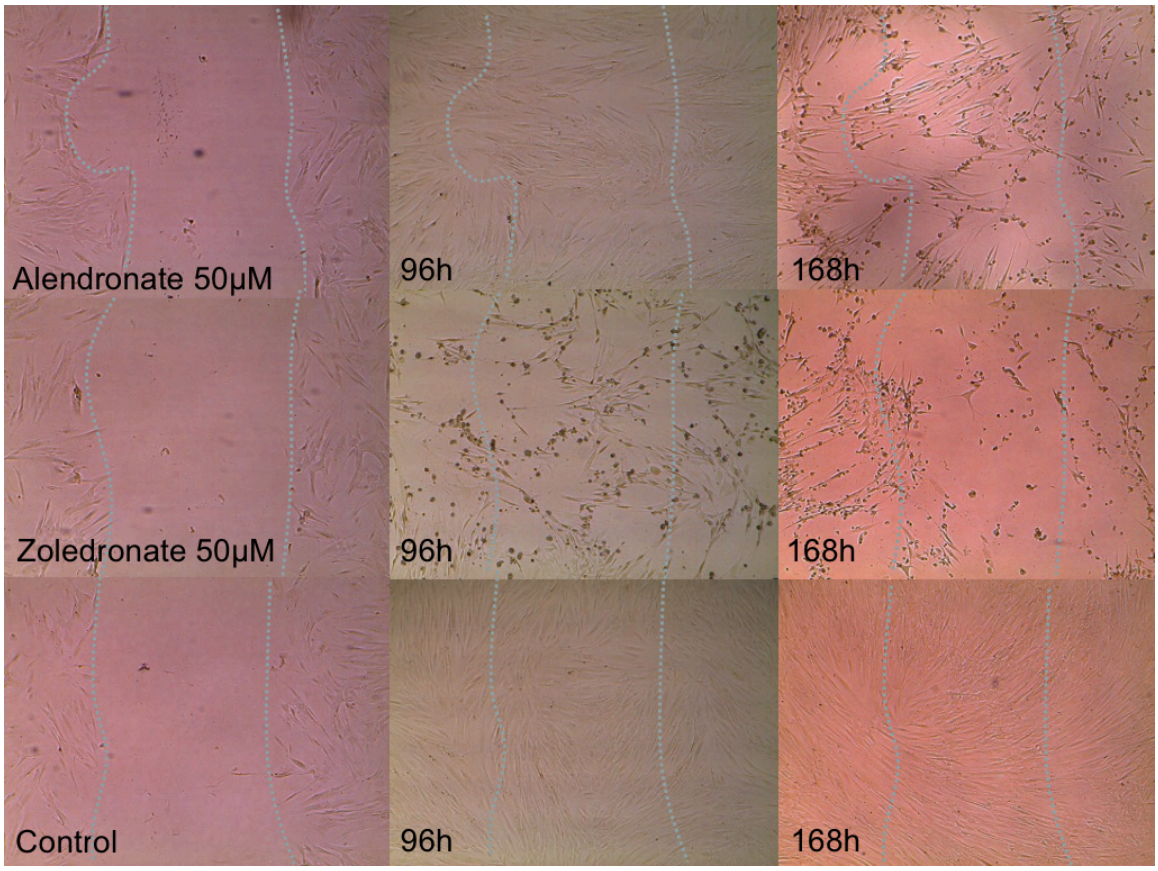

Figure 9. Human gingival fibroblasts exposed to alendronate 50 μM, zoledronate 50 μM, or control in 24-well plate scratch assay at 0, 96, and 168 hours after scratch and antiresorptive addition.

3.5 Non-scratch assay in 24-well plates

Antiresorptives were toxic to HGFs in the 24-well plate non-scratch assay even without mechanical damage (Figure 10). Cells exposed to a concentration of zoledronate 50 μM already appeared apoptotic at 24 hours after the addition of antiresorptive. By 168 hours, ibandronate 50 μM, zoledronate 50 μM, zoledronate 5 μM + denosumab 10 μg/mL, and alendronate 50 μM all demonstrated obvious severe cell death. In 24-well plates exposed to both antiresorptive and *P. gingivalis* LPS, zoledronate 50 μM demonstrated similar early cell death, with alendronate

50 μM also appearing apoptotic at 96 hours. Findings were analogous to the inflexion points of adherence/cell death observed in xCELLigence experiments.

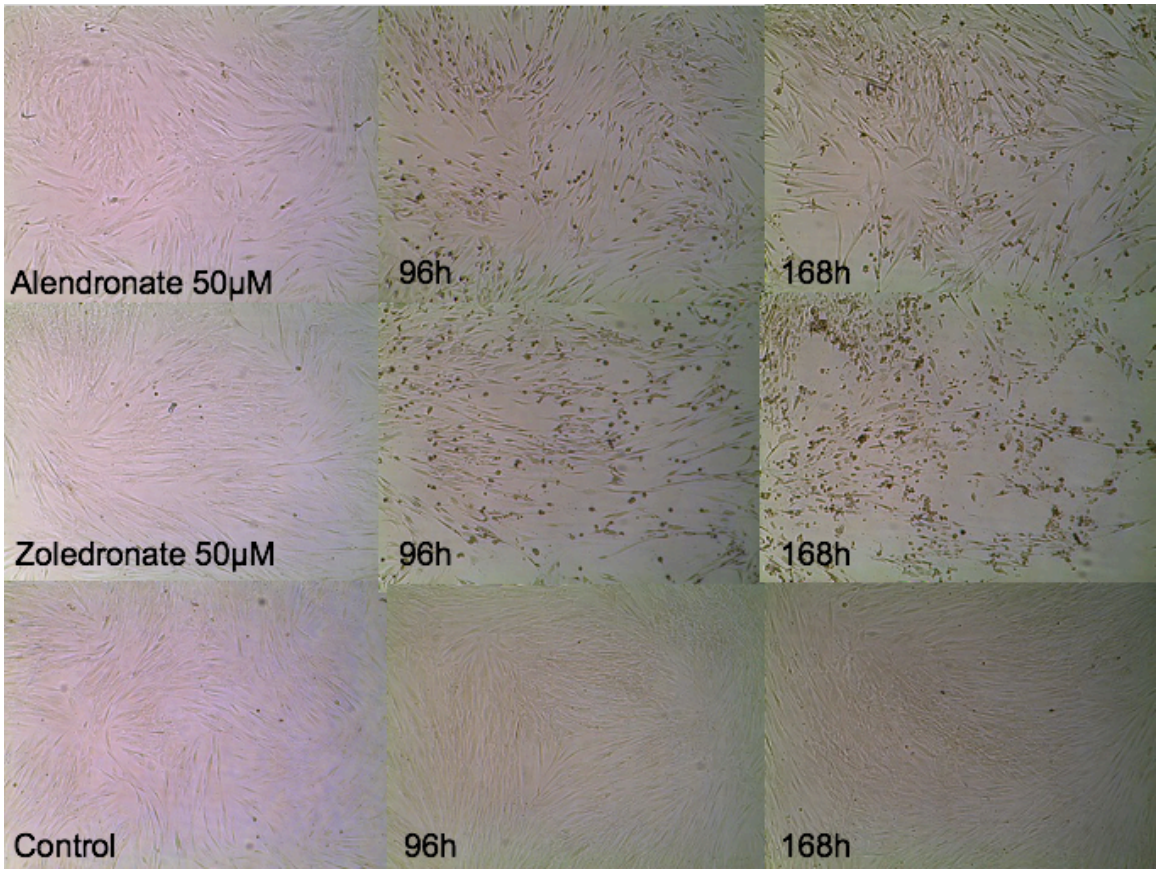

Figure 10. Human gingival fibroblasts exposed to alendronate 50 μM with lipopolysaccharide (LPS), zoledronate 50 μM with LPS, or control in 24-well plates at 0, 96, and 168 hours after antiresorptive addition.

3.6 Analysis of cell viability/cell death with fluorescence staining

Live/Dead staining results confirmed xCELLigence adherence curves at distinct time points after antiresorptive addition, consistent with the inflexion points of adherence/cell death described in Table 2. Obvious wound healing effects were observed at 96 hours after the addition of the antiresorptive and/or scratch (Figure 11). Fibroblasts exposed to antiresorptives demonstrated severe cell death upon

administration of zoledronate 50 μM and alendronate 50 μM. HGFs in the scratch assay demonstrated effects on wound healing in the following concentrations: clodronate 500 μM, ibandronate 5 μM and 50 μM, zoledronate 5 μM, zoledronate 5 μM + denosumab 10 μg/mL, alendronate 0.5 μM and 50 μM with obvious cell death in zoledronate 50 μM.

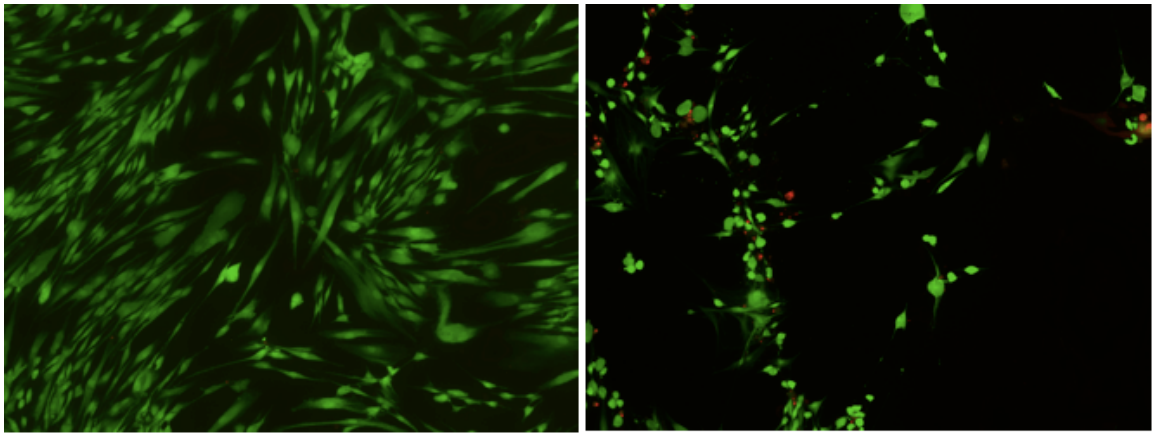

Figure 11. Human gingival fibroblasts exposed to zoledronate 50 μM or control in a 24-well plate LIVE/DEAD assay at 96 hours after antiresorptive addition and scratch. Green fluorescence depicts membrane-permeant calcein in living cells and red fluorescence depicts membrane-impermeant ethidium homodimer-1 in compromised cells.

3.7 Scanning electron microscopy

Scanning electron microscopy of 12-well plates indicated a confluent HGF layer in controls demonstrating normal cell morphology in comparison to deteriorated cell morphology, a clear reduction of adherence, and significant cell death at 96 hours after the addition of zoledronate 50 μM (Figure 12). The disruption of the confluent cell layer was more severe in the zoledronate 50 μM scratch assay compared to the non-scratch assay, though both were drastically altered compared to controls.

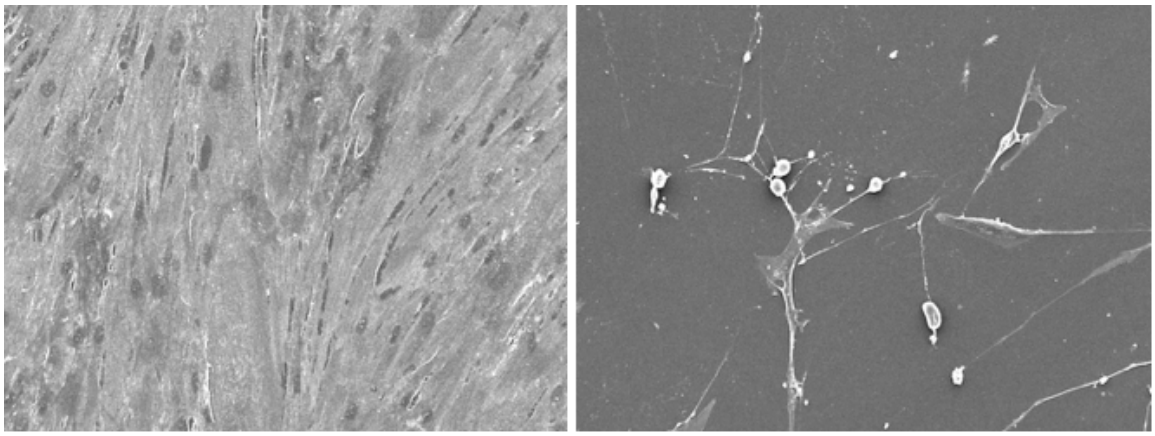

Figure 12. Scanning electron microscopy of human gingival fibroblasts exposed to zoledronate 50 μM and confluent control cell layer in 6-well plates at 96 hours after scratch assay and antiresorptive addition. 500x magnification.

3.8 Co-culture insert from THP-1 co-culture

The Greiner co-culture inserts containing THP-1 cells from the 24-well plate co-culture were stained with hematoxylin and revealed THP-1 cells remaining on the floor of the insert at 24 hours and 96 hours after the addition of antiresorptives (Figure 13). There was evidence of macrophage differentiation of THP-1 cells exposed to concentrations of, among others, alendronate 0.5 μM and zoledronate 50 μM.

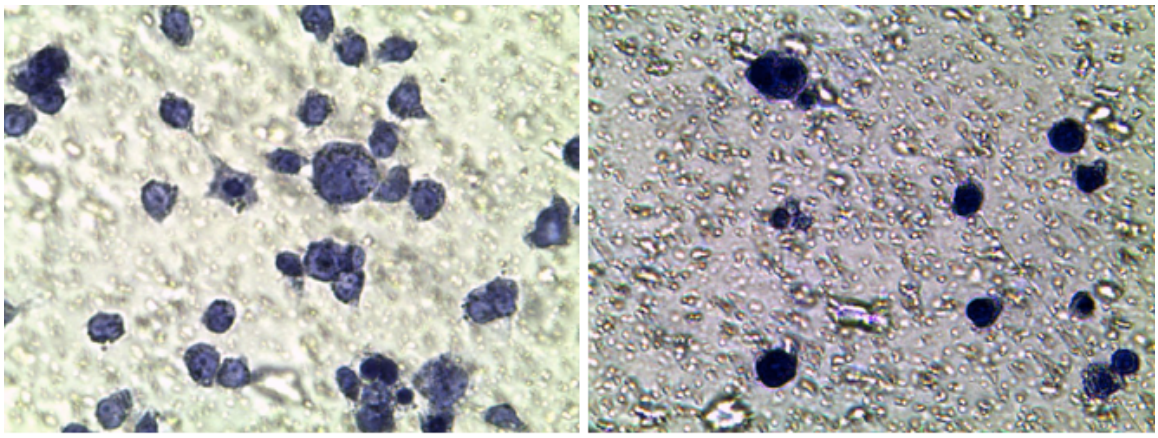

Figure 13. Hematoxylin staining of 0.4 μm porous Greiner inserts with adherent THP-1 cells and differentiated macrophages exposed to ibandronate 0.5 μM at 24 hours and zoledronate 50 μM at 96 hours after antiresorptive addition. 40x magnification.

3.9 OPG, RANKL, IL-8, and TNF expression with qRT-PCR

High concentrations of zoledronate (and slightly denosumab) in combination with LPS demonstrated high values of OPG gene expression (zoledronate: 773 gene copies; denosumab: 6.01 gene copies) in contrast to control (0.28 gene copies; Figure 14). Antiresorptives by themselves did not affect the expression of OPG without LPS. The expression of RANKL by HGF was only slightly influenced by zoledronate 50 μM with LPS (2.49 gene copies; Figure 15).

High concentrations of zoledronate in the presence of LPS exhibited elevated values of IL-8 gene expression (16.9 gene copies) compared to controls (.007 gene copies; Figure 16). For TNF, zoledronate 50 μM (and slightly denosumab 40 μg/mL) in the presence of LPS demonstrated elevated gene expression (zoledronate: 443 gene copies; denosumab: 2.66 gene copies; control: 0 gene

copies; Figure 17). Antiresorptives by themselves did not affect the expression of TNF without the addition of LPS.

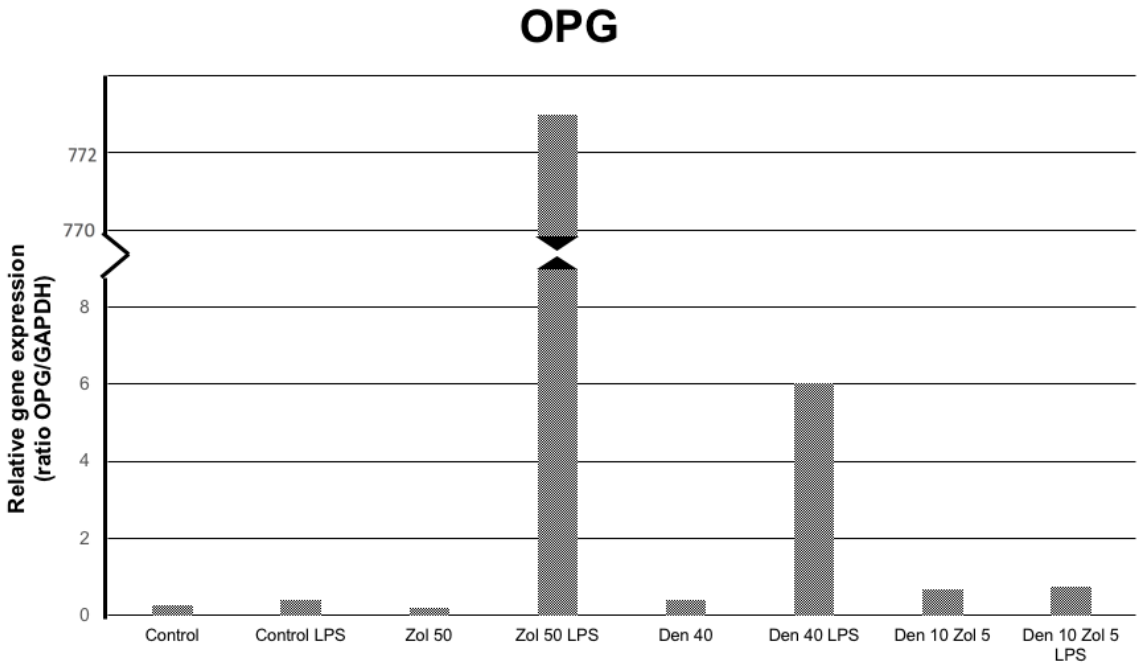

Figure 14. Relative gene expression of osteoprotegrin with and without lipopolysaccharide. LPS = lipopolysaccharide; Zol = zoledronate; Den = denosumab.

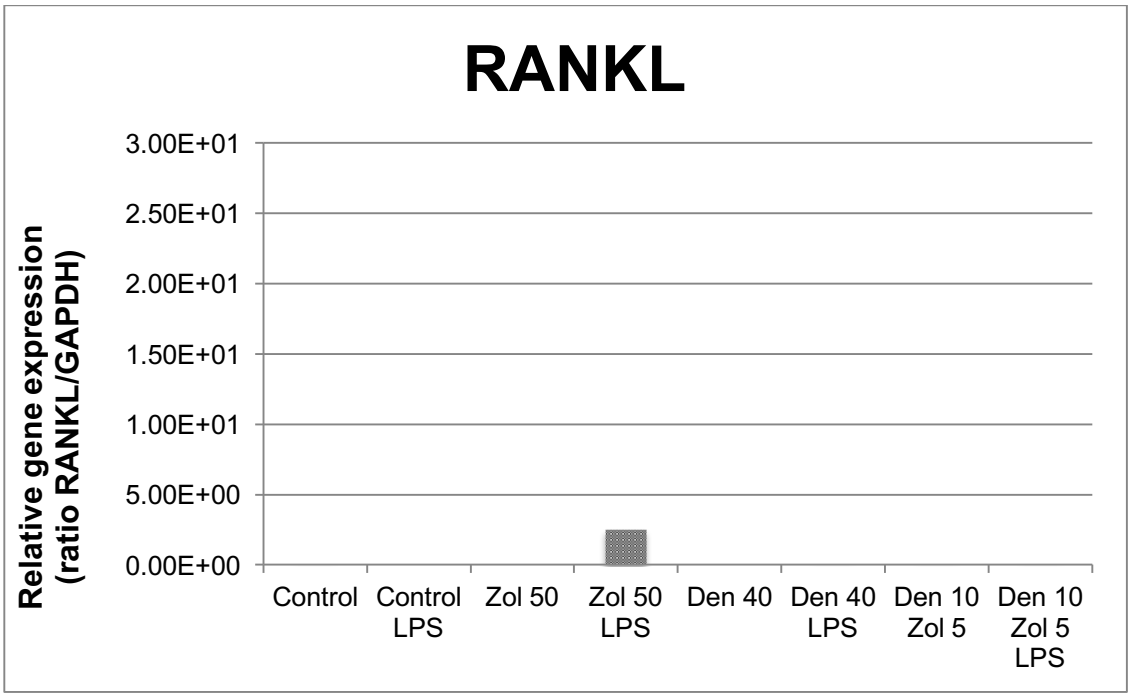

Figure 15. Relative gene expression of RANKL with and without lipopolysaccharide. LPS = lipopolysaccharide; Zol = zoledronate; Den = denosumab.

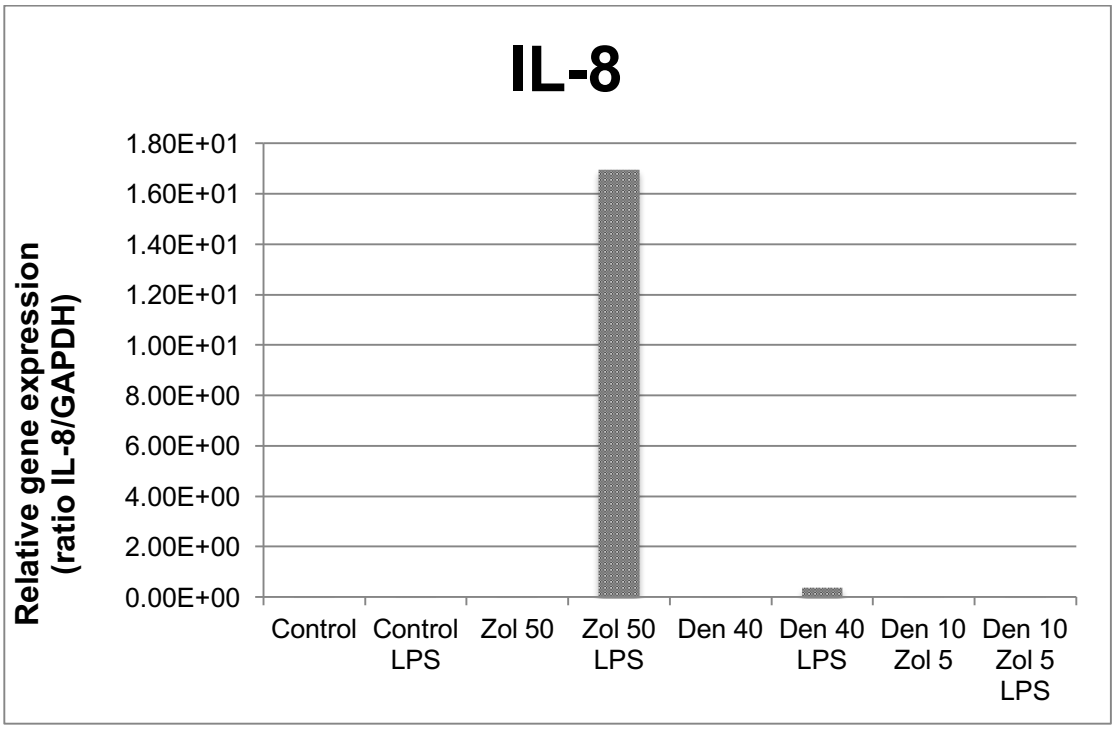

Figure 16. Relative gene expression of IL-8 with and without lipopolysaccharide. LPS = lipopolysaccharide; Zol = zoledronate; Den = denosumab..

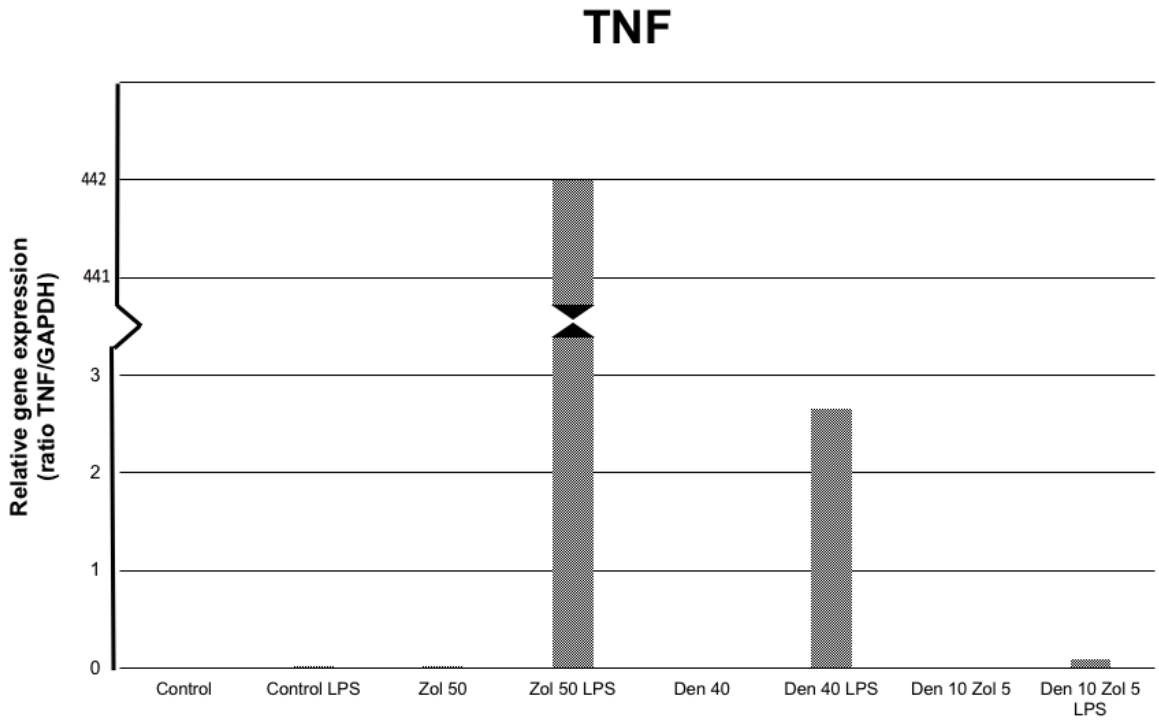

Figure 17. Relative gene expression of TNF with and without lipopolysaccharide. LPS = lipopolysaccharide; Zol = zoledronate; Den = denosumab..

3.10 IL-1β, IL-6, and VEGF expression with ELISA

All antiresorptives significantly elevated the expression of IL-1β in both the scratch and non-scratch assay in contrast to control (Figure 18), including the control stimulated with LPS in co-culture. In contrast, IL-6 levels were significantly decreased in HGFs exposed to high concentrations of nitrogen-containing BPs compared to the control (Figure 19). For VEGF, all antiresorptives elevated the expression of VEGF in contrast to control (including the control stimulated with

LPS in co-culture); this was statistically significant with the exception of higher concentrations of clodronate (Figure 20).

A

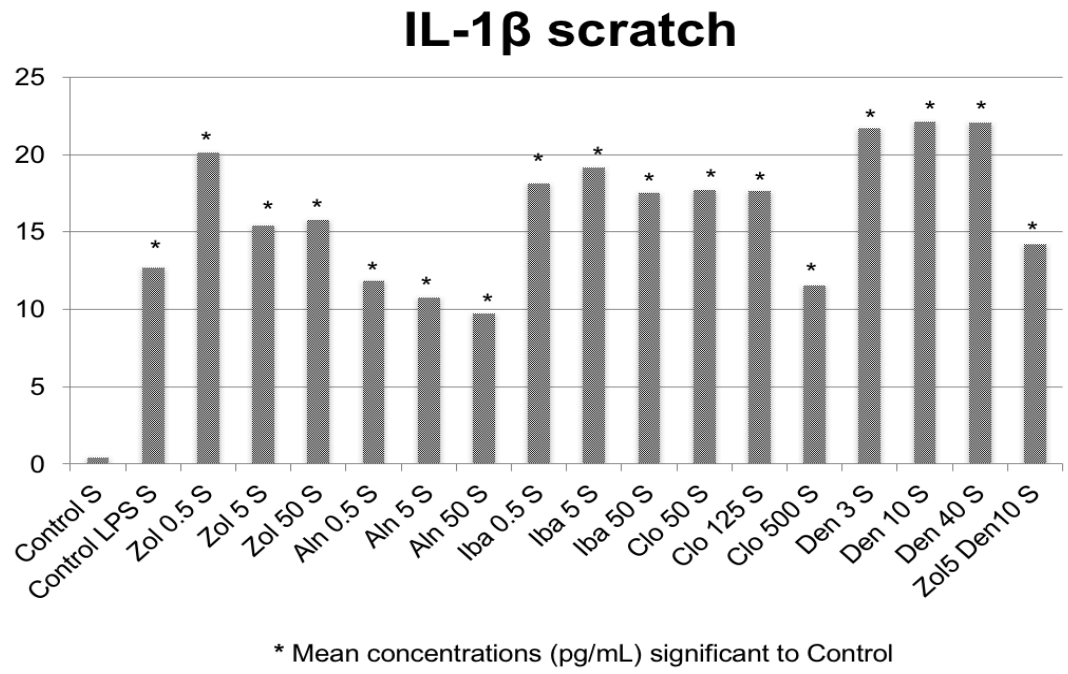

* Mean concentrations (pg/mL) significant to Control

B

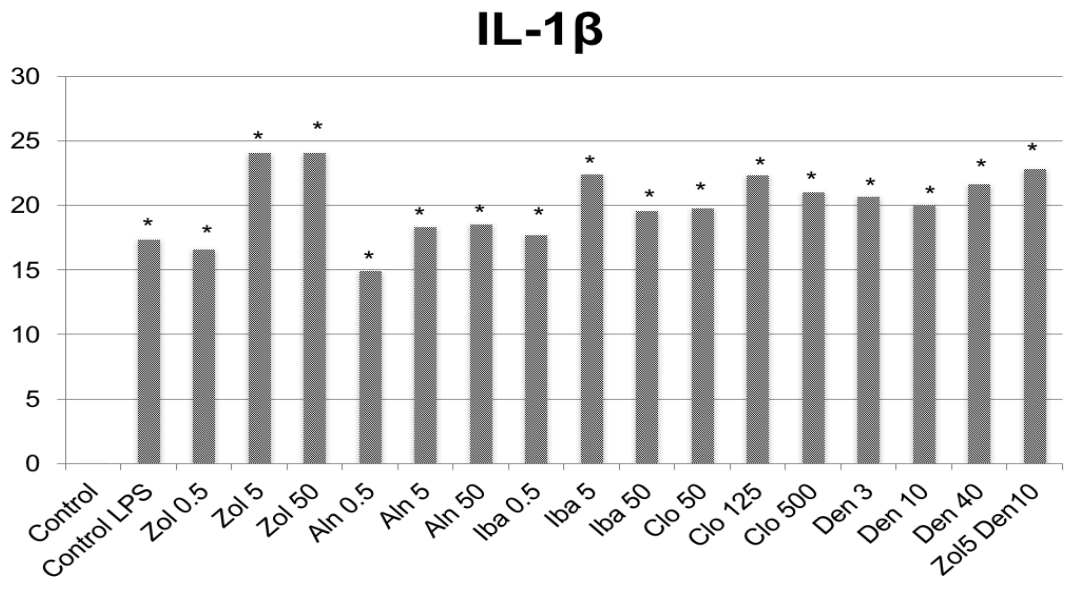

* Mean concentrations (pg/mL) significant to Control

Figure 18. IL-1β ELISA with (A) and without scratch (B). LPS = lipopolysaccharide; Zol = zoledronate; Aln = alendronate; Iba = ibandronate; Clo = clodronate; Den = denosumab.

A

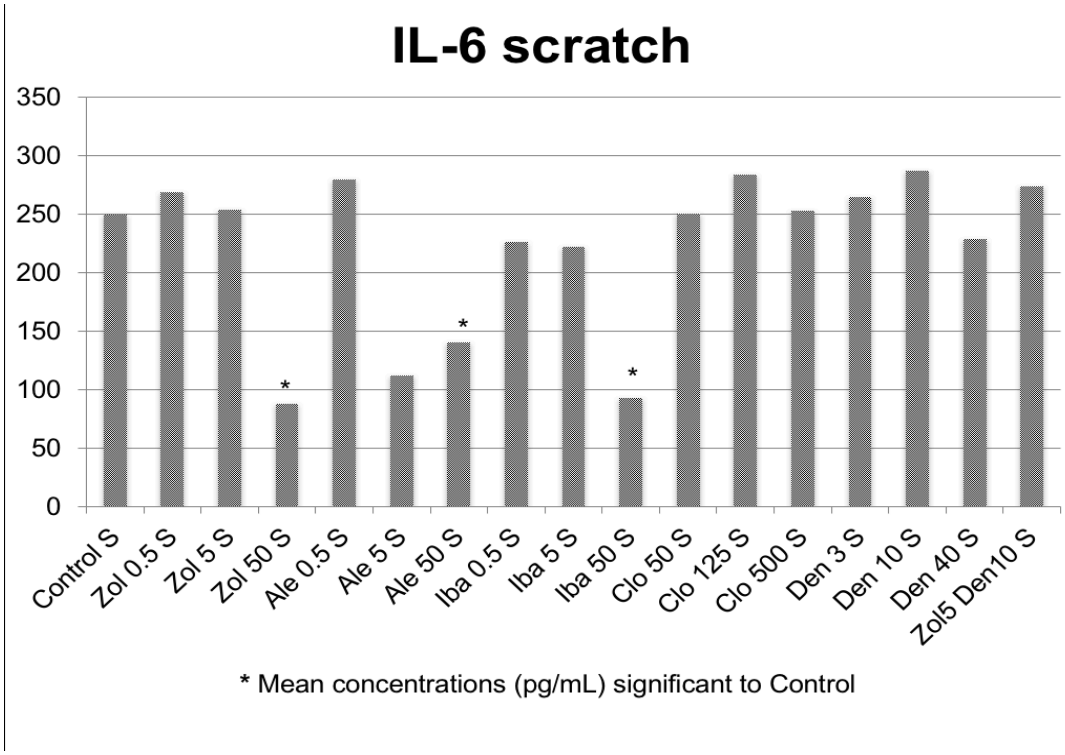

B

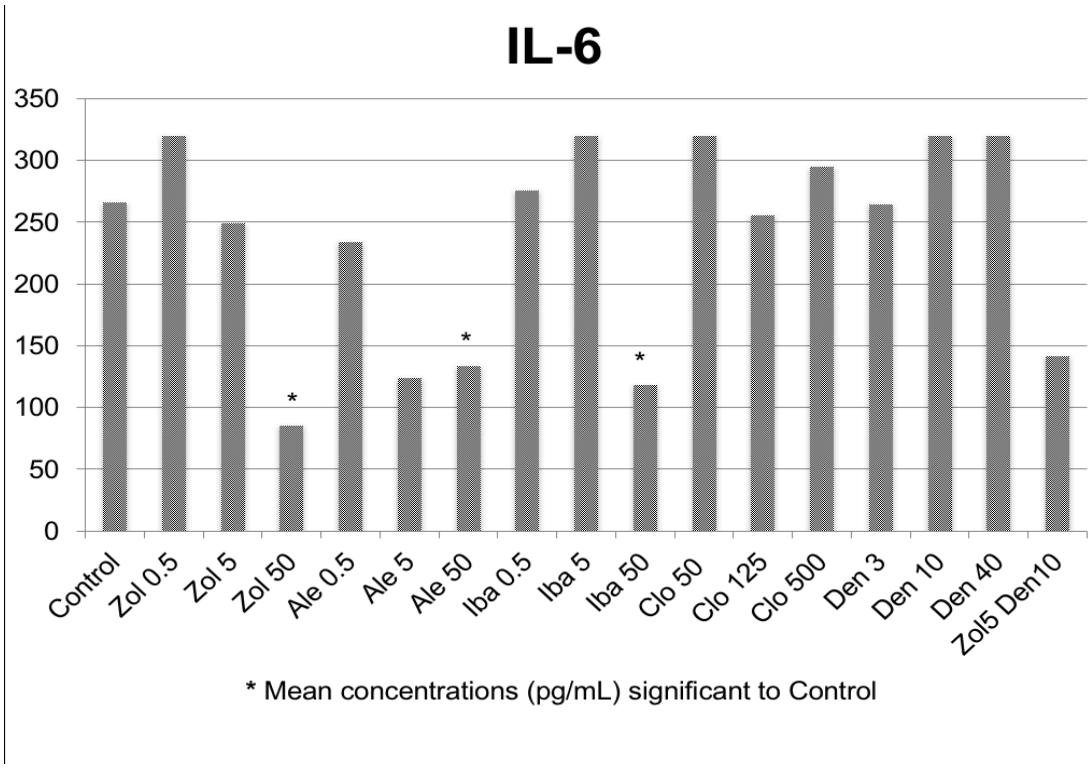

Figure 19. IL-6 ELISA with (A) and without scratch (B). LPS = lipopolysaccharide; Zol = zoledronate; Aln = alendronate; Iba = ibandronate; Clo = clodronate; Den = denosumab.

A

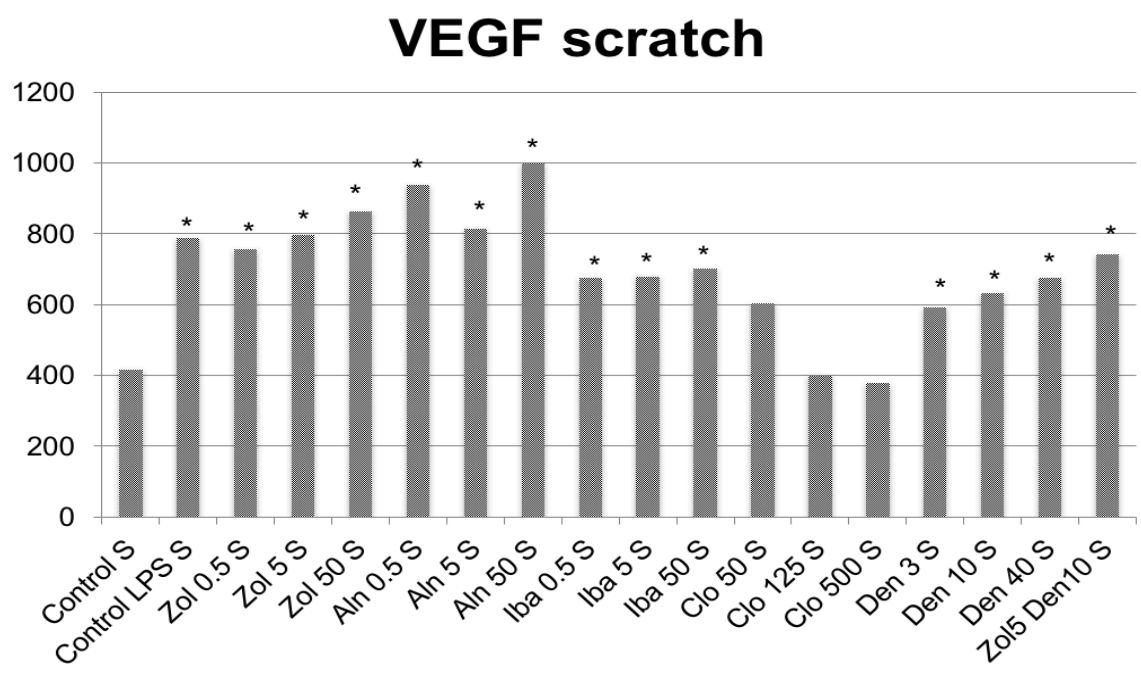

* Mean concentrations (pg/mL) significant to Control

B

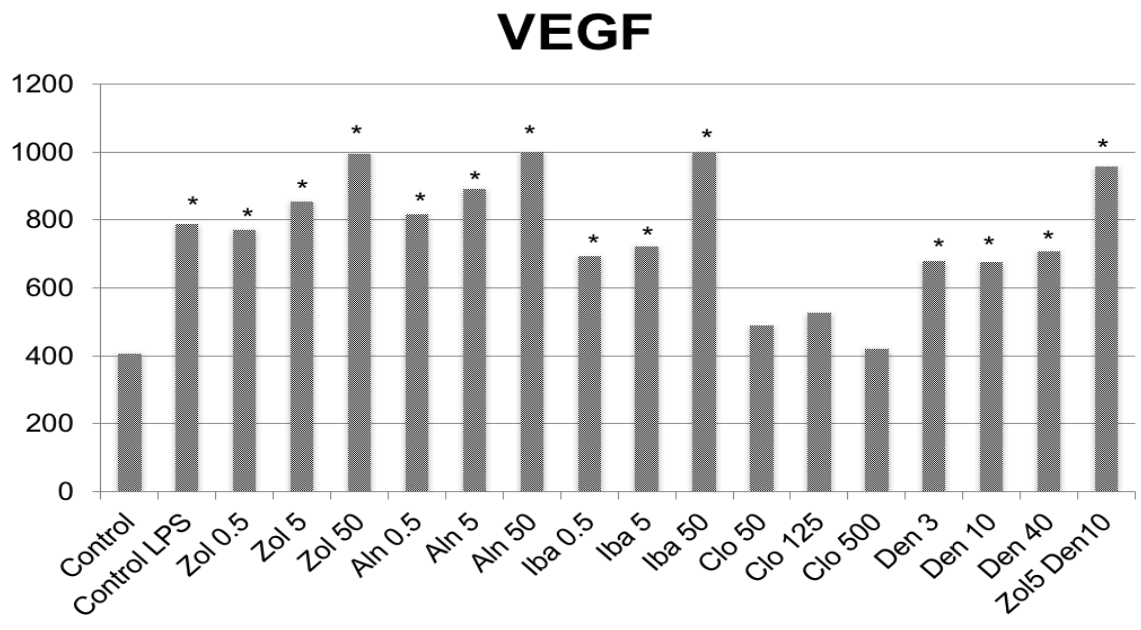

* Mean concentrations (pg/mL) significant to Control

Figure 20. VEGF ELISA with (A) and without scratch (B). LPS = lipopolysaccharide; Zol = zoledronate; Aln = alendronate; Iba = ibandronate; Clo = clodronate; Den = denosumab.

Part II Histologic examination

3.11 Patient groups and histologic bone samples

A total of 158 bone samples were collected from 107 patients with BRONJ (32/107), DRONJ (4/107), Mixed ONJ (8/107), bone exposed to BP (BP-exposed; 24/107), bone exposed to BP and denosumab (BPDN-exposed; 5/107), ORN (10/107), osteoporosis (7/107), OM (8/107), and bone from healthy individuals (9/107). Two patients with necrotic bone secondary to other chemotherapies (1/107) and transplanted bone (1/107) were excluded from the analysis due to small patient group size. Patients in the osteoporosis group and DRONJ group were not previously exposed to antiresorptive therapies. The majority of bone samples were obtained from the right mandible (n=53) and left mandible (n=44), with others from the left (n=29) and right maxilla (n=21). Of the bone biopsies from patients with BRONJ, DRONJ, and Mixed ONJ, 46 samples were labelled as border bone, 26 were labelled as sequestrum bone, and 5 as newly formed bone.

3.12 Antiresorptive dosing

The mean duration of BP or denosumab therapy was 28.08 months (range: 1-181 months) with a total average of 17.0 non-oral doses (range: 1-123 doses) and 7.86 oral doses (range: 1-144 doses; Table 6). The BP-exposed and BRONJ group had the longest mean duration of antiresorptive treatment with 47.5 months (range: 4-144 months) and 44.1 months (range: 2-181 months), respectively. The BRONJ (29.7 doses; range 1-123 doses) and Mixed ONJ (29.4 doses; range: 1-62 doses) groups demonstrated the highest mean number of

non-oral doses, while the BPDN-exposed group exhibited the longest duration of oral doses (18 months; range: 0-48 months).

Disease group	Mean months of antiresorptive treatment (range)	Mean number of non-oral doses (range)	Mean months of oral doses (range)
BRONJ	44.1 ± 42.8 (2-181)	29.7 ± 30.8 (1-123)	10.5 ± 20.3 (0-72)
DRONJ	13.8 ± 10.7 (1-24)	14.0 ± 11.0 (1-25)	-
Mixed ONJ	37.8 ± 23.8 (14-77)	29.4 ± 21.5 (1-62)	6.0 ± 14.6 (0-42)
BP-exposed	47.5 ± 36.7 (4-144)	25.3 ± 22.9 (1-72)	15.5 ± 37.3 (0-144)
BPDN-exposed	33.0 ± 26.7 (3-54)	2.6 ±2.7 (1-7)	18.0 ± 24.7 (0-48)

Table 6. Mean duration and number of antiresorptive doses for antiresorptive-related disease groups. BRONJ = bisphosphonate-related osteonecrosis of the jaw; DRONJ = denosumab-related osteonecrosis of the jaw; Mixed ONJ = bisphosphonate and denosumab osteonecrosis of the jaw; BP-exposed = bone exposed to bisphosphonates; BPDN-exposed = bone exposed to bisphosphonates and denosumab.

3.13 Clinical characteristics of patients treated with antiresorptives

Patient were treated with antiresorptives for primary diagnoses of breast cancer (n=26), prostate cancer (n=16), osteoporosis (n=17), multiple myeloma (n=4), and other cancer (n=16). Patients received zoledronate (n=49), alendronate (n=14), denosumab (n=12), ibandronate (n=12), pamidronate (n=3), and risendronate (n=3). A total of 84 patients received intravenous administration of

BPs, and 24 patients received oral BPs. The 12 patients who received denosumab were administered the medication via subcutaneous injection. Out of 81 patients asked about the presence of pain, 29 patients reported pain at the clinical visit. The onset of osteonecrosis was mostly associated with dental extractions (n=28) or pressure sores from dental prostheses (n=15), while in 13 patients another association was reported (i.e., implantitis, periodontitis, or spontaneous onset). A total of 16 patients were classified as Stage 3 MRONJ, 28 patients as Stage 2, and only 1 patient as Stage 1. Complete healing (no exposed or probeable bone with no complaint of pain) was reported in 29 patients, and no healing was observed in 66 patients.

3.14 H&E stain findings

Mixed ONJ, ORN, BRONJ, and DRONJ exhibited more infectious infiltration compared to healthy and osteoporosis groups which had no signs of infection. Bone exposed to BP exhibited the most pseudoepithelial changes. Mixed ONJ and BRONJ exhibited more granulation tissue along with pseudoepitheliomatous hyperplasia in non-necrotic lesions. Osteoporosis, OM, and BPDN-exposed exhibited more fibrous tissue; in the osteoporosis group the appearance was more organized. Mixed ONJ and BRONJ also demonstrated more areas of scallopped resorption.

3.15 RANKL stain findings

The mean RANKL stain positivity was highest for BRONJ (2.22) and Mixed ONJ (1.75), and lowest for BP-exposed (0.59), DRONJ (0.43), and Healthy (0.53; Tables 7 and 8). This was statistically significant for BRONJ ($p = .021$) when compared to the healthy group.

3.16 TRAP stain findings

The mean TRAP stain positivity was highest for Mixed ONJ (2.88), BRONJ (2.60), and BP-exposed (1.83), and lowest for Healthy (0.38). This was

statistically significant for Mixed ONJ (p = .002), BRONJ (p < .001), and BP-exposed (p = .017) when compared to the healthy group. The mean number of osteoclasts positive for TRAP stain per view was highest for Mixed ONJ (0.78) and BRONJ (0.63), and lowest for Healthy (0.11) and OM (0.011). This was statistically significant for Mixed ONJ (p = .041), BRONJ (p = .034) when compared to the healthy group.

3.17 OPG stain findings

The mean OPG positivity was highest for DRONJ (2.89) and Mixed ONJ (2.75) and lowest for Healthy (1.00) and ORN (1.14).

	BRONJ	**Mixed ONJ**	**DRONJ**	**BP-exposed**	**BPDN-exposed**
RANKL Mean Positivity (0-8)	2.22**	1.75	0.43	0.69	0.80
TRAP Mean Positivity (0-8)	2.60**	2.88**	0.77	1.83**	1.40
TRAP Mean Number of Osteoclasts per View	0.63**	0.78**	0.14	0.30	0.17
OPG Mean Positivity (0-8)	1.89	2.75	2.89	2.26	1.57
Mean Osteocyte Lacunae per μm^2	0.00036	0.00034	0.00026 ***	0.00033 ***	0.00029 ***
CD14 Mean Positivity (0-8)	2.59**	2.13	0.80	1.09	2.37
CD68 Mean Positivity (0-8)	4.30**	4.73**	0.97	2.21	2.06
Mean Percent Medullary Space to Bone	13.78**	12.30**	19.69	10.40**	9.63**
Mean Width of Osteoid Trabeculae (μm)	434.81	601.71**	504.75	476.96	654.36

Table 7. Histologic and histomorphometric findings of bone samples for BRONJ, Mixed ONJ, DRONJ, BP-exposed, and BPDN-exposed groups. ** indicates statistical significance p < .05 when compared to Healthy or * compared to Osteoporosis. BRONJ = bisphosphonate-related osteonecrosis of the jaw; Mixed ONJ = mixed osteonecrosis of the jaw;**

DRONJ = denosumab-related osteonecrosis of the jaw; BP-exposed = bisphosphonate-exposed bone; BPDN-exposed = bisphosphonate and denosumab-exposed bone; RANKL = receptor activator of nuclear factor kappa-B ligand; TRAP = tartrate-resistant acid phosphatase; OPG = osteoprotegerin.

	ORN	OM	OP	Healthy
RANKL Mean Positivity (0-8)	0.77	0.75	1.51	0.53
TRAP Mean Positivity (0-8)	0.87	0.87	1.69	0.38
TRAP Mean Number of Osteoclasts per View	0.50	0.11	0.46	0.11
OPG Mean Positivity (0-8)	1.14	1.60	1.33	1.00
Mean Osteocyte Lacunae per μm^2	0.00029***	0.00033	0.00041	0.00032
CD14 Mean Positivity (0-8)	1.59	0.56	2.71**	0.69
CD68 Mean Positivity (0-8)	2.00	1.51	2.37	0.78
Mean Percent Medullary Space to Bone	10.92**	9.03**	18.15**	28.09
Mean Width of Osteoid Trabeculae (μm)	460.69	434.63	336.74	259.07

Table 8. Histologic and histomorphometric findings of bone samples for ORN, OM, OP, and Healthy groups. ** indicates statistical significance p < .05 when compared to Healthy or * compared to Osteoporosis. ORN = osteoradionecrosis; OM = secondary osteomyelitis; OP = primary osteoporosis; RANKL = receptor activator of nuclear factor kappa-B ligand; TRAP = tartrate-resistant acid phosphatase; OPG = osteoprotegerin.**

3.18 Toluidine blue stain findings

DRONJ (0.000090; p = .007; Figure 21), BP-exposed (0.000103; p = .028), BPDN-exposed (0.000118; p = 0.022), and ORN (0.000050; p = 0.004) demonstrated statistically significantly fewer osteocyte lacunae per μm^2 compared to Osteoporosis (0.000171; Figures 22 and 23). The blood supply by Haversian systems exhibited no significant differences (Figure 24). There was even a tendency for a higher Haversian canal density in DRONJ, BRONJ and Mixed ONJ sample groups with intact blood vessels observed. The bony structures appeared more unorganized in MRONJ disease variants with the presence of higher numbers of bony reversal lines compared to Osteoporosis or Healthy (Figure 25).

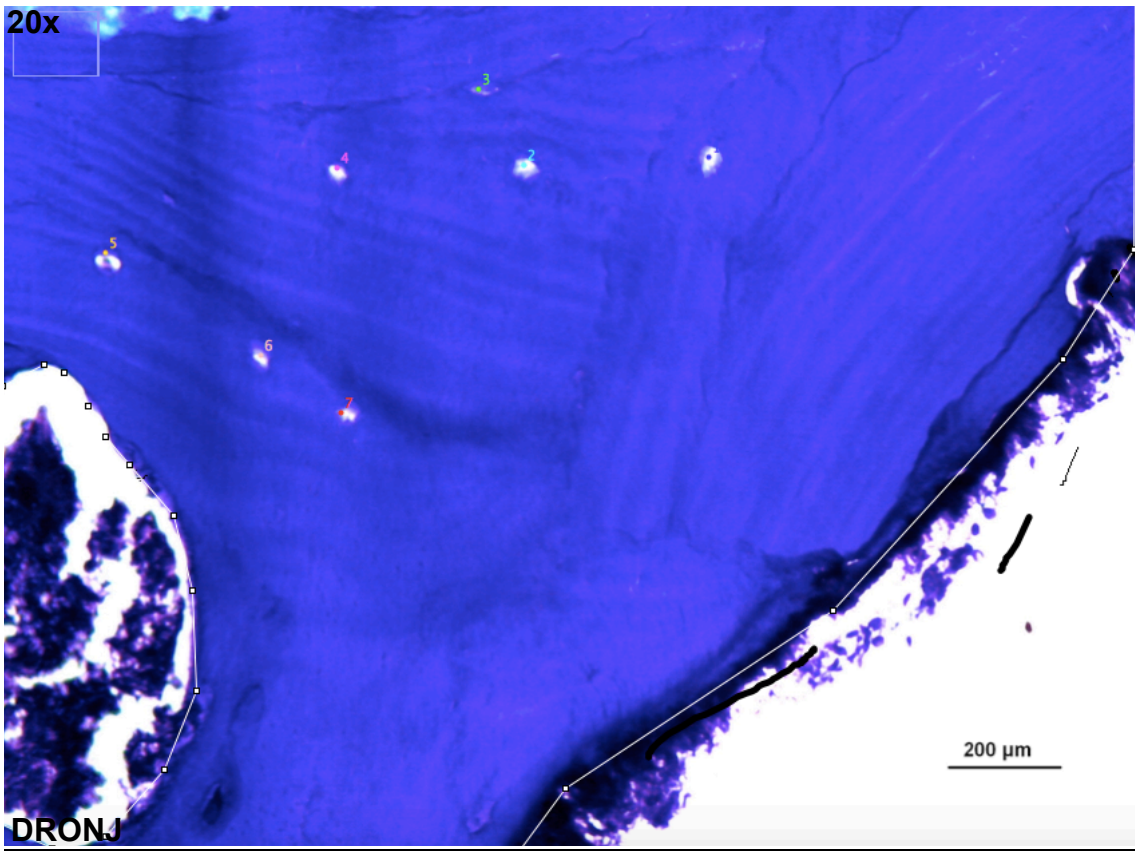

Figure 21. Toluidine blue staining of an outlined area of bone fragment in a patient with denosumab-related osteonecrosis of the jaw demonstrating

numbered sparse, empty osteocyte lacunae with bacteria rimming. 20x magnification.

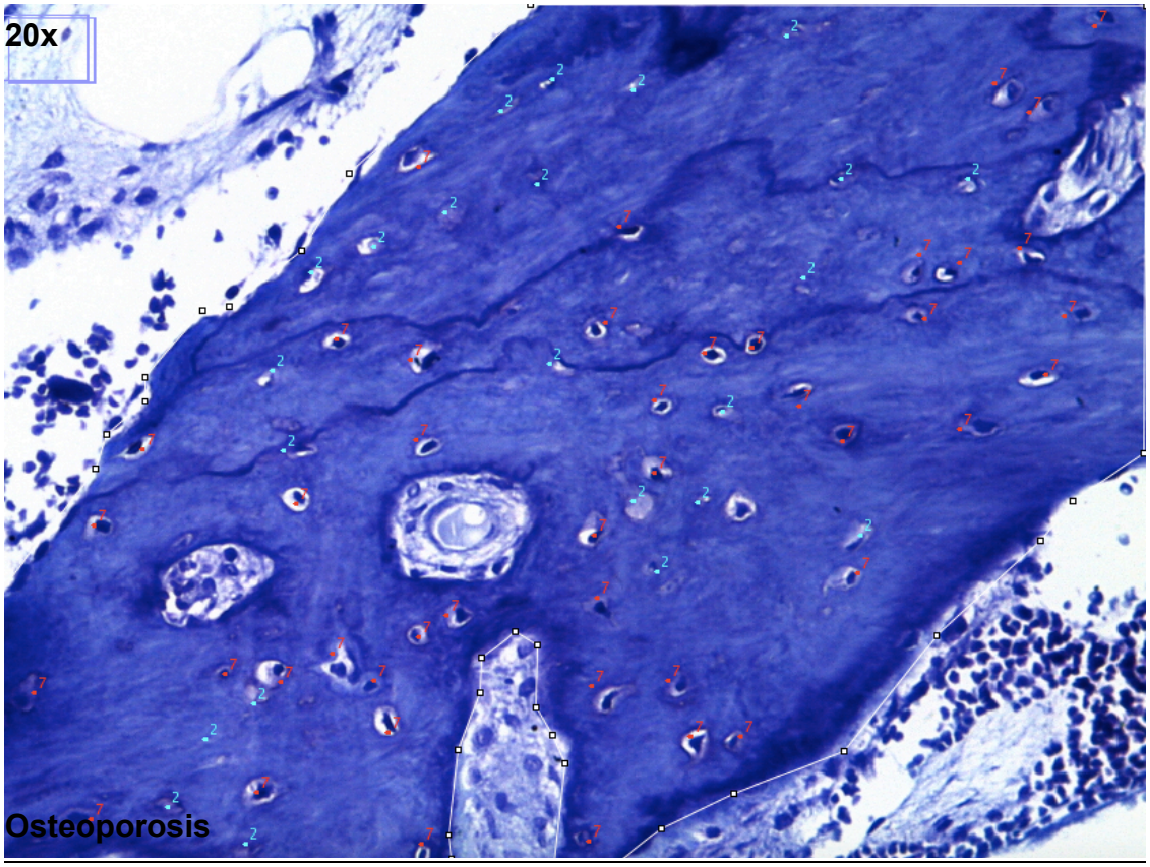

Figure 22. Toluidine blue staining of an outlined area of bone fragment in an patient with osteoporosis demonstrating numbered osteocyte lacunae with the majority containing living osteocytes. 20x magnification.

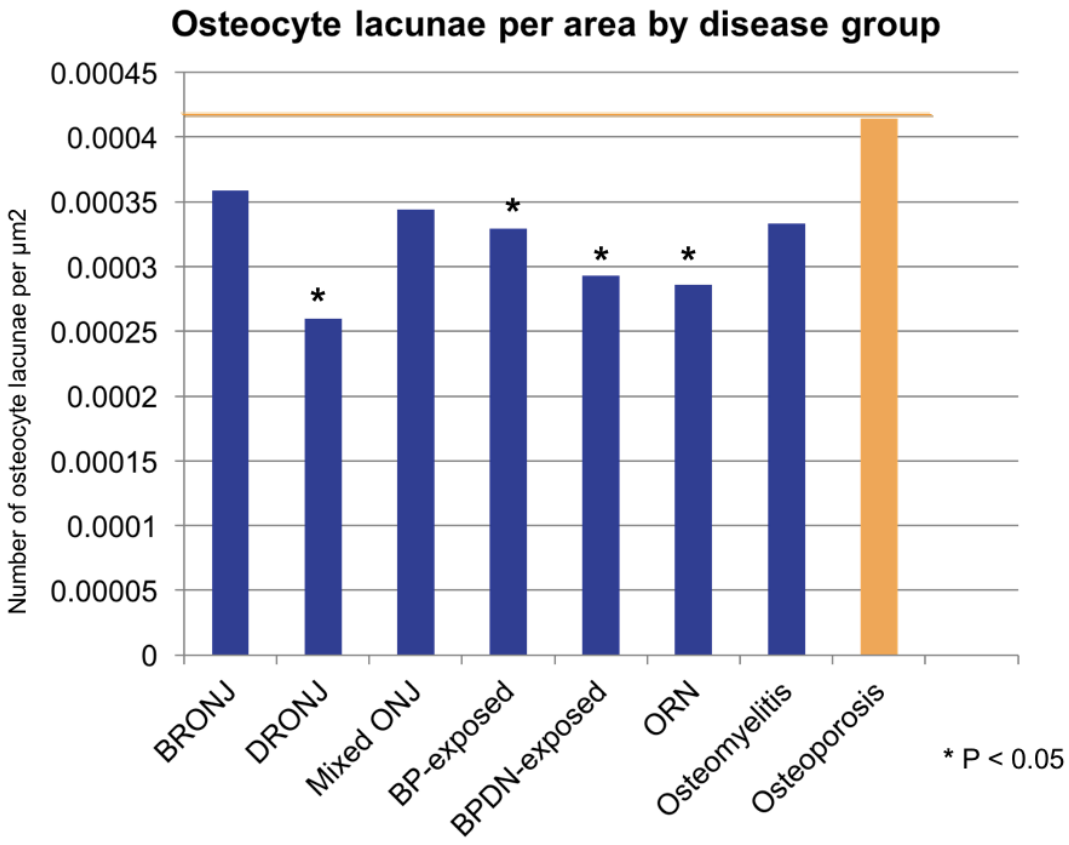

Figure 23. Number of osteocyte lacunae per µm^2 by disease group. Asterisk indicates significance p < .05 compared to the osteoporosis group. BRONJ = bisphosphonate-related osteonecrosis of the jaw; DRONJ = denosumab-related osteonecrosis of the jaw; ONJ = osteonecrosis of the jaw; BP = bisphosphonate; DN = denosumab; ORN = osteoradionecrosis.

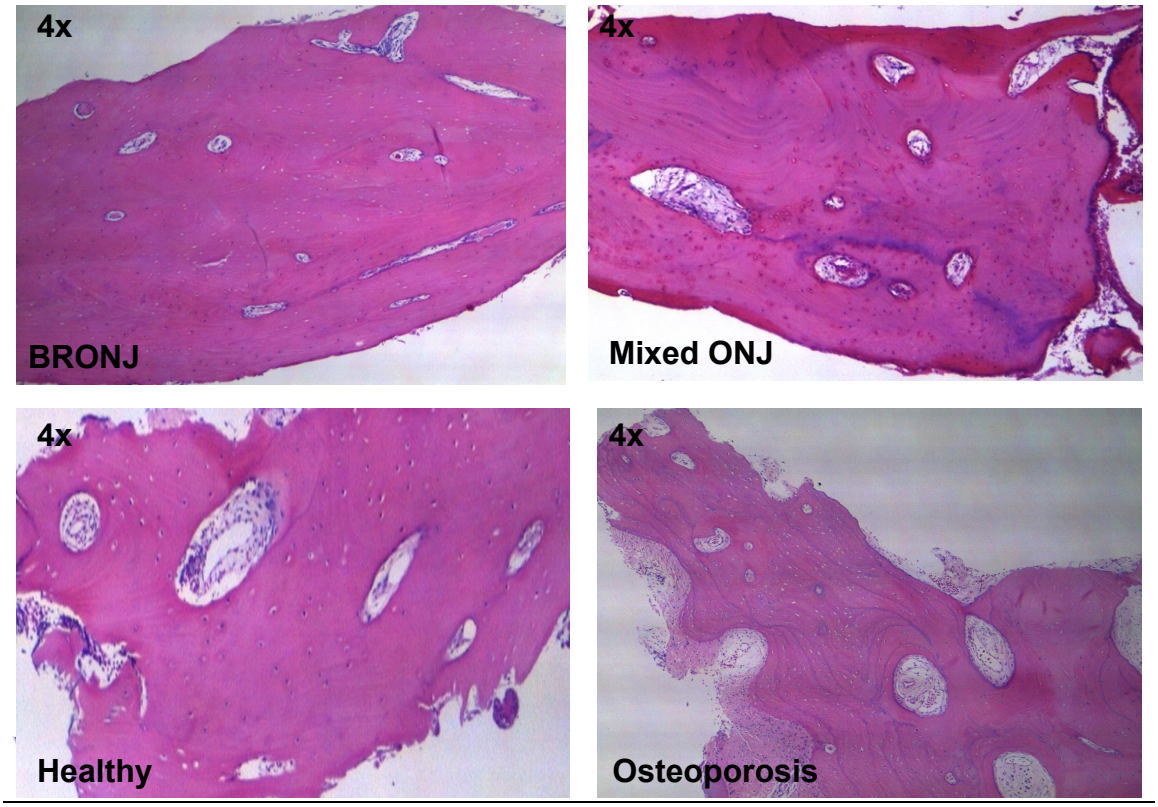

Figure 24. Hematoxylin and eosin staining of Haversian canal architecture in bone samples of bisphosphonate-related necrosis of the jaw and mixed necrosis of the jaw compared to healthy and osteoporosis groups. 4x magnification. BRONJ = bisphosphonate-related osteonecrosis of the jaw; ONJ = osteonecrosis of the jaw.

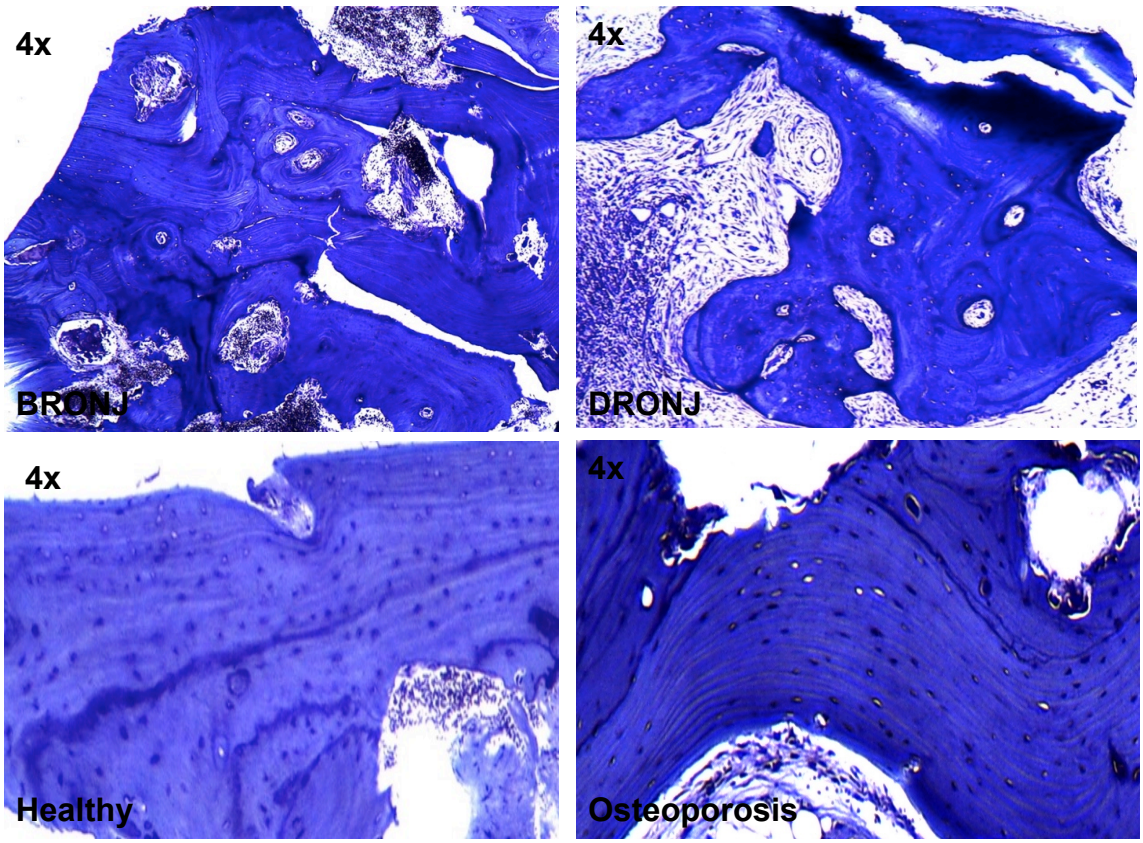

Figure 25. Toluidine blue staining of disorganized bone remodeling in bisphosphonate- and denosumab-related osteonecrosis of the jaw compared to healthy and osteoporosis disease groups. 4x magnification.

3.19 CD14 stain findings

The mean CD14 positivity was highest for Osteoporosis (2.71) and BRONJ (2.59), and lowest for OM (0.56) and Healthy (0.69). This was statistically significant for Osteoporosis ($p = .044$) and BRONJ ($p = .008$) when compared to the healthy group.

3.20 CD68 stain findings

The mean CD68 macrophagic cell positivity was highest for Mixed ONJ (4.73) and BRONJ (4.30), and lowest for Healthy (0.71). This was statistically significant for Mixed ONJ ($p = .001$) and BRONJ ($p < .001$) when compared to the healthy group as well as to the osteoporosis group.

3.21 Micro-CT measurements

Healthy bone demonstrated the highest mean percentage of medullary space to bone (28.09%), while OM (9.03%), BPDN-exposed (9.63%), BP-exposed (10.40%), ORN (10.92%), Mixed ONJ (12.30%), BRONJ (13.78%), Osteoporosis (18.15%) and DRONJ (19.69%) all demonstrated a significant decrease in the ratio of medullary space to bone (Figure 26). This was statistically significant for OM ($p < .001$), BPDN-exposed ($p = .001$), BP-exposed ($p < .001$), ORN ($p < .001$), Mixed ONJ ($p < .001$), BRONJ ($p < .001$), and Osteoporosis ($p = .030$). Osteonecrotic disease variants exhibited an increased mean trabecular width with BPDN-exposed (654.36 μm), Mixed ONJ (601.71 μm), DRONJ (504.75 μm), BP-exposed (476.96 μm), ORN (460.69), and BRONJ (434.81 μm), while Healthy (259.07 μm) exhibited the narrowest trabecular width. This was statistically significant for Mixed ONJ ($p = .033$). Of the bone biopsies from patients with BRONJ, DRONJ, and Mixed ONJ, 46 samples were labelled as border bone, 26 were labelled as sequestrum bone, and 5 as newly formed bone. Analysis was performed both including and excluding sequestrum bone samples, but no significant difference was observed. The presented values above include sequestrum bone samples.

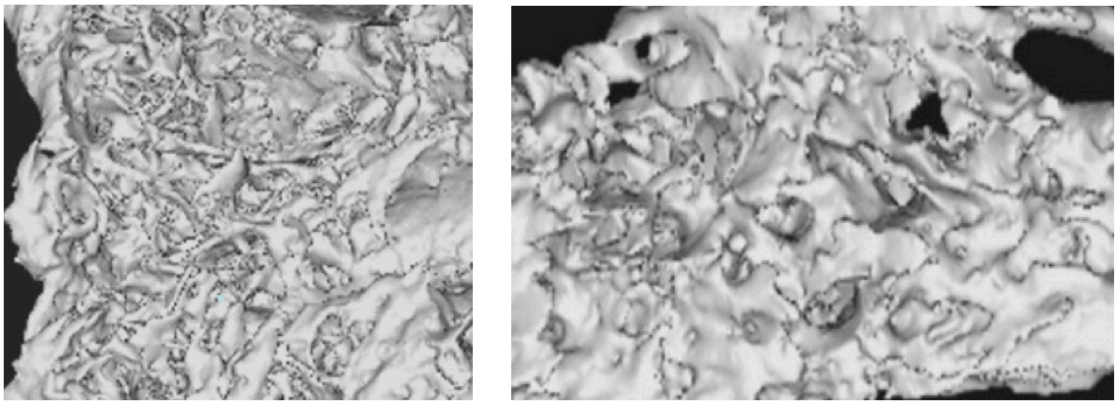

Figure 26. Micro-computed tomography 3D reconstructions of bone samples from a patient with osteoporosis (left) compared to a patient diagnosed with denosumab-related osteonecrosis of the jaw exhibiting thickened plate-like bone trabeculae (right).

Part III Radiographic evaluation

3.22 Patient population

A total of 37 patients (20 females and 17 males) age 44 to 92 years old were diagnosed with BRONJ (n=28), DRONJ (n=6), and Mixed ONJ (n=3), with the majority at stage 2 (n=27) and stage 3 (n=9; Table 9). A total of 22 patients reported pain upon clinical examination. Patients were treated with antiresorptives for primary diagnoses of breast cancer (14/37), prostate cancer (10/37), multiple myeloma (7/37), osteoporosis (3/37), and other (3/37). A total of 28 patients reported concurrent chemotherapies, and 11 patients were taking opioid medications at the time of the first visit. Five patients reported a smoking history, while 32 were non-smokers.

3.23 Clinical characteristics

The onset of osteonecrosis was mostly associated with dental extractions (n=20) or pressure sores from dental prostheses (n=16), while in 8 patients another

association was reported (i.e., implantitis, periodontitis, or spontaneous onset). Necrotic sites were reported in the right mandible (n=22), left mandible (n=19), right maxilla (n=6), and left maxilla (n=4). Most patients were managed operatively (29/37) rather than non-operatively (8/37). The mean duration between the first visit and an operation was 136.7 ± 176.1 days (range: 84 to 622 days). Complete healing (no exposed or probeable bone with no complaint of pain) was observed in 19 patients, and non-healing was reported in 18 patients. Patients who received operative treatment were more likely to be healed compared to patients who received non-operative treatment ($p = .001$), even when controlling for MRONJ stage, pain, and number of non-oral and oral doses.

3.24 Antiresorptive dosing

The total mean number of non-oral doses was 27 doses (range: 1-100 doses), with 26.3 ± 22.1 doses (range: 1-100 doses) for BRONJ, 10.8 ± 9.9 doses (range: 1-25 doses) for DRONJ, and 29.0 ± 26.2 doses (range: 1-51 doses) for Mixed ONJ. The mean duration of oral doses was 7 months (range 3-84 months), with 4.4 ± 16.5 months (range: 0-84 months) for BRONJ and 34.0 ± 48.0 months (range: 0-68 months) for Mixed ONJ. The majority of patients were treated with zoledronate (27/37) and denosumab (8/37), while others were treated with alendronate (3/37), risendronate (2/37), pamidronate (2/37), and ibandronate (2/37). Antiresorptives were administered intravenously (27/37), orally (5/37), and via subcutaneous injection for denosumab (8/37).

3.25 Imaging findings

Necrotic lesions were imaged with panoramic radiograph (n=134), CBCT (n=30), bone scintigraphy (n=18), CT (n=11), and MRI (n=1). We excluded MRI from the follow-up analysis due to the small sample size. The mean duration of radiographic follow-up was 654.2 ± 417.6 days (range: 163-1990 days). The most reported radiographic signs (Figure 27) were cancellous bone sclerosis (34/37), cortical bone sclerosis (32/37), cortical bone erosion (32/37; Figure 28), persistent

extraction sockets (26/37; Figure 29), sequestrum (24/37; Figure 30), thickened lamina dura (24/37), bony fistula (17/37), activity on bone scintigraphy studies (11/37), inferior alveolar nerve canal changes (10/37), maxillary sinus involvement (7/37), jaw bone fracture (4/37), and cervical lymph node involvement (2/37). There were no obvious differences in radiographic findings with regard to antiresorptive type, MRONJ disease variant, presence of pain, and healing. More radiographic findings were found in the mandible (p = .017).

	Number of patients		**Number of patients**
MRONJ type		**Primary disease**	
BRONJ	28	Breast cancer	14
DRONJ	6	Osteoporosis	3
Mixed ONJ	3	Prostate cancer	10
		Multiple myeloma	7
		Other cancer	3
Medications		**Stage**	
Zoledronate	27	1	1
Alendronate	3	2	27
Risendronate	2	3	9
Pamidronate	2	**Treatment**	
Ibandronate	2	Operative	29
Denosumab	8	Non-operative	8
Precipitating factor		**Healing**	

Extraction	20	Healed	19
Dentures	16	Not healed	18
Other	8		
Pain		**Smoking history**	
Yes	22	Yes	5
No	14	No	32

Table 9. Patient characteristics for medication-related osteonecrosis of the jaw disease variants, primary disease, antiresorptive type, staging, precipitating factor, presence of pain, smoking history, treatment type, and healing outcome. MRONJ = medication-related osteonecrosis of the jaw; BRONJ = bisphosphonate-related osteonecrosis of the jaw; DRONJ = denosumab-related osteonecrosis of the jaw.

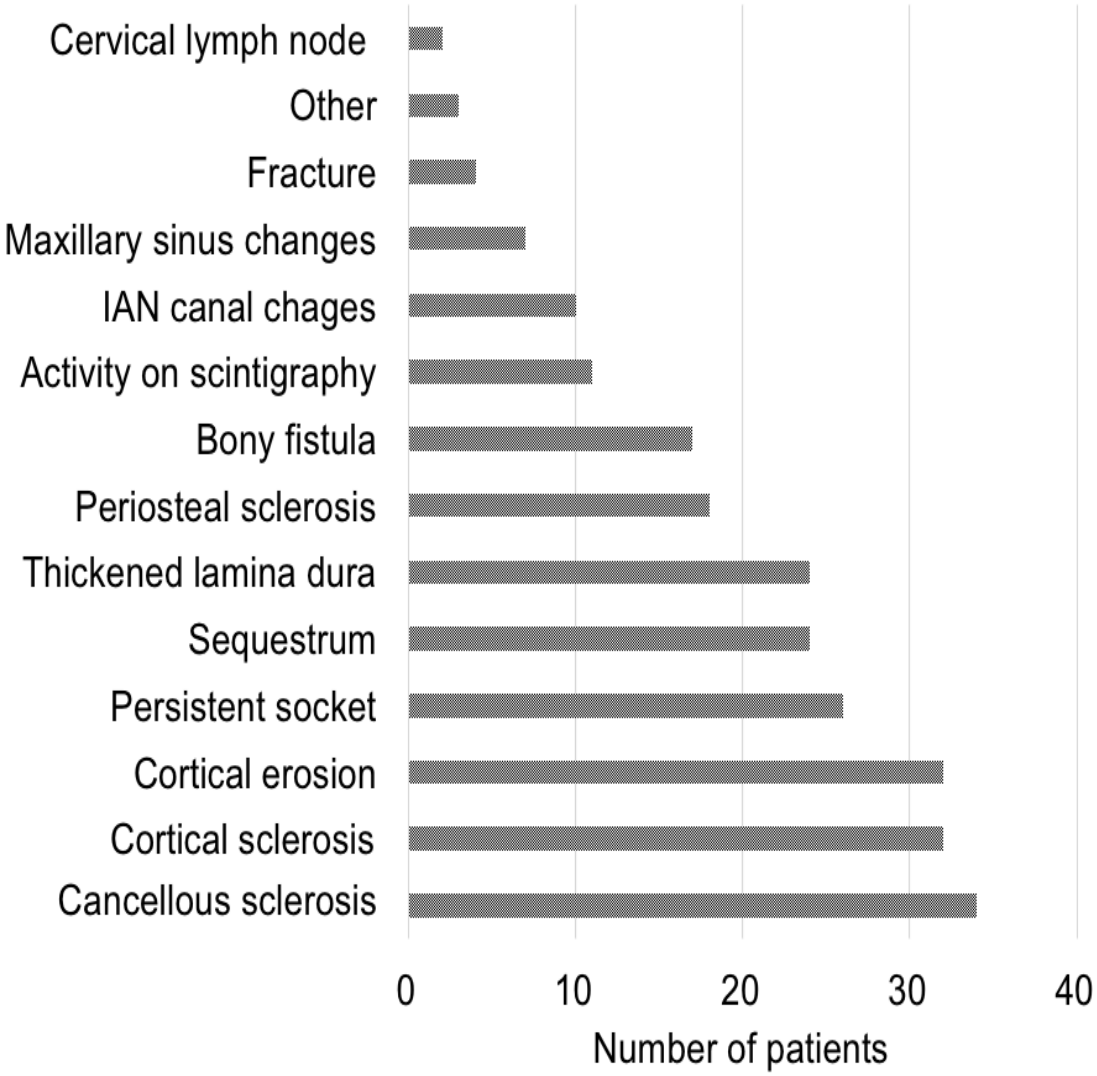

Figure 27. Most common imaging findings for patients diagnosed with medication-related osteonecrosis of the jaw. IAN = inferior alveolar nerve canal.

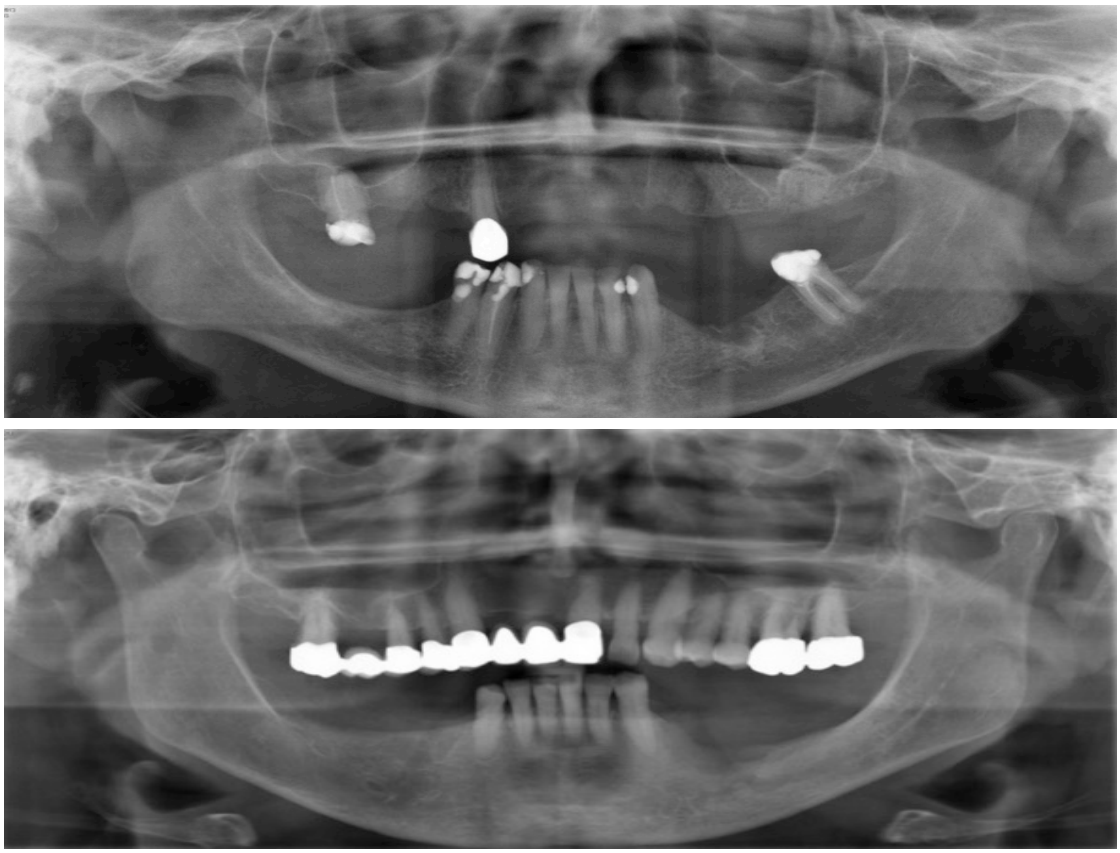

Figure 28. Cortical bone erosion of the left mandible in patients treated with zoledronate (upper) and denosumab (lower) as evidenced by panoramic radiograph imaging.

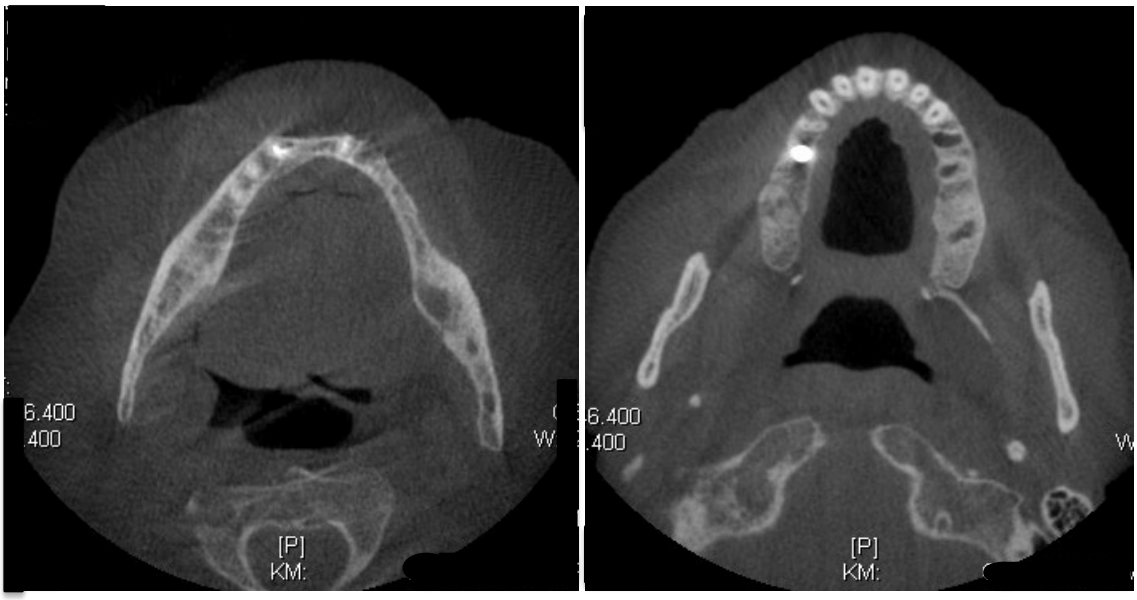

Figure 29. Persistent extraction sockets and bony fistula demonstrated on cone-beam computed tomography in a patient with bisphosphonate-related necrosis of the jaw in the right and left mandible (left) and a patient with denosumab-related necrosis of the jaw in the left and right maxilla (right).

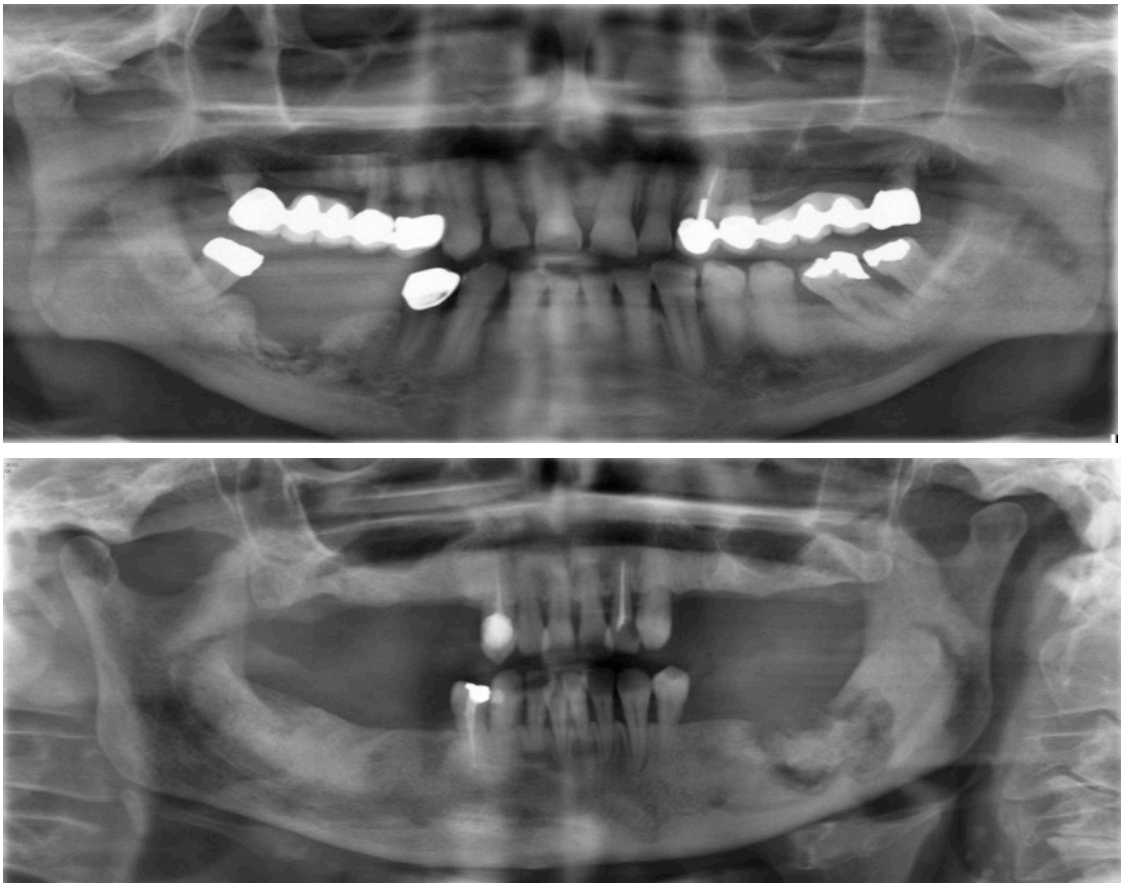

Figure 30. Bone sequestrum in the right mandible of a patient treated with zoledronate (upper) and in the left mandible of a patient treated with ibandronate, zoledronate, and risendronate (lower) as evidenced by panoramic radiograph imaging.

3.26 Comparison of imaging modalities

CBCT was better for visualizing bony fistula, fracture, and the extent of the sequestrum (68.2% detectability) compared to CT (30.8% detectability). CBCT detected 18.4% more findings than panoramic radiograph in intraindividual comparisons of simultaneous panoramic radiograph and CBCT studies (Figure 31). CBCT was particularly superior for denosumab patients with poor healing despite minimal radiographic signs, for which panoramic radiograph did not

demonstrate the extent of the lesion (Figure 32). CT was helpful for visualizing maxillary sinus involvement and cervical lymph node involvement. Panoramic radiograph was useful for visualizing bone sclerosis, although the extent was not as precise as 3D imaging modalities.

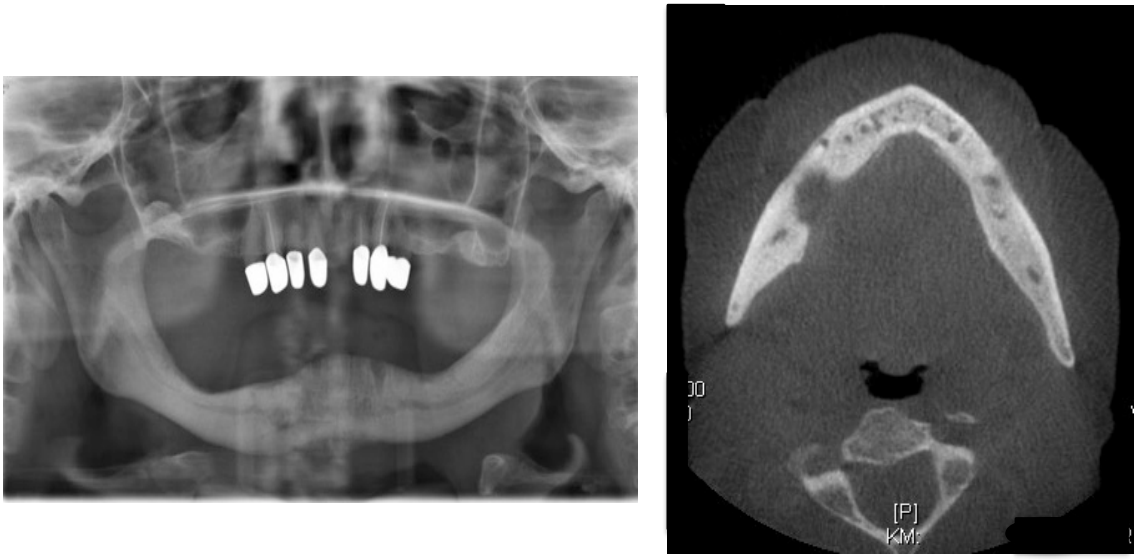

Figure 31. Intraindividual comparision of simultaneous panoramic film (left) and cone-beam computed tomography (right) in a patient with mixed osteonecrosis of the jaw demonstrating the superiority of the three-dimensional imaging modality in detailing the extent of cortical bone erosion in the right mandible from the lingual to buccal plate.

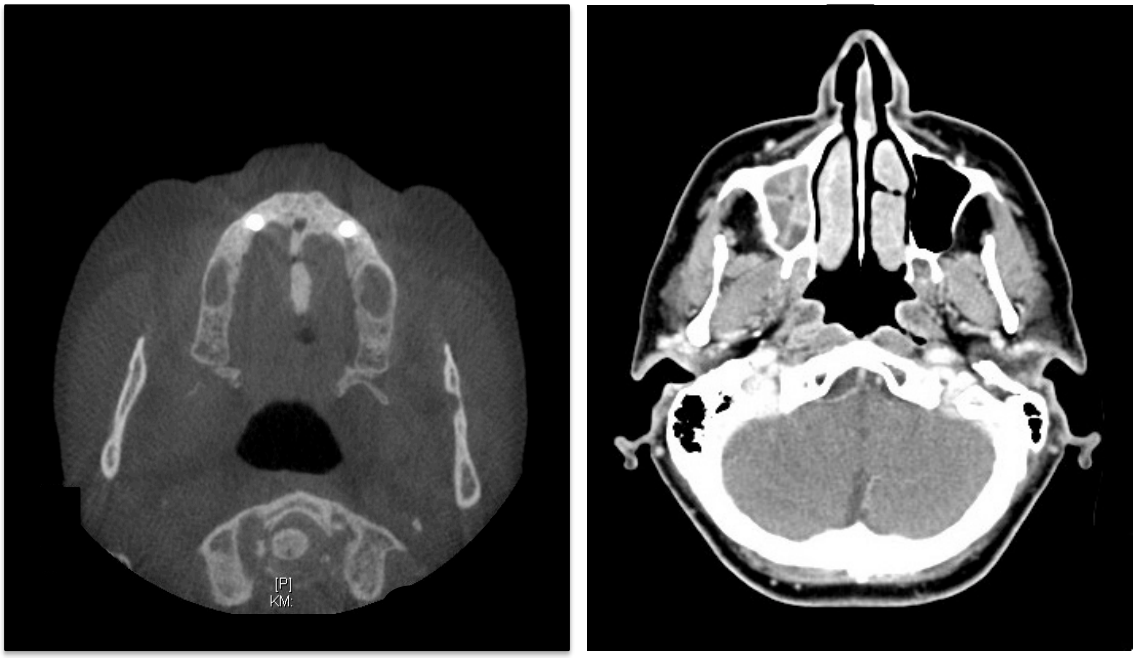

Figure 32. Two patients with denosumab-related osteonecrosis of the jaw. Cone-beam computed tomography demonstrating bony fistula in necrotic sites in the right maxilla (left). Conventional computed tomography of a patient with maxillary sinus involvement associated with a site of osteonecrosis in the right maxilla (right).

3.27 Radiographic changes over time

Patients who received operative treatment were more likely to exhibit improved or stable sequestrum lesions ($p = .024$), even when controlling for age ($p = .011$) and presence of pain ($p = .014$). Patients in the operative group were also more likely to have improved or stable bony fistulas compared to non-operatively managed patients ($p = .015$), even when controlling for age. The improvement or worsening of other radiographic findings such as persistent extraction socket, cortical bone erosion, cortical bone sclerosis, cancellous bone sclerosis, periosteal sclerosis, and thickened lamina dura did not exhibit a dependency on having had operative treatment. An attempt was made to describe the general improvement or worsening of radiographic signs at 6 month, 12 month, 24

month, and overall follow-up, but our follow-up data was not statistically sufficient.

4 Discussion

Although the first incidence of MRONJ was described over fifteen years ago with zoledronate[10], the pathogenesis of the disease continues to be a subject of debate. As a result, there is no consensus on a unified treatment or prevention paradigm. Treatment of MRONJ is difficult and costly, and disease sequela can include pain, infection, inability to eat, extraoral fistula, and pathologic fracture, all of which significantly impact the quality of life for patients.[8, 9] This doctoral project aimed to provide a more profound picture of how BPs and denosumab could influence the expression patterns of HGFs and participating cells in MRONJ *in vitro*, while also including retrospective histologic and radiographic studies to correlate the altered bone structure with different disease variants and degree of antiresorptive exposure.

Our research found that fibroblast cell death and delayed wound healing was observed after administration of antiresorptives, in particular with high and medium concentrations of nitrogen-containing BPs. This was increased by the introduction of bacterial LPS and a co-culture with a THP-1 mononuclear cell line. There was also evidence of an alteration in the immune response, with an elevated immune reaction and possible dysfunction as a result of antiresorptive exposure. In both the cellular assays with gingival fibroblasts and the histologic study, we noted some effects of altered osteoclast activation and inhibition through RANKL and OPG, although with no evidence of an anti-angiogenic influence (Figure 33). Upon examination of the bone tissues in the histologic and radiographic study, results suggested that a limited osteocyte network and over-ossification of the bone could play in a role in MRONJ. Many of these findings could have important implications

for researchers investigating MRONJ and provide clinical relevance for treating practioners.

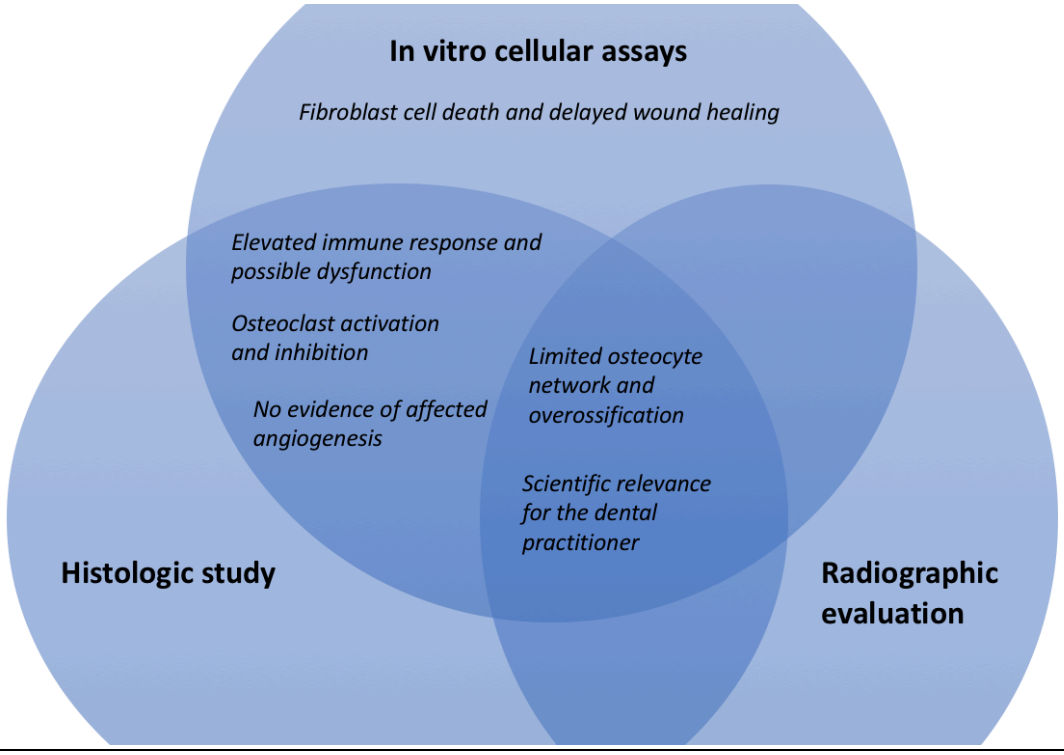

Figure 33. Key research findings and their interconnections in the *in vitro* cellular assays, histologic study, and radiographic evaluation.

4.1 Fibroblast cell death and delayed wound healing

In experiments with gingival fibroblasts, we found that these cells of the soft tissue were susceptible to certain antiresorptive medications at high and medium concentrations. Additional concentrations were affected with the introduction of LPS and a further co-culture experiment with THP-1 cells, including low concentrations of BP and combinations of zoledronate and denosumab, respectively. Live/Dead staining results confirmed xCELLigence adherence curves, and a reduction of adherence was associated with HGF cell death dose-dependently. Scanning electron microscopy also further displayed the drastically

altered morphology of HGFs and the deterioration of the fibroblast cell layer exposed to antiresorptives.

Although MRONJ is primarily considered a bone lesion, defective or delayed oral mucosa epithelialization raises the question of the role of soft tissue in disease pathogenesis.[86] As BPs are renally excreted after a few hours in circulation, the medication concentration in tissues outside bone should theoretically be minimal.[87] However, apoptosis and decreased proliferation have been observed in several cell types including cervical, prostate, and intestinal epithelial cells after exposure to BPs *in vitro*.[88-90] Reported clinical effects include chemical esophagitis and ulceration occurring in patients who suck on BP tablets.[91, 92] How BPs in saliva or gingival cervicular fluid may have apoptotic effects on oral mucosa remains controversial.[69] Some authors proposed that BPs could have a direct cytotoxic effect on oral mucosal cells due to a leakage of the drug on the overlying mucosa, with greater severity when administered intravenously.[25] Irritation of the oral mucosa could easily be further exacerbated by a dental extraction or other microtrauma. To this effect, if high concentrations of BPs in the oral cavity can disrupt the mucosa, it may be reasonable to consider how high concentrations in the underlying bone could produce a similar toxic effect.[25] A decreased pH due to infection could further increase the acidic environment of the osteoclastic bone resorption sites, increase the liberation of more BPs to the surrounding mucosa and bone.[93-95]

The first study investigating the toxic effects of the soft tissue caused by BPs was conducted on oral keratinocytes.[41] Several research groups since have confirmed decreased keratinocyte proliferation rates and viability, increased apoptotic changes, and decreased migratory capacity in keratinocytes exposed to BPs.[96, 97] Pabst et al. found that both pamidronate and zoledronate induced apoptosis at concentrations of 50 μM and decreased cellular viability of gingival keratinocytes at 5 μM.[96] Histologic samples of gingival tissue obtained from

BRONJ patients demonstrated swollen and hypereosinophilic cells with a picnotic nucleus in the mucosal layers of the oral cavity.[98] Cytotoxic effects have also been reported with periodontal ligament fibroblasts exposed to alendronate in concentrations higher than 1 μM.[99] Agis et al. reported decreased cellular activity in periodontal fibroblasts which underwent apoptosis *in vitro*; however, these adverse effects of zoledronate were mitigated by the presence of serum.[100]

Gingival fibroblasts comprise approximately 65% of the total cell population in healthy gingival connective tissue.[101] There have been a handful of studies on HGF cell lines or primary culture cells in response to BPs.[40, 70, 95, 102, 103] Scheper et al. reported that zoledronic acid released from the bone affects gingival fibroblasts as well as oral keratinocytes, inducing early apoptosis and reducing cell growth.[43] Simon et al. reported toxicity of both zoledronate and pamidronate on gingival fibroblasts.[104] Another study demonstrated that alendronate, zoledronate, and pamidronate decreased collagen production and cell survival in primary HGFs.[44] Significant apoptosis and inhibited cellular proliferation at concentrations of 1, 5, and 10 μM of zoledronate on HGFs were observed to increase with concentration and time up to 7 days.[105] Soydan et al. reported cytotoxic effects of both parentally administered pamidronate and orally administered alendronate, which induced apoptosis and inhibited proliferation in primary HGFs *in vitro*, particularly at concentrations ranging from 10-100 μM.[69]

We observed earlier gingival fibroblast death with higher concentrations of nitrogen-containing BPs (zoledronate, alendronate, and ibandronate) in the xCELLigence experiments, with cell death at 63-78 hours compared to controls of 90-149 hours. These results were exacerbated with the introduction of LPS and a co-culture of THP-1 cells, which affected medium and low concentrations of nitrogen-containing BPs, as well. Other studies also confirmed the increased toxicity of aminobisphosphonates on a variety of cell types including endothelial cells, fibroblasts, and osteogenic cells compared to non-nitrogen-containing

clodronate.[95] Nitrogen-containing BPs are not metabolized and therefore accumulate in the bone[106], whereas non-nitrogen containing BPs such as clodronate are rapidly excreted by the kidneys with far less uptake by cells.[107] BP uptake into bone is in direct proportion to the local rate of bone turnover, and the alveolar ridges of the maxilla and mandible exhibit a high turnover rate.[108, 109]

Nitrogen-containing BPs function by inhibiting farnesyl pyrophosphate synthase, an enzyme in the mevalonate pathway (Figure 34).[70] Lorenzo et al. proposed that the mechanism could be due to a leakage of BP from the jaw bone, particularly after a dental extraction, resulting in the inhibition of the farnesyl pyrophosphate synthase enzyme in surrounding cells.[98] There has been evidence of suppressed epithelial cell growth by nitrogen-containing BPs via inhibition of the mevalonate pathway and a consequent reduction in cholesterol synthesis.[110] This also results in decreased synthesis of the metabolite geranylgeraniol, interfering with cell cycle progression and blocking cytokinesis.[111] Geranylgeraniol is necessary for membrane localization of intracellular proteins, including caspase 3, a main regulator of cellular apoptosis, and the small GTP-binding proteins Ras, Rho, Rac, and Rap, which are involved in a number of signaling pathways.[69, 112] Disturbance of these important pathways leads to an inhibition of cell migration, cell metabolism, and ultimately, apoptosis. Alendronate 30 nM/ml and risedronate 10 nM/ml were found to inhibit human epidermal keratinocyte proliferation *in vitro* by means of farnesyl pyrophosphate synthase inhibition.[110] Suri et al. reported that dose-dependent apoptosis and loss of viability in intestinal epithelial cells was prevented when BP-induced inhibition of farnesyl pyrosphosphate synthase was bypassed with the addition of the downstream product geranylgeraniol.[113] Other researchers have demonstrated the same effect with gingival fibroblasts, where proliferation, cellular apoptosis, and migration could be partially rescued by geranylgeraniol *in vitro*.[70, 71, 111]

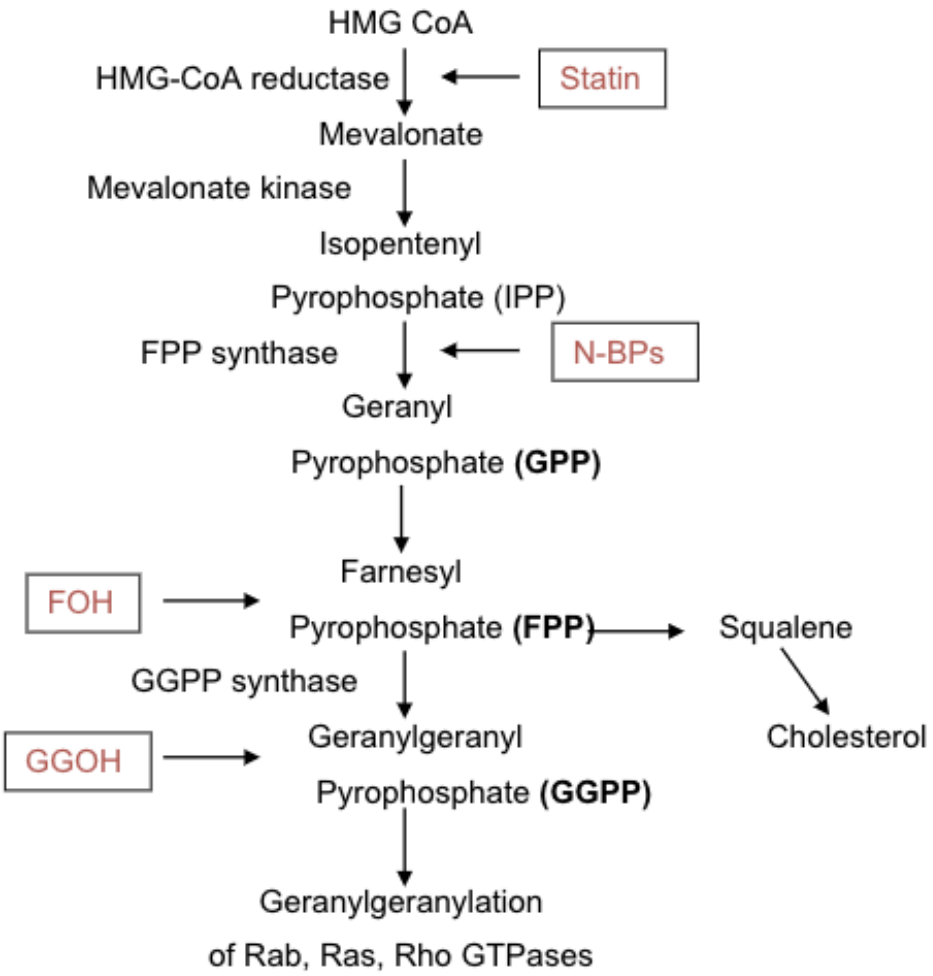

Figure 34. The Mevalonate Pathway.[111] N-BPs = nitrogen-containing bisphosphonates; FOH = farnesol; GGOH = geranylgeraniol.

We also observed effects on wound healing in the 24-well plate scratch assay. Impaired wound healing was observed early on (after 72 to 96 hours) in nitrogen-containing BPs, a non-nitrogen containing BP, as well as a combination of zoledronate and denosumab (specifically, clodronate 500 μM, ibandronate 5 μM and 50 μM, alendronate 50 μM, zoledronate 5 μM + denosumab 10 μg/mL, and zoledronate 5 μM), with obvious severe fibroblast cell death in zoledronate 50 μM.

By 168 hours, ibandronate 50 μM, alendronate 50 μM, zoledronate 5 μM + denosumab 10 μg/mL also demonstrated obvious severe cell death compared to healthy-appearing confluent controls. When comparing our *in vitro* observations of increased cell death and delayed wound healing which intensified with time to studies in patient populations, the incidence of BRONJ indeed does increase with the time of exposure, from 1.5% among patients treated for 4–12 months to 7.7% for treatment of 37–48 months.[114]

Defective or delayed epithelialization of the oral mucosa has also been observed in almost all cases of BRONJ.[98] If the local medication concentration is high enough, it inhibits proliferation of adjacent epithelial cells[42] and slows healing of the physical breach in the mucosa.[98] Landesberg et al. administered pamidronate to oral keratinocytes at concentrations of 3, 10, 30, 100 μM, and reported inhibited cell proliferation and impaired wound healing at the concentration of 100 μM with no evidence of cellular apoptosis. The cell layer was closed at 72 hours for the lower concentrations of pamidronate and the control group.[41] Pabst et al. observed cellular apoptosis of oral keratinocytes as well as impairment of migration in a scratch assay with 50 μM of nitrogen-containing zoledronate, ibandronate, and pamidronate within 48 hours, and non-nitrogen containing clodronate within 72 hours.[96] Kobayshi et al. conducted a wound healing assay which demonstrated that zoledronate 1–10 μM inhibited the migration of murine oral keratinocytes but not fibroblasts.[115]

For HGFs, zoledonate, pamidronate, and ibandronate have been reported to affect healing in a previous wound healing scratch assay.[95] Previous studies have observed that zoledronate impedes proliferation and the migratory capacity/wound healing of gingival fibroblasts, suggesting that the downregulation of type-I collagen transcription could be a mechanism, as it is necessary to deposit the granulation tissue needed for re-epithelization in keratinocyte and fibroblastic cell lines.[103, 104] Komatsu et al. also reported a reduction of type-I collagen

expression via transforming growth factor beta (TGF-β) suppression in HGFs exposed to zoledronate at serum concentrations of 1.47 μM. They proposed that zoledronate-induced suppression of TGF‑β resulted in decreased HGF viability and migratory activity and overall impaired fibrous tissue formation by HGFs possibly through the inhibition of the Smad‑dependent signal transduction pathway.[74] A theory of diminished keratinocyte growth factor (KGF) production has also been suggested as a factor in the mechanism of delayed epithelial healing. KGF induces growth and migration of gingival epithelial cells, and the combination of oral bacteria and pamidronate was observed to promote apoptosis of gingival fibroblasts, a major source of KGF production, resulting in delayed epithelial healing combined with bone death.[40]

With the addition of LPS, impediments to wound healing and observed gingival fibroblast cell death occurred earlier and were affected by an increased number of medications. Zoledronate 50 μM displayed signs of cell death as early as 24 hours. By 48 hours, wound healing was affected in clodronate 500 μM, denosumab 40 μg/mL, ibandronate 5 μM and 50 μM, zoledronate 0.5 μM and 5 μM, zoledronate 5 μM + denosumab 10 μg/mL, alendronate 50 μM, with zoledronate 50 μM already having already progressed to severe cell death. By 96 hours, alendronate 50 μM also exhibited severe cell death. A murine model of oral bacteria in BRONJ exhibited unhealed gingival epithelium and delayed bone regeneration in mice after tooth extraction following 15 days of exposure to pamidronate 1mg/kg and *Fusobacterium nucleatum (F. nucleatum)*.[40] The accompanying *in vitro* study also demonstrated significantly more gingival fibroblast apoptosis when exposed to the combination of pamidronate and *F. nucleatum* compared to only BP, only bacteria, or control. Zoledronate 1–10 μM has been documented to promote the adherence of *Streptococcus mutans* to hydroxyapatite and the proliferation of oral bacteria obtained from healthy individuals, suggesting that zoledronate may increase bacterial infection.[115] Although BRONJ has been shown to develop in rat models without inflammation or oral infection[33], a critical role of oral bacteria

in the pathogenesis of BRONJ is supported by clinical studies where the frequency of necrosis is significantly decreased with the elimination of bacteria-permeated dental plaque and antibiotic administration prior to dental surgery.[116-118]

Our results demonstrated that antiresorptives were toxic to HGF even without mechanical damage. In the non-scratch 24-well plate experiments, zoledronate 50 resulted in early cell death at 24 hours, while ibandronate 50 μM, zoledronate 50 μM, zoledronate 5 μM + denosumab 10 μg/mL, and alendronate 50 μM progressed to severe cell death at 168 hours. The addition of LPS worsened the effects of alendronate 50 μM, which appeared apoptotic earlier at 96 hours. Due to the features of the periodontal anatomy in which the alveolar ligament, periosteum, gingival mucosa, and the dental cervix are connected, contact between BP and the soft tissues is likely to occur in the absence of traumatic events such as dental extraction.[98] Scheper et al. demonstrated the release of low levels of zoledronate (0.25–3 μM) from bone, which may induce mucosal cell apoptosis and inhibit proliferation.[43] Spontaneous cases occur in about 30% of patients[30], which are typically localized to areas that are easily injured with thin overlying mucosa, such as in the mylohyoid ridge region.[41] This may explain the onset of necrosis due to a number of dental prostheses pressure sores in both our histologic (27%) and radiographic studies (43%), which may point to oral mucosal cell death without direct trauma to the oral tissues. One clinical study reported that 87% of adult patients exhibited traumatic ulcerations in the first week after placement of dentures, followed by 50% in the second week, and 7% in the third week.[119] Niibe et al. also observed a statistically significant incidence of MRONJ in patients with removable dentures compared to those with no prosthesis.[120]

Our experiments present some of the first results investigating the singular effect of denosumab on HGFs, which inhibited wound healing at high concentrations but otherwise did not dismantle the fibroblast cell layer. Oral soft tissue toxicity was previously not reported with denosumab.[7] A murine model has demonstrated that

denosumab administration resulted in a significant increase in CD3 and gamma delta (γδ) T cells locally, which may suggest a relationship between denosumab and inflammation with delayed connective tissue repair.[121] In addition, monocytes and macrophages have been reported to produce isopentenyl pyrophosphate (IPP) in response to BP therapy, which also activates γδ T cells and initiates immune responses found in disease states.[122, 123] It has been noted that γδ T cells cause a release in TNF and the initiation of the inflammatory acute phase response, which was also evidenced by elevated TNF expression in our *in vitro* assays.[124] Denosumab has been associated clinically with non-specific dermatologic reactions, which could be attributed to the suboptimal tissue specificity of recombinant molecules.[125, 126] RANKL and RANK are also expressed in immune cells including T lymphocytes, B cells, and dendritic cells.[127, 128] Since RANKL and RANK expressed in skin cells activates T regulatory cells to diminish autoimmune and hypersensitivity responses, an inhibition of RANKL may disturb normal immune activity.[126, 129] In our experiments with THP-1 cells, a co-culture with the monocytic/macrophagic cell line resulted in significantly earlier HGF cell death with a combination of denosumab and zoledronate, indicating a potential immunologic influence.

These results are one of the first to address the effect of combined concentrations of zoledronate and denosumab, which attempted to simulate the actual clinical situation of patients who have received BP therapy before initiating denosumab.[7] Since the half-life of BPs could be up to ten years[103], it may be realistic for patients in a clinical setting to have residual BP effects while receiving denosumab. In order to untangle the distinct differences in BP-specific, denosumab-specific, and combination zoledronate and denosumab effects, we included three different concentrations of BP combined with denosumab. In particular, the concentrations of zoledronate 5 μM + denosumab 10 μg/mL demonstrated severe cell death with impaired wound healing, which was also seen with the introduction of LPS. This combination also resulted in HGF death without mechanical damage, which was

interestingly not observed with the denosumab-only group. This implies that there may be an influence of BP on HGFs which may be different from the effect exerted by denosumab alone.[130]

4.2 Elevated immune response and possible dysfunction

Our experiments revealed high levels of IL-8 and TNF gene expression with zoledonate 50 μM in the presence of LPS when compared to control groups with and without LPS. Denosumab 40 μg/mL in the presence of LPS also demonstrated slightly elevated TNF expression. When HGFs were cultured with THP-1 cells, IL-1β was elevated with all concentrations of antiresorptive except for control. IL-6 levels were suppressed significantly in high concentrations of nitrogen-containing BPs.

Previous research in the field of periodontics has demonstrated an increased production of proinflammatory cytokines such as IL-1, IL-6, and TNF in the periodontitis disease state (Figure 35); these cytokines prime neutrophils and stimulate bone resorption.[131] These same cytokines are also elevated in the pathogenesis of oral mucositis following cancer therapy leading to macrophagic tissue destruction.[132] IL-8 is produced by epithelial cells, and is responsible for chemotaxis and angiogenesis by recruiting neutrophil migration and increasing monocyte adhesion in the blood vessels.[66] De Colli proposed that the overproduction of IL-6, IL-1, and TNF-α are closely linked to the occurrence of inflammation due to their regulation of COX-2 expression, resulting in the production of key inflammatory mediators.[58] Periodontal microbiota such as *P. gingivalis*, although capable of direct host tissue destruction, are also able to communicate with fibroblasts and epithelial cells to stimulate the production of host mediators and cytokines.[133, 134] The synthesis of IL-1α, IL-1β, and TNF-α in various cell lines *in vitro* have been induced by LPS from *Actinobacillus actinomycetemcomitans*

(A. actinomycetemcomitans) and *P. gingivalis*.[135-138] These cytokines play an important role in inflammatory osteoclastic bone resorption in periodontal disease.[62, 139]

P. gingivalis LPS induces IL-1 release from macrophages[140] and IL-1β from fibroblasts *in vitro*[141] as well as *in vivo*.[138] Inflammation caused by LPS is also mediated at least in part by IL-1β. The LPS from *P. gingivalis* is a potent stimulator of bone resorption *in vitro*.[139] IL-1β has also been demonstrated to play an important role in osteoclastic bone resorption *in vitro* [142, 143] and *in vivo*.[62-64]

As a part of the innate immunity response, TNF-α plays a central role in the inflammatory reaction, alveolar bone resorption, and the loss of connective tissue attachment in periodontal disease.[144] TNF-α is locally produced by a number of cell types, including neutrophils, which exhibit increased chemotaxis and production of proinflammatory cytokines.[131] Macrophages represent an important source of TNF-α, that, under dysregulation, contribute to host tissue destruction.[145] The loss of fibroblasts that occurs during infection with periodontal pathogens is also mediated by TNF.[61] Graves et al. indicated that the destruction of the periodontium may very well represent an overreaction of the host response to periodontal pathogens caused by excessive production of IL-1 and TNF.[61] In murine models, BRONJ was seen to be associated not with infection but instead with severe inflammation and immunosuppression[33, 146]; therefore, immune dysregulation could be a factor in BRONJ pathogenesis.

Other authors have suggested a mechanism of reduced host defense against infection induced by antiresorptive medications.[16] In previous experiments we demonstrated that BPs suppressed macrophage differentiation, migration, and phagocytosis *in vitro*.[34, 36] Partial inhibition of early T and B lymphocyte development has been observed in RANKL-deficient mice.[52] It is also conceivable that recombinant denosumab molecules not completely specific for

RANKL could react with other receptors in the TNF family to produce disruptions in the immune system.[126] In our experiments with HGFs, we noted that denosumab in combination with LPS did indeed increase the levels of TNF, as well as IL-1β. Clinically, severe infections requiring hospitalization including cases of diverticulitis, cellulitis, and erysipelas have been reported with denosumab treatment.[147, 148] One could hypothesize that denosumab could play a role in exacerbating chronic infection, which may be relevant in the field of clinical periodontics, although there is no literature addressing this to date.

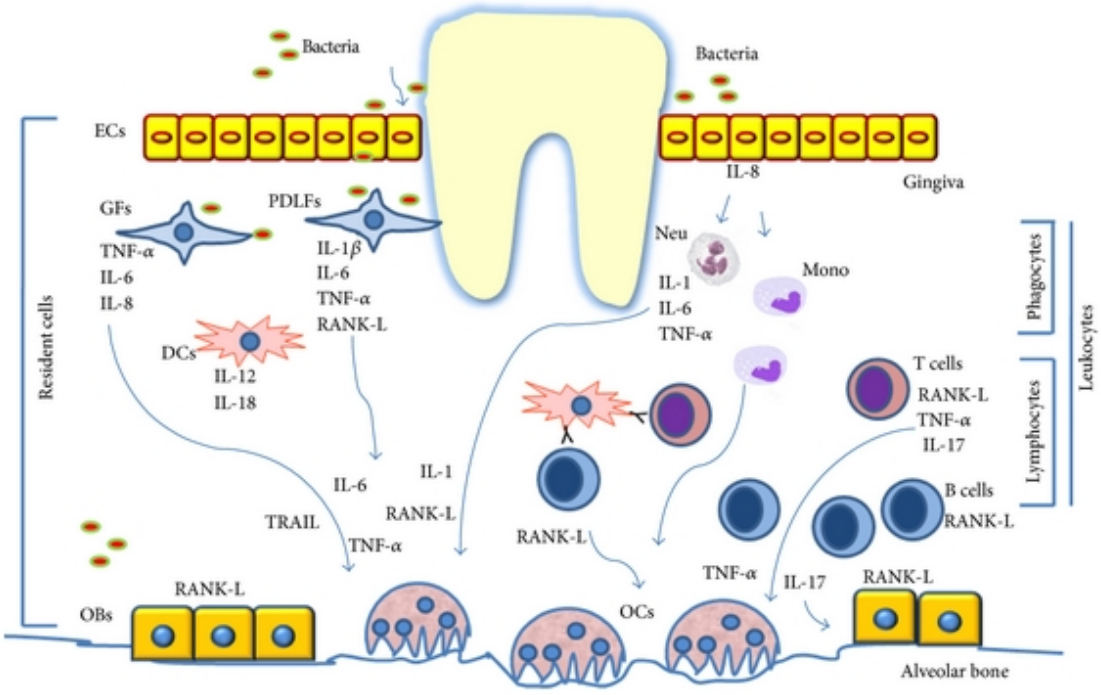

Figure 35. Network of cytokines involved in periodontal disease.[145]

Increases of IL-1β, TNF, and IL-8 in HGFs exposed to antiresorptives in our experiments suggest a pro-inflammatory environment as seen in other diseases of the oral cavity such as periodontitis and mucositis. However, we found that levels of IL-6 were elevated for every concentration including the control except for the

highest concentrations of zoledronate, alendronate, and ibandronate. Since zoledronate 50 μM, alendronate 50 μM, ibandronate 50 μM were the most toxic concentrations for HGF viability, the lack of expression in these concentrations was a point of interest. IL-6 is an important regulator of the immune system; IL-6 levels are normally present in healthy patients and are then increased in a periodontal disease state.[149] IL-6 plays a major role in B cell differentiation in the adaptive immune response.[65] B cells are activated and transformed into plasma cells, which produce antibodies against bacterial antigens. Since IL-6 is necessary for this switch to a more sophisticated immune response, an absence or decrease of IL-6 in high concentrations of aminobisphosphonates could suggest a dysfunction in the later stages of the immune response. It could be possible that HGFs exposed to antiresorptives and bacterial challenge remain in the initial pro-inflammatory stage, unable to activate the acquired immune system and resolve inflammation. However, other research groups have also reported increased IL-6 levels expressed by HGFs exposed to BPs.[58, 101]

Saracino et al. suggested that a switch to a pro-inflammatory microenvironment could play in a role in pathogenesis after observing an increase of TNF-α in keratinocytes exposed to zoledronate 5 μM and 50 μM.[42] Our results also seem to support the theory that antiresorptives in combination with infection/LPS promote an immunologic reaction in HGF cells, which could be indicative of some type of ineffective immunologic overstimulation leading to local immune dysfunction.[35, 36] The results of our histologic study seemed to corroborate with this idea. We did see more signs of infectious infiltration in BRONJ, DRONJ, and Mixed ONJ compared to healthy and osteoporosis samples, as well as a significantly higher Allred Score with CD14 and CD68 for BRONJ and Mixed ONJ bone specimens compared to healthy control groups. There was also evidence of macrophage differentiation of THP-1 cells exposed to antiresorptives and LPS in co-culture with fibroblasts, along with release of the aforementioned cytokines.

CD14 is a glycoprotein released by monocytes and macrophages localized on cell membranes, and is mainly expressed by macrophagic cells and to a lesser extent by neutrophil granulocytes.[35] CD14-positive monocytes can differentiate into various cells and interact with and bind to LPS, a potent activator of macrophages.[150] CD14 plays in a role in activating a signalling pathway for optimal inflammatory gene expression induced by LPS from *Escherichia coli* or *P. gingivalis* through toll-like receptors in macrophages.[150]

CD68 is also expressed by macrophages/monocytes, and is particularly useful as a marker for the various cells of the macrophage lineage, including monocytes, histiocytes, giant cells, Kupffer cells, and osteoclasts.[151, 152] Expression levels of CD68 are also connected to the phagocytic activity of macrophages.[35] Hoefert et al. observed an decreased CD68 infiltration and CD68/CD14 ratio in BRONJ specimens compared to jaw bone specimens of patients with OM or ORN.[35] Other groups have reported an increased macrophage cell density in BRONJ-affected jaw bone compared to ORN and control groups[153], and comparable results in murine models for CD68 positivity in rats treated with BPs.[154]

Macrophages, like osteoclasts, can internalize and be affected by BPs.[155] In addition to their role in initiating the immune response against pathogens, macrophages are also crucial to tissue homeostasis and regeneration.[156] An excessive response of the macrophage lineage may indicate some disproportionate reaction from the innate immune system. The increased macrophagic infiltration in BRONJ specimens could be stimulated by local infection but also by the action of BPs.[153] Wehrhan et al. found an increased macrophage cell density in BRONJ-affected jaw bone, and proposed that it could be due to a BP-caused shift from the M2 to a M1 macrophage cell type.[153] M2 macrophages are associated with tissue homeostasis and regeneration, while M1 macrophages cause tissue destructive inflammation.[157, 158] M1 phenotype activation has been also associated with an increase in TNF-α and IL-1β, which was also

confirmed in our *in vitro* assays.[159] Additionally, recent groups have also reported that IL-6 is important for the switch in macrophage polarization.[153] Thus, a BP-derived shift towards M1 polarization might prevent a M2 macrophage-mediated wound healing response in BRONJ affected sites[35, 160], resulting in a continued inflammatory process which is unable to resolve. This failure to switch from an inflammatory M1 type to a regenerative M2 type has also been observed in unhealed chronic venous ulcers.[161]

The immunomodulatory capacity of BPs has been proposed due to direct anti-tumor effects in patients treated with BPs for malignant diseases in the absense of bone involvement.[162, 163] There is evidence that BP treatment decreases RANKL expression and consequently reduces nuclear factor kappa-B activation, a gene regulator implicated in many cancers which also has a role in increasing macrophage polarization to the M2 phenotype.[164-167] A shift from M2-polarized macrophages to M1 might explain the clinically observed anti-tumor/tissue destructive effects of BPs even in the absence of bone metastases[168], as well as the predominance of the tissue-destructive phenotype potentially leading to the development of BRONJ.[153] This theory was further supported by the work of Zhang et al., who noted that the adoptive transfer of M2 macrophages could reduce BRONJ severity in mice.[160] Zoledronate but not denosumab has been demonstrated to suppressed THP-1 macrophagic differentiation and cell function.[34] Our results likewise lead us to propose that denosumab could have a different mechanism of action than BPs in causing tissue destruction. Macrophage involvement and absent IL-6 levels were observed in our *in vitro* and histologic studies involving BRONJ but not DRONJ, which we hypothesize to be more associated with disturbed T and B cell immunity, local inflammation, suboptimal tissue specificity and TNF family activation, and over-suppression of bone turnover.

4.3 Osteoclast activation and inhibition

In our experiments with connective tissue cells, we observed that the expression of RANKL by HGFs was not significantly influenced by antiresorptives. However, high doses of zoledronate 50 μM with LPS (and slightly denosumab 40 μg/mL) with LPS elevated the expression of OPG compared to controls with and without LPS. RANKL is a member of the TNF cytokine family and is secreted by fibroblasts, as well as osteoblasts and other stromal cells, to promote osteoclast activation and differentiation.[169, 170] OPG is a cytokine receptor also from the TNF family which functions as a decoy receptor for RANKL, inhibiting the RANK-RANKL interaction and thus osteoclastogenesis by tightly binding to RANKL.[171] Fibroblasts, as well as osteoblasts and cells of the immune system, can produce both OPG and RANKL. LPS has also been demonstrated to have a direct effect on fibroblasts, causing them to increase the expression of RANKL and IL-6.[172] Since RANKL levels were low and levels of OPG were higher in our experiments of fibroblasts exposed to both zoledronate and denosumab, our results could indicate that fibroblast signaling in osteoclastic bone remodelling is suppressed in the presence of a combination of infection/LPS and antiresorptive, but not antiresorptive alone. Therefore it seems a bacterial challenge is needed to increase the expression of OPG, thereby inhibiting RANKL and bone resorption.

Previous studies have confirmed our results with HGFs, where OPG was detected at high levels in gingival fibroblast cultures, and RANKL could not be detected.[173] Tipton et al. also found that OPG levels increased and RANKL levels decreased when HGFs were exposed to alendronate or pamidronate at concentrations of 0.01 nM to 1 μM, and these effects were amplified when stimulated by LPS.[101] Human periodontal ligament cells stimulated with LPS inhibited osteoclastogenesis by producing more OPG than RANKL through the induction of IL-1β and TNF-α.[174] This correlated with our observations of increased OPG, IL-1β, and TNF cytokine expression with decreased RANKL gene expression.

Our histologic study of bone specimens revealed that RANKL staining was most positive for BRONJ ($p = .021$ compared to Healthy) and Mixed ONJ, and least positive for Healthy and DRONJ. The results for TRAP stain corroborated with this as Mixed ONJ ($p = .002$), BRONJ ($p < .001$), and BP-exposed ($p = .017$) exhibited a higher Allred Score compared to the healthy group. The number of osteoclasts counted were also highest for Mixed ONJ ($p = .041$), BRONJ ($p = .034$), and lowest for Healthy. In contrast, OPG positivity was highest for DRONJ and Mixed ONJ and lowest for Healthy, although the results were not of statistical significance. It is of interest to find an increased number of osteoclasts in BRONJ-affected bone, since the accepted mechanism of action of BPs is to prevent osteoclast function.[175] Most research groups have reported a decrease or absence of multinucleated osteoclasts and no signs of bone remodeling in necrotic BRONJ sites[176, 177], although a statistically significant higher number of osteoclasts in tissue samples of patients with BRONJ has been previously reported.[178, 179]

Baron et al. suggested that BP-induced osteoclast inhibition could trigger a feedback loop resulting in the increase of RANKL and subsequent osteoclast differentiation.[5] Hansen et al. propose that this increase in osteoclasts is probably not only related to resorption of sequestrated bone[180], but also the dysfunctional degradation of vital and functional jaw bone.[178] Of the 20% to 80% of absorbed BP taken up by bone, a high percentage has been reported at sites of bone formation and even higher for sites of bone resorption.[95] In our study, we also noticed that Mixed ONJ and BRONJ exhibited more areas of scallopped resorption in both necrotic and vital bone, with multinucleated osteoclastic cells in Howship lacunae participating in bone destruction and resorption. These areas of osteonecrosis also appeared to be patchier in tissue specimens of BP-treated patients when compared with larger regions of necrotic bone in ORN.[179]

Higher numbers of osteoclasts could be also explained by a stimulating presence of bacteria in the oral cavity. An association between infection with *Actinomyces* and osteolysis has been long established.[181] The increased recruitment of osteoclasts in *Actinomyces*-positive osteonecrosis as reported in a previous study argues for a stimulatory effect of a microbial presence.[178] Some bacteria have been demonstrated to directly regulate the production of RANKL in human periodontal ligament cells, gingival fibroblasts, B cells, and macrophages, resulting in increased bone resorption.[16, 182] *A. actinomycetemcomitans* and *P. gingivalis*, both common pathogens in periodontitis, have been shown to cause a similar increase in bone erosion in animal models and have been cited as possible agents in BRONJ development.[138, 183] These gram-negative anaerobic bacteria contain a complex inflammatory LPS in their cell walls which can independently participate in host cell cytokine synthesis and bone resorption. Proteins from *P. gingivalis* have been reported to directly regulate RANKL and OPG production in human periodontal ligament fibroblasts and HGFs, increasing osteoclastogenesis.[184] This may explain MRONJ cases exhibiting extensive sequestration despite antiresorptive-suppressed bone turnover. Osteoclasts stimulated by bacteria could additionally activate inflammatory cells and induce the synthesis and release of cytokines such as TNF, IL-1, and IL-6, as observed in periodontitis.[185] Reports of scallopped bone on surfaces affected by BRONJ[179, 186, 187] has also been attributed to bacteria, cytokines, and associated fibroblast-like cells which have the ability to directly resorb bone independent of osteoclasts via the release of various acids and proteases.[28, 188-191] This suggests that the theory of osteoclast inhibition alone does not explain the elective localization of the disease in maxillofacial area, and that other mechanisms must play a role in the pathogenesis of BRONJ.[98]

Hansen et al. proposed that pseudoepitheliomatous hyperplasia could play a role in allowing bacteria to reach the bone, since they observed the presence of

bacteria situated between the bone and altered epithelium in several cases of BRONJ.[179] While pseudoepitheliomatous hyperplasia normally occurs as a rare complication of chronic osteomyelitis of long bones such as the tibia, it occurs seldomly in the jaw.[192] Typically, this lesion is distinguished by nonkeratinized squamous epithelium without signs of atypia exhibiting a distinct centrifugal involvement of medullary spaces.[179] In our histologic study, we observed that BP-exposed bone exhibited more pseudoepithelial changes. Zustin et al. observed the appearance of pseudoepitheliomatous hyperplasia in the bone specimens of 11 out of 17 BRONJ patients and suggested that it could be a response of the oral tissues to re-epithelialize and create a physical barrier from inflamed regions.[193] We also observed pseudoepitheliomatous hyperplasia in BRONJ and Mixed ONJ, with the presence of granulation tissue in non-necrotic bone samples, which has associated in the literature with bacterial debris in Mixed ONJ and BRONJ.[194, 195]

In our study, pseudoepitheliomatous hyperplasia occurred more frequently in cases associated with BPs than denosumab, particularly in non-necrotic bone still able to respond to injury via epithelial changes. Hokugo et al. proposed that this reaction could be due to an upregulation of TNF-α and interferon gamma (IFN-γ) induced by increased T helper cytokines.[37] In our laboratory studies, we also noted a greater increase of TNF levels in gingival fibroblasts upon administration of zoledronate compared to denosumab. Furthermore, we observed that fibrous tissue was more frequently found in the osteoporosis, osteomyelitis, and BPDN-exposed groups with a more organized appearance in osteoporosis samples. Favia et al. reported collagen deposition in non-necrotic bone from ONJ patients.[39] Interestingly, fibrotic diseases are believed to be associated with the M2 polarization of macrophages, which is much less tissue-destructive than the M1 profile.[196]

Besides bacterial stimulation of osteoclasts, an increased positivity of osteoclastic staining in our study could also be explained by the presence of osteoclasts that survive but are non-functional. Previous results have shown that zoledronate inhibits bone healing by suppressing osteoclast activation despite positive TRAP staining.[106] Lim et al. observed that with a concentration of 1 µM zoledronate in rats, cells were stained with TRAP but failed to fuse and form active osteoclasts. Osteoclasts detected in inflammatory areas from treated patients were small and contained few nuclei.[39] It was discovered that osteoclasts, which arise from macrophagic precursors, normally also express a M2-like cytokine profile, but are induced by nitrogen-containing BPs to a shift towards an M1-like pro-inflammatory profile.[197] Since osteoclasts are formed by the fusion of mononuclear cells, some authors propose that a shift from a M2 to a M1 macrophage progenitor microenvironment in BRONJ-affected bone could additionally block the the fusion of hematopoietic precursors into multinucleated, mature osteoclasts.[153, 198] Since BPs could also inhibit bone resorption by preventing mature osteoclast formation, this may result in an accumulation of functionally inactive osteoclasts.[5, 198] In organ culture, some BPs have been observed to inhibit the generation of mature osteoclasts, possibly by preventing the fusion of osteoclast precursors.[199] Williams et al. proposed that these impaired osteoclasts are then unable to remove bacteria-infested bone in MRONJ lesions, leading to bone death.[200]

Since osteoclasts and macrophages derive from a common precursor, another hypothesis is that positive RANKL or TRAP stains for osteoclast-like cells could, in fact, actually be macrophages with osteoclast-like functions, as no truly specific osteoclast markers are available. Positive TRAP staining has been reported for osteoclast precursors before fusion and activation.[201] Since intermediate cell types in the continuum between macrophages and osteoclasts do exist, including mononuclear osteoclasts and polynuclear macrophages[198], there could be a cell type that, when converted by certain cytokines, begins to dysfunctionally resorb

the bone. This could perhaps occur despite or even due to antiresorptive inhibition of mature osteoclasts and expressed with positive TRAP and RANKL staining. Macrophages, osteoclast-like cells, and fibroblast-like cells have all been demonstrated to participate in osteoclast-independent bone resorption.[28, 189, 202] There has been evidence of mononuclear macrophage-like cells at sites of cartilage resorption which expressed a TRAP-positive osteoclast phenotype.[203] Immune modulators and hormones have been observed to induce mature macrophages to differentiate into osteoclasts *in vitro*.[204] Our previous study with THP-1 cells also revealed that zoledronate affected macrophagic differentiation and function.[34] However, macrophagic activity was not affected by denosumab. This concurred with the results from our histologic study, where DRONJ samples did not demonstrate evidence of macrophagic-osteoclastic involvement, nor cells positive for RANKL and TRAP staining like the BRONJ group. This may be due to the explicit effects of denosumab on RANKL inhibition and supports the idea of a different mechanism of action between DRONJ and BRONJ. The influence of exclusive denosumab effects may have been previously confounded due to DRONJ patients who were often initially exposed to other antiresorptives in prior studies. However, in our study, the DRONJ group represented a cohort of patients without a history of other prior antiresorptives. Of interest is the variable results for Mixed ONJ, which may depend on whether the necrotic lesion is influenced more predominantly by BP or denosumab effects.

4.4 No evidence of affected angiogenesis

We did not find any evidence of decreased angiogenesis in any of our investigations. Results from ELISA quantifications of VEGF revealed that all concentrations with and without antiresorptive medications were elevated, indicating no signs of anti-angiogenic effects on HGFs exposed to antiresorptives. We also observed IL-8 gene expression with zoledronate 50 μM in the presence of LPS. Since IL-8 is also responsible for monocyte adhesion in the blood vessels,

it can also serve as a marker for affected angiogenesis.[66] In the histology study, the blood supply by Haversian systems showed no significant observable differences; interestingly, there was even a slight tendency for a higher Haversian canal density in bone affected by DRONJ, BRONJ and Mixed ONJ with observable intact vasculature.

Anti-angiogenic properties of antiresorptives have long been indicated as a mechanism for MRONJ development.[31, 88, 205, 206] A reduction of blood vessels in ONJ patients[207] as well as inhibition of vascular endothelial cell proliferation and migration has been reported.[208] Others hypothesize that anti-angiogenic effects could be attributed to incorrect processing of vascular endothelial growth factor receptor 2 (VEGFR2) on endothelial cells resulting in an intracellular accumulation induced by zoledronate.[209] Yamashita et al. found that while VEGF-A was not affected by zoledronate, VEGF-C, which is responsible for lymphangiogenesis, was suppressed in rats.[210]

We did not observe any evidence for anti-angiogenic effects in our experiments. Other *in vivo* studies have also failed to demonstrate a strong relationship between BP treatment and reduced angiogenesis.[211, 212] In fact, several groups have even reported an upregulation of VEGF-A and bone morphogenetic protein 2 (BMP-2) gene expression, suggesting that fibroblasts respond to zoledronic acid by producing a pro-angiogenic environment.[111, 213] Tseng et al. reported that IL-8 levels were significantly upregulated in osteoclasts treated with zoledronate. Both human bone specimens and a canine model of BRONJ exhibited a visible and intact vasculature despite being surrounded by areas of nonviable osteocytes.[179, 214] An increased or continued vascular flow to affected regions could even permit more BPs to enter and accumulate in the bone and extracellular fluid.[109]

4.5 Limited osteocyte network and over-ossification

The results of our histologic study demonstrated significantly fewer total numbers of osteocytes per μm^2 in DRONJ ($p = .007$), BP-exposed ($p = .028$), BPDN-exposed ($p = .022$), and ORN ($p = .004$) compared to Osteoporosis. DRONJ lesions exhibited a decreased amount of osteocytes initially when compared to the healthy group, and this distinction became even more clear when compared to the osteoporosis group since both cancer patients (breast and prostate) and osteoporosis patients frequently begin antiresorptive therapy in an osteopenic state. A decreased osteocyte density was also reported by other groups in both patients treated with alendronate compared to osteoporosis and those with active BRONJ compared to healthy groups[215, 216], but has thus far not been investigated for DRONJ. The bone structures also appeared more unorganized in MRONJ disease variants with the presence of higher numbers of bone reversal lines than Osteoporosis or Healthy. This was in accordance with the findings of Kim et al., who also reported evidence of increased thick, irregular bone reversal lines and immature woven bone in BRONJ.[217] Previous authors have concluded that changes in bony histomorphometrics could be a consequence of the prolonged effects of antiresorptives on bone metabolism and structure.[39, 218]

Haversian canals surround blood vessels and nerve cells throughout the bone. The lamellae are concentric layers surrounding the canal which contain osteocytes in their lacunae. Osteocytes communicate with each other and the Haversian canal through cytoplasmic extensions spanning small interconnecting canals called canaliculi.[219] Osteocytes control osteoclast and osteoblast activity by monitoring several hundred μm^3 of bone via dendrites in canaliculi by means of mechanicosensation and mechanicotransduction.[216, 220] They are believed to detect bone stress and respond by producing signals such as nitric oxide and sclerostin within the lacuno-canalicular network to initiate bone formation or resorption (Figure 36).[221-223]

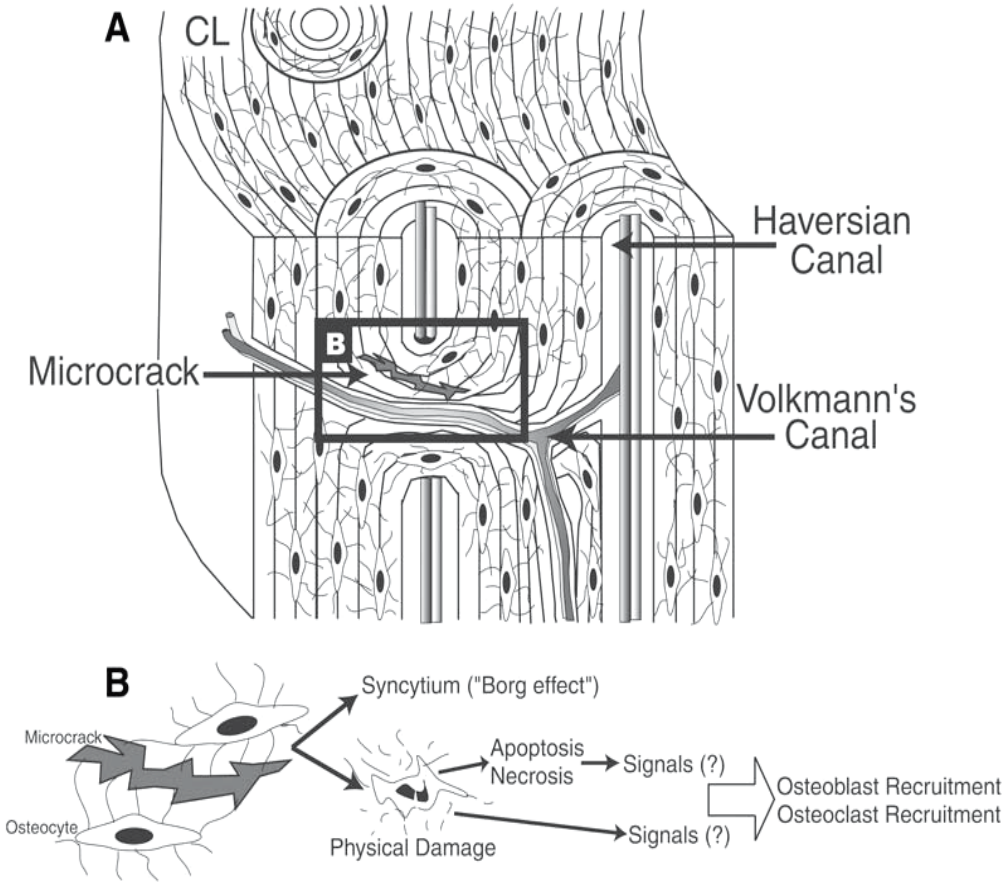

Figure 36. Osteocyte involvement in signaling bone damage.[224]

Our findings lead us to hypothesize that MRONJ, and in particular DRONJ, could develop by means of a limited osteocyte network and consequent disturbed and disorganized bone remodeling. This decrease in osteocyte networks could be due to the antiresorptive-induced over-suppression of bone turnover and subsequent over-ossification which crowds out osteocytes. Micro-CT results revealed that every ONJ variant exhibited a lower mean percentage of medullary space to bone compared to the healthy group. Mixed ONJ ($p = .033$), BPDN-exposed, DRONJ, BP-exposed, ORN, BRONJ also exhibited the widest trabecular width, while the healthy group had the narrowest trabecular width.

Results from the radiographic study also indicated that cortical and cancellous bone sclerosis were the two most frequently observed radiographic findings in the patient population affected by BRONJ, DRONJ, and Mixed ONJ, along with higher numbers of patients with a thickened lamina dura surrounding the teeth. This dense trabecular network with reduced medullary space and clinically visibly sclerosing bone upon radiographic examination could be an indication of the mechanism of over-ossification leading to subsequent osteocyte apoptosis, supporting the theory of suppressed bone turnover and trabecular thickening.

It has been demonstrated that denosumab suppresses bone remodeling even more than alendronate by directly affecting bone microarchitecture.[225, 226] Decreased bone turnover upon micro-CT with reduced porosity and increased bone mineral density was documented in postmenopausal women treated with denosumab for osteoporosis in the FREEDOM study.[227] Similar histomorphometric indices of increased total bone mineral density, remodelling suppression, and microarchitectural changes in cortical bone was observed with denosumab when compared to alendronate-treated patients.[228] A mouse model of fracture healing compared bone volume and bone mineral density between alendronate and denosumab, and found that denosumab-treated bone exhibited a more dense appearance on micro-CT with almost no distinct trabeculae formed.[229] A bone scintigraphy study reported no differences in bone turnover of the mandible compared to other skeletal sites in patients receiving BPs and denosumab.[230] However, since the jaw bone has been recognized to have a higher bone turnover than other skeletal sites to begin with[22, 214, 231], likely due to large forces of mastication or the need to clear numerous oral bacteria[109], a comparable turnover rate to the femur would indeed indicate decreased bone remodelling in the mandible. Osteopetrosis due to the genetic absence of RANKL has been previously described[232], with a difference in skeletal site turnover due to osteoclast heterogeneity.[233] Experiments with transgenic rodent models suggested that osteoclast type and

subsequent suppression may be skeletal site-specific, as normalizing osteoclast function in long bones did not produce a similar result in the jaws.[233]

Rapid over-ossification could cause bone fatigue and microdamage in bone with atypical fragility.[126] Anastasilakis et al. reported that patients on long-term denosumab exhibited a “frozen bone” phenomenon with increased risk of atypical fragility possibly due to the over-suppression of bone turnover.[126] Excessive loading of the cortical bone induces the formation of microcracks; these areas of damaged bone are subsequently resorbed with evidence of osteocyte apoptosis in these respective regions.[234, 235] More microfractures have been identified by scanning electron microscopy in MRONJ bone samples compared to osteomyelitis, osteoradionecrosis, and osteoporosis.[236] Continous microtrauma from the daily forces of jaw movement could further exacerbate osteocyte death in fragile bone, and when combined with a lack of adequate bone remodeling, could lead to necrosis.[32]

It has been also suggested that over-ossification leading to the expansion of the bone compartment could result in ischemic-necrotic changes despite the absence of reduced angiogenesis following antiresorptive therapy.[39] Favia et al. noted that the histomorphometric features seen in their study of BRONJ patients was similar to what occurs in osteopetrosis, where the metabolic demand of bone would increase but would not be compensated by a concurrent and adequate increase of blood supply.[39] This could also be due to a disturbance of the osteocyte system, where a decreased density of osteocytes and their corresponding sensory and vascular channels could imply that the nutrition for bone would have a longer distance to travel, resulting in silently expanding areas of matrix necrosis. This could provide a compatible picture connecting our observations of overossified bone and decreased number of osteocytes coinciding with unaffected markers of angiogenesis (VEGF and IL-8) and intact Haversian canals. The bone could be increasing in density, but not

provided with enough nutrition via blood supply to compensate for this increased metabolic demand, resulting in ischemic-necrotic changes. This could also explain why other anti-angiogenic agents such as bevacizumab have been seen to exacerbate these effects when combined with antiresorptives.[7, 108]

Antiresorptives have furthermore been implicated in having a direct toxic effect on osteocytes[237], since it has been demonstrated that BPs can become embedded in the osteocyte lacunae.[238] Previous studies have revealed that BPs at low concentrations inhibit osteocyte apoptosis.[239, 240] However, at high concentrations osteocyte cell death is increased.[241] Allen et al. propose that high concentrations of antiresorptive medications may accumulate near the osteocyte and induce apoptosis.[28] Osteocytes exposed to zoledronate have also exhibited more variable distribution patterns in cortical bone which increased with drug exposure time.[242] A reduction in the number of osteocytes was directly related to the increase in distance from bone channels.[242] This increased heterogeneity in osteocyte distribution in the matrix, with longer cell-to-cell distance, could affect mechanotransduction and fluid flow and decrease the functional adaptability of the bone.[243] The distribution of osteocytes is normally optimized in terms of transport costs of nutrients and cellular signals between cells and blood vessels.[244] A dense and well-organized osteocyte network is considered essential to facilitate fluid flow and diffusion of ions, hormones, and signaling molecules.[245, 246] A disruption in the system could lead to a low quality of the bone material, as evidenced by the irregular bone reversal lines and disorganized structural appearance of our histologic samples.

As antiresorptives are capable of inducing an inflammatory reaction as discussed in previous sections, TNF-α, IL-1β, and high oxidative stress have also been demonstrated to modulate an increase in osteocyte apoptosis.[247-250] We observed a marked increase of TNF and IL-1β in our experiments with gingival fibroblasts and in co-culture with THP-1 cells with high concentrations of

zoledronate, denosumab, the combination of zoledronate and denosumab, clodronate, and ibandronate. The formation of apoptotic bodies in osteocytes could also stimulate the recruitment and activation of macrophages and osteoclasts for localized bone destruction[251], as evidenced by a recent *in vivo* study.[154]

4.6 Scientific relevance for the dental practioner

As the current patient population ages, more patients may be compromised by osteoporosis and oncologic tumors and treated with antiresorptive medications. The fields of oral and maxillofacial surgery, oral medicine, and dentistry will be confronted with a growing number of patients presenting with bone necrosis of the facial skeleton. The role of soft tissue in the pathogenesis of MRONJ is to date particularly not well defined, and may be crucial in discerning how the underlying bone is exposed, infected, and unable to heal.

Our experiments demonstrated that assumed high and medium concentrations of BPs led to gingival fibroblast cell death, which may indicate clinically that certain dosages of antiresorptives interfere with soft tissue coverage of the jaw bones with risk of bone exposure. This has also been demonstrated with oral keratinocyte cells and BPs at concentrations between 5 and 100 µM[96], strengthening the theory of a combined intrinsic and extrinsic pathway of toxicity which includes soft tissue as a key component of MRONJ pathogenesis.[41] The oral epithelium is unique in that no fat, fascia, or muscle layers buffer it from the underlying bone.[252] Since fibroblasts and cells of the immune system can also express RANKL, OPG, and IL-6, disturbance of these cells could result in disruption of the mucosal layer, bacterial infiltration, and affected bone metabolism leading to osteolysis.

We also observed that the risk of soft tissue damage was influenced by the bacterial challenge simulated by *P. gingivalis* LPS exposure. A bacterial challenge such as periodontitis has been associated with risk of MRONJ.[187, 253] Since necrotic bone lesions have been reported to contain mainly anerobic bacteria representative of the microflora found in destructive periodontitis, dental practioners should consider intensified periodontitis control and treatment in antiresorptive-exposed patients.[187, 254] Sedghizadeh et al. detected many common periodontal pathogens within biofilms of bone affected with BRONJ, including species from *Fusobacterium*, *bacillus*, *actinomyces*, *staphylococcus*, *streptococcus*, *Selenomonas*, *Treponema*, and *spirochetes*.[254] Hallmer et al. found periodontal pathogens in all necrotic jaw samples from patients affected with both BRONJ and DRONJ, including *P. gingivalis*, *Tannerella forsythia*, and *Treponema denticola*, which have been demonstrated to cause high levels of bone resorption *in vitro*. [253, 255, 256] Destructive periodontitis is associated with a T helper immune response, with a particularly strong stimulus from *P. gingivalis* and activation of RANKL-induced osteoclasts. Previous research has indicated that patients treated with BPs exhibit more *P. gingivalis* species in necrotic specimens than the patients treated with denosumab, suggesting a more active role of BPs in inducing an optimal environment for periopathogenic bacteria.[253]

In our clinical studies, we observed that dental prostheses-induced pressure sores were often the precipitating event before the presentation of an osteonecrotic lesion. The severity and accompanied healing complications of prostheses pressure sores could be explained by our laboratory results with evidence of HGF apoptosis. Soft tissue affected by antiresorptives may be more prone to breakdown especially when accompanied by prolonged mechanical pressure from prosthetic devices. Pressure sores are a common phenomenon observed with dental prostheses, and a growing body of evidence points to weight-bearing areas of soft tissue[257] as a risk factor which influences the

prognosis[258] of MRONJ.[259-261] Among 21 MRONJ cases, Niibe et al. observed a statistically significant difference between patients with removable dentures and those with no prosthesis.[120] It may be prudent for dental practioners to remain just as vigilant for the risk of MRONJ in pressure-bearing areas of dental prostheses as with direct trauma from extractions or dental surgery.

Additionally, we found that the soft tissue may be inherently at risk for damage by antiresorptives even without invasive mechanical manipulation such as dental extraction or local surgery. HGFs were seen to undergo cell death even without an inflicted wound in our experiments. Practioners should be aware of the risk of MRONJ even in patients not receiving local surgical procedures. This could explain our clinical cases of spontaneous instances of MRONJ, which predominantly occur where the mucosal layer is particularly thin.[93] Spontaneous incidences of necrosis has been reported in MRONJ patients to be as high as 36%[261] and 42%.[262] Vescovi et al. reported approximately 32% of untriggered cases in a cohort of 567 BRONJ patients.[263] Spontanenous cases have ranged from mild to severe[264, 265], and antiresorptive toxicity to the fibroblast layer could be implicated in the development of this complication.

Reported radiologic findings in the BRONJ literature have included cortical surface irregularities, persistent extraction sockets, sequestration, lytic or radiolucent changes, and an increase in sclerosis with progressing disease severity.[82, 84] To date, radiographic changes in DRONJ have not been addressed beyond case reports in literature. Our analysis of all available radiographic images revealed that dental practioners can expect osteosclerosis, cortical bone erosion, and persistent extraction sockets as the most common radiographic signs of MRONJ. Other studies have also noted that osteosclerosis was frequently observed in all stages of BRONJ, which corresponded to our proposed mechanism of over-ossification and subsequently reduced osteocyte

network from the histologic results.[176, 266] Similar radiographic features of cortical thickening have been reported with osteopetrosis, with clinical findings of brittle bone susceptible to infection.[267, 268] Focal or diffuse osteosclerosis was a consistent finding in patients with stage 0 MRONJ without exposed bone in the clinically symptomatic area.[269] We also noted evidence of osteosclerosis prominent in areas of necrosis, frequently with extension beyond the lesion. However, we did not find any differences that would allow us to differentiate BRONJ, DRONJ, and Mixed ONJ upon radiologic exam. There were also no obvious differences in radiographic findings with regard to antiresorptive type, MRONJ disease variant, presence of pain, and healing.

CBCT was more effective in the visualization of bony fistula, fracture, and the extent of the sequestrum compared to CT, and also detected 18.4% more findings than panoramic radiograph in intraindividual comparisons of simultaneous panoramic radiograph and CBCT imaging studies. CBCT was particularly superior for DRONJ patients with poor healing but minimal radiographic signs upon panoramic radiograph imaging, which did not demonstrate the extent of the lesion. CT was helpful for visualizing maxillary sinus involvement and lymph node involvement. However, radiographic signs observed on CT and MRI have been reported to be non-specific for the disease.[270] Furthermore, though they exceeded panoramic radiographs in the detectability of BRONJ lesions, CT and MRI were reported to underestimate the extent of the intra-operative lesion within a range of 50%.[85] Panoramic radiograph was useful for visualizing sclerosis, though did not provide as much detail as 3D imaging modalities. Bianchi et al. found that CBCT was superior than panoramic radiograph in detecting six common radiologic signs, since panoramic radiograph often missed the diagnosis of sequestration.[83] CBCT could be recommended for all MRONJ variants, particularly in cases where panoramic radiograph does not demonstrate the extent of the lesion per clinical judgement.

We observed that patients who receive operative intervention were more likely to have improved outcomes upon both clinical exam and evaluation of radiographic signs. Patients who were operated on were more likely to exhibit improved or stable sequestrum lesions upon radiographic exam; this remained statistically significant even when controlling for age and presence of pain. Patients in the operative group were also more likely to have improved or stable bony fistulas observed on radiographs compared to non-operatively managed patients, which remained statistically significant when controlling for age. Operated patients were also more likely to be healed compared to patients who received non-operative treatment, regardless of controlling for MRONJ stage, pain, and number of medication doses. Ruggiero and Kohn reported that operative management such as alveolectomy, marginal resection, or segmental resection was 28 times more likely to have an improved outcome compared to non-operative management in a retrospective study of 337 patients.[262] Positive outcomes and cure rates were also reported in other investigations for patients treated operatively for MRONJ[271-274]; however, details regarding radiographic changes were sparse.

4.7 Study limitations

A major limitation of our laboratory experiments with HGFs was that we were not able to simulate the oral mucosa as a whole *in vitro*. Although we attempted to account for the interactions of gingival fibroblasts with a macrophagic cell line of the local immune system, it would be ideal to be able to observe the effects of the cellular composition of the entire epithelium and connective tissue in response to antiresorptive medications, along with interactions with the underlying bone. Ravosa et al. investigated both oral keratinocytes and fibroblast cells lines in a study with various concentrations of zoledronate and found that oral fibroblasts were more susceptible to BPs than epithelial cells.[103] Scheper et al. observed fibroblast growth inhibition at low BP concentrations which

affected keratinocytes with increasing concentration.[45] A 3-dimensional oral mucosal wound-healing model was established using a mixture of fibroblasts in a collagen stromal bed with keratinocytes plated on top days later.[97] This transwell containing the fibroblast/keratinocyte bed was air-lifted for the administration of BP and impaired proliferation and migration of oral mucosal cells was observed.[275] A more comprehensive model including cells of the immune system, endothelial network, and underlying bone would be ideal to elucidate the exact interactions in the pathogenic process of MRONJ. This could be considered with the use of hydroxyapatite scaffolds underneath the above-mentioned 3-dimensional oral mucosal model.

The oncologic nature of the THP-1 cell used in co-culture may also have some limitations with respect to their immortalized character.[48] This may have contributed to fluctuations in measurements of the co-culture, and future studies may consider isolated human monocytes. Future research would also benefit from expanded analyses of additional cytokines associated with hard and soft tissue homeostasis, including TGF-β, matrix metalloproteinases (MMPs), CXCL12, and CXCR4, with investigation of Smad-dependent signaling pathway inhibition. Further analyses to clarify the influence of IL-6 is recommended.

Our histologic study was affected by small sample sizes of less common diseases such as DRONJ, Mixed ONJ, and bone exposed to both BPs and denosumab. This was because our patient cohort, unlike other case series, included patients treated with denosumab not previously exposed to other antiresorptives in order to isolate the behavior of agent-specific osteonecrosis and eliminate confounding histories. Bone specimens in general were characterized by a high heterogeneity and sometimes poor sample quality. Histomorphometric analyses with micro-CT could have also been influenced according to which views were selected at random for the measurement of trabecular width or the percentage of medullary space to bone. A dearth of long-

term follow-up data limited our attempt to describe changes in radiographic signs over time. Due to the retrospective nature of both clinical investigations, we were unable to perform more comprehensive time-to-event statistical analyses.

4.8 Future areas of research

Newer cases of MRONJ are being reported with other medication classes[18-20] used in cancer therapy, and the use of potent nitrogen-containing BPs to treat osteoporosis is increasing in practice.[276] Therefore, clinicians and researchers may expect to see an increase in the incidence of MRONJ. Our next project will expand experiments with HGFs to TKIs, mTOR inhibitors, and VEGF inhibitors, alone and in combination with BPs. Recently, De Colli et al. reported that newly synthesized sulfonamide-containing BPs did not affect HGF viability and adhesion when compared to zoledronate. Future studies could also be directed to investigating new molecules which may be better tolerated by soft and hard tissues.[277]

4.9 Conclusion

MRONJ is a disease growing in prevalence for which the pathogenesis remains unclear. We propose that the etiology of MRONJ could be attributed to a multifactorial process involving both the hard and soft tissues of the maxillo-mandibular region (Figure 37). This could include over-suppressed bone turnover as a mechanism combined with soft tissue toxicity, immune dysfunction, disturbed bone resorption, and a bacterial presence, which could help explain why these lesions are not present elsewhere in the skeleton. The anatomical features of thin oral mucosa with no fat or fascia separating it from the underlying bone in combination with the sustained forces of daily jaw movement and constant bacterial exposure make the oral cavity a unique location for the occurrence of MRONJ. We found that antiresorptives resulted in HGF death and

delayed wound healing, which was medication dose-dependent. There was also evidence of an alteration of the immune response, in particularly in co-culture with THP-1 cells, which demonstrated an excessive production of IL-1β and TNF and suppressed levels of IL-6 in high concentrations of nitrogen-containing BPs. This was exacerbated by bacterial LPS, which has been demonstrated along with IL-1β and TNF to activate the inflammatory response and cause bone resorption.[62, 139, 190]

Osteoclast inhibition was noted in gingival fibroblasts, but bone specimens exhibited cells positively stained for RANKL and TRAP for BRONJ and Mixed ONJ disease groups. We suggest this could be due to an M2 to M1 pro-inflammatory cytokine profile shift resulting in dysfunctional and destructive osteoclastic-macrophagic cells unable to resolve a continued process of inflammation and bone resorption. The alveolar process is unique from other skeletal sites as it endures significant mechanical force adjacent to a thin epithelium constantly exposed to bacterial agents.[231] It could also be possible that bacterial invasion combined with a dysfunctional immune response could give rise to a cell type in the macrophage-osteoclast continuum with the capability to resorb functional and vital bone, accounting for the presence of sequestra in MRONJ.

We suggest that a suppressed normal bone turnover could result in over-ossification of bone and crowding out of osteocytes leading to a decreased osteocyte network unable to maintain bone homeostasis. A consequent increased metabolic demand where nutrition for bone would have a longer distance to travel could generate silently expanding areas of matrix necrosis. We did not observe any evidence of inhibited angiogenesis in both the *in vitro* and histologic studies. This could be a compensatory mechanism of the vasculature to respond to an increasing metabolic demand due to a dearth of osteocyte networks. The destructive cycle could be further perpetuated when vascular flow

to the affected regions could function in allowing more antiresorptives to enter the bone and extracellular fluid.

Our results also lead us to believe that the pathogenesis of MRONJ due to BPs and denosumab could develop via differing mechanisms of action resulting in similar clinical appearances of necrosis. BRONJ lesions appear to be affected more by soft tissue toxicity and an inability to activate the acquired immune response resulting in a dysfunctional macrophagic-osteoclastic cell-induced bone destruction. DRONJ seems to be more influenced by over-ossification and a decreased osteocyte network due to its RANKL-inhibiting pharmacologic action, which could lead to ischemic-necrotic changes seen in necrosis. When combined with mechanical trauma, infection, and further immunosuppression from concurrent therapies, these factors may lead to the development of MRONJ.

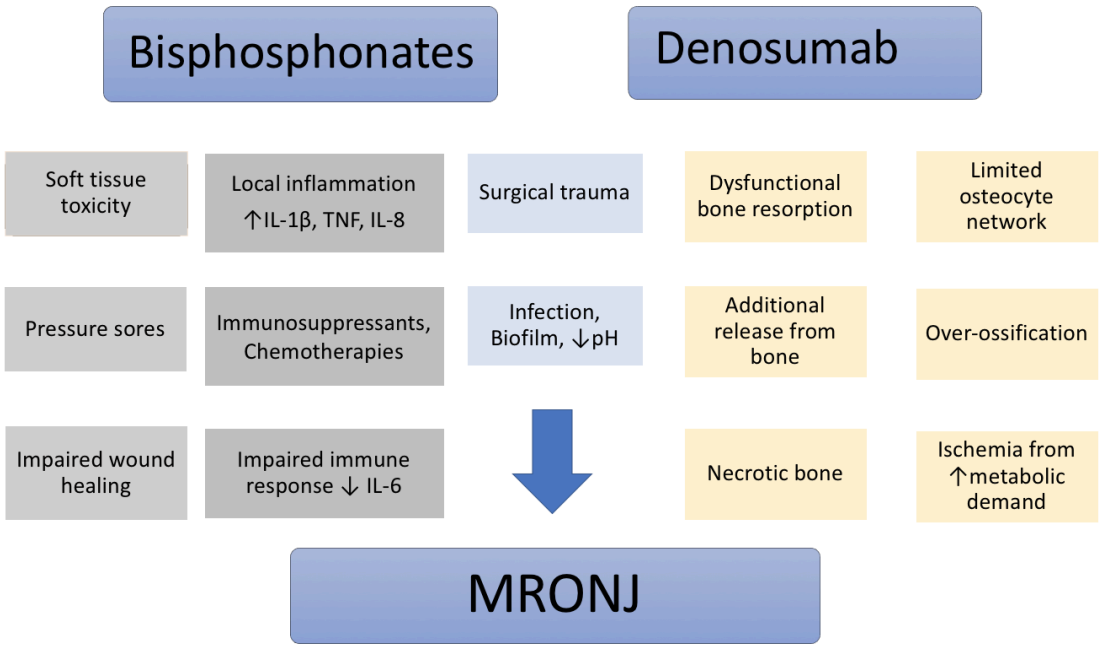

Figure 37. Proposed model of the pathogenesis of medication-related osteonecrosis of the jaw (MRONJ). The etiology of MRONJ could be attributed to a multifactorial process involving soft tissue toxicity,

mechanical damage and surgical trauma, local inflammation, immune suppression and dysfunction, infection and biofilm alteration, dysfunctional bone resorption, over-ossification and a limited osteocyte network, and impaired wound healing leading to necrotic bone exposure.

5 Summary

Although the first incidence of MRONJ was described over fifteen years ago, to date the pathogenesis of the disease remains unclear. As a result, there is no consensus on a unified treatment or prevention protocol. Treatment of MRONJ is difficult and costly, and disease sequela can include pain, infection, inability to eat, extraoral fistula, and pathologic fracture, all of which significantly impact the quality of life for patients.

Since the role of soft tissue in the pathogenesis of MRONJ is particularly not well defined, this doctoral project aimed to investigate the role of BPs and denosumab to induce or inhibit cell death and inflammation in the expression patterns of HGFs, and to observe the influence on wound healing and angiogenesis in response to antiresorptive therapy. A novel real-time *in vitro* assay was performed on HGFs with and without the addition of bacterial LPS and a co-culture of mononuclear cells to observe the effect of various antiresorptives (zoledronate, ibandronate, alendronate, clodronate, denosumab, and combinations of zoledronate and denosumab) at estimated low, middle, and high concentrations using the xCelligence system. A wound healing assay was also performed, and gene and protein expression was analyzed for various cytokines and mediators, including IL-1β, IL-6, IL-8, VEGF, TNF, OPG, and RANKL.

Retrospective histologic and radiographic studies were also conducted to correlate the altered bone structure with different disease variants and degree of antiresorptive exposure in *in vivo* studies of the accompanying hard tissue. A total of 158 bone biopsies were collected from patients with various infectious, inflammatory, and necrotic jaw diseases and stained with H&E, RANKL, OPG, TRAP, toluidine blue, CD14, and CD68. Micro CT of the samples were additionally analyzed. Radiographic records of 37 MRONJ patients were reviewed for imaging findings before and after disease management. Radiographic signs of necrosis were noted in MRONJ disease variants and imaging techniques were compared

to evaluate the correlation of the clinical presentation and outcomes with imaging findings in a total of 86 radiographic studies.

Our results revealed that higher concentrations of antiresorptives resulted in HGF cell death (zoledronate 50 μM at 66.0 hours; alendronate 50 μM at 64.0 hours; ibandronate 50 μM at 66.0 hours, all $p < .05$ compared to controls at 90.4 hours) and impaired wound healing (clodronate 500 μM, ibandronate 5 μM and 50 μM, alendronate 50 μM, zoledronate 5 μM + denosumab 10 μg/mL, and zoledronate 5 μM). These effects increased with the introduction of bacterial LPS (aledronate 5 μM and 0.5 μM additionally affected, $p < .05$) and in co-culture with a mononuclear cell line (zoledronate 5 μM and zoledronate 5 μM + densumab 40 μg/mL additionally affected, $p < .05$). There were also signs of altered immune response, with an elevated immune reaction and possible dysfunction as a result of exposure to antiresorptives. Increased levels of TNF (443 gene copies of zoledronate 50 μM with LPS and 2.66 gene copies of denosumab 40 μg/mL with LPS compared to 0 in control), IL-8 (16.9 gene copies of zoledronate 50 μM with LPS compared to 0.007 gene copies in control), IL-1β (all concentrations increased, $p < .05$), and CD14 and CD68 expression (Mixed ONJ and BRONJ $p < .001$) were observed, perhaps due to a sustained inflammatory response, while an IL-6 response was missing for high concentrations of nitrogen-containing BPs (all $p < .05$), which may suggest a deficiency in the shift from innate to acquired immunity.

Osteoclast inhibition was noted in HGFs which demonstrated an increased expression of OPG upon exposure to zoledronate (773 gene copies) and denosumab (6.01 gene copies) compared to 0.28 in control, with low levels of RANKL. However, bone specimens exhibited cells positively stained for RANKL (BRONJ $p = .021$) and TRAP (Mixed ONJ $p = .002$; BRONJ $p < .001$; BP-exposed $p = .017$). There was no evidence of an anti-angiogenic effect as evidenced by levels of VEGF and IL-8 as well as the appearance of intact Haversian systems in the bone. Upon examination of the bone tissues in the histologic and radiographic

study, results suggest that a limited osteocyte network (mean number of osteocyte lacunae per μm^2 in DRONJ: 0.00026, $p < .05$) and over-ossification of the bone (decreased ratio of medullary space to bone $p < .01$ for MRONJ variants; increased trabecular width of 601.71 μm in Mixed ONJ; $p = .03$; presence of sclerosis upon radiographic exam in 92% of MRONJ patients) could play in a role in disease development. Our findings lead us to believe that the precise pathogenesis could differ based on whether the offending agent is a BP or denosumab, which still may result in a similar appearance of necrosis. From our clinical studies, patients who received operative treatment were more likely to exhibit complete healing compared to patients who received non-operative management ($p = .001$). CBCT was more effective to visualize bony fistula, fracture, and the extent of the sequestrum (68.2% detectability) compared to CT (30.8% detectability), and detected 18.4% more findings than panoramic radiograph in simultaneous comparisons.

Many of these findings could have important implications for researchers investigating MRONJ and provide clinical relevance for treating practitioners. This was the first investigation of HGFs in real-time, particularly with a wide range of BP concentrations. To study the effect of denosumab on HGFs, as well to introduce a combination of zoledronate and denosumab concentrations to simulate a realistic clinical situation, were also novel research objectives. Furthermore, these results present previously unreported details on the features of DRONJ, Mixed ONJ, BP-exposed bone, and BP-and denosumab-exposed bone, particularly as we were able to identify features of denosumab-specific ONJ without influence from previous BP therapy.

6 References

1. Campisi, G., et al., *Epidemiology, clinical manifestations, risk reduction and treatment strategies of jaw osteonecrosis in cancer patients exposed to antiresorptive agents.* Future Oncol, 2014. **10**(2): p. 257-75.
2. Russell, R.G., *Bisphosphonates: the first 40 years.* Bone, 2011. **49**(1): p. 2-19.
3. Green, J.R., *Chemical and biological prerequisites for novel bisphosphonate molecules: results of comparative preclinical studies.* Semin Oncol, 2001. **28**(2 Suppl 6): p. 4-10.
4. Nancollas, G.H., et al., *Novel insights into actions of bisphosphonates on bone: differences in interactions with hydroxyapatite.* Bone, 2006. **38**(5): p. 617-27.
5. Baron, R., S. Ferrari, and R.G. Russell, *Denosumab and bisphosphonates: different mechanisms of action and effects.* Bone, 2011. **48**(4): p. 677-92.
6. Bekker, P.J., et al., *A single-dose placebo-controlled study of AMG 162, a fully human monoclonal antibody to RANKL, in postmenopausal women.* J Bone Miner Res, 2004. **19**(7): p. 1059-66.
7. Ruggiero, S.L., et al., *American Association of Oral and Maxillofacial Surgeons position paper on medication-related osteonecrosis of the jaw--2014 update.* J Oral Maxillofac Surg, 2014. **72**(10): p. 1938-56.
8. Ruggiero, S.L. and B. Mehrotra, *Bisphosphonate-related osteonecrosis of the jaw: diagnosis, prevention, and management.* Annu Rev Med, 2009. **60**: p. 85-96.
9. Khan, A.A., et al., *Diagnosis and management of osteonecrosis of the jaw: a systematic review and international consensus.* J Bone Miner Res, 2015. **30**(1): p. 3-23.
10. Marx, R.E., *Pamidronate (Aredia) and zoledronate (Zometa) induced avascular necrosis of the jaws: a growing epidemic.* J Oral Maxillofac Surg, 2003. **61**(9): p. 1115-7.
11. Diz, P., et al., *Denosumab-related osteonecrosis of the jaw.* J Am Dent Assoc, 2012. **143**(9): p. 981-4.
12. Boonyapakorn, T., et al., *Bisphosphonate-induced osteonecrosis of the jaws: prospective study of 80 patients with multiple myeloma and other malignancies.* Oral Oncol, 2008. **44**(9): p. 857-69.
13. Kuhl, S., et al., *Bisphosphonate-related osteonecrosis of the jaws--a review.* Oral Oncol, 2012. **48**(10): p. 938-47.
14. Migliorati, C.A. and J.S. Covington, 3rd, *New oncology drugs and osteonecrosis of the jaw (ONJ).* J Tenn Dent Assoc, 2009. **89**(4): p. 36-8; quiz 38-9.
15. Vahtsevanos, K., et al., *Longitudinal cohort study of risk factors in cancer patients of bisphosphonate-related osteonecrosis of the jaw.* J Clin Oncol, 2009. **27**(32): p. 5356-62.
16. Katsarelis, H., et al., *Infection and medication-related osteonecrosis of the jaw.* J Dent Res, 2015. **94**(4): p. 534-9.

17. Epstein, M.S., H.D. Ephros, and J.B. Epstein, *Review of current literature and implications of RANKL inhibitors for oral health care providers.* Oral Surg Oral Med Oral Pathol Oral Radiol, 2013. **116**(6): p. e437-42.
18. Guarneri, V., et al., *Bevacizumab and osteonecrosis of the jaw: incidence and association with bisphosphonate therapy in three large prospective trials in advanced breast cancer.* Breast Cancer Res Treat, 2010. **122**(1): p. 181-8.
19. Koch, F.P., et al., *Osteonecrosis of the jaw related to sunitinib.* Oral Maxillofac Surg, 2011. **15**(1): p. 63-6.
20. Fleissig, Y., E. Regev, and H. Lehman, *Sunitinib related osteonecrosis of jaw: a case report.* Oral Surg Oral Med Oral Pathol Oral Radiol, 2012. **113**(3): p. e1-3.
21. Troeltzsch, M., et al., *Physiology and pharmacology of nonbisphosphonate drugs implicated in osteonecrosis of the jaw.* J Can Dent Assoc, 2012. **78**: p. c85.
22. Kumar, V. and R.K. Sinha, *Evolution and etiopathogenesis of bisphosphonates induced osteonecrosis of the jaw.* N Am J Med Sci, 2013. **5**(4): p. 260-5.
23. Garetto, L.P., et al., *Remodeling dynamics of bone supporting rigidly fixed titanium implants: a histomorphometric comparison in four species including humans.* Implant Dent, 1995. **4**(4): p. 235-43.
24. Han, Z.H., et al., *Effects of ethnicity and age or menopause on the remodeling and turnover of iliac bone: implications for mechanisms of bone loss.* J Bone Miner Res, 1997. **12**(4): p. 498-508.
25. Reid, I.R., M.J. Bolland, and A.B. Grey, *Is bisphosphonate-associated osteonecrosis of the jaw caused by soft tissue toxicity?* Bone, 2007. **41**(3): p. 318-20.
26. Matsuura, T., et al., *Distinct characteristics of mandibular bone collagen relative to long bone collagen: relevance to clinical dentistry.* Biomed Res Int, 2014. **2014**: p. 769414.
27. Perez-Amodio, S., et al., *Calvarial osteoclasts express a higher level of tartrate-resistant acid phosphatase than long bone osteoclasts and activation does not depend on cathepsin K or L activity.* Calcif Tissue Int, 2006. **79**(4): p. 245-54.
28. Allen, M.R. and D.B. Burr, *The pathogenesis of bisphosphonate-related osteonecrosis of the jaw: so many hypotheses, so few data.* J Oral Maxillofac Surg, 2009. **67**(5 Suppl): p. 61-70.
29. Ruggiero, S.L., et al., *Osteonecrosis of the jaws associated with the use of bisphosphonates: a review of 63 cases.* J Oral Maxillofac Surg, 2004. **62**(5): p. 527-34.
30. Marx, R.E., et al., *Bisphosphonate-induced exposed bone (osteonecrosis/osteopetrosis) of the jaws: risk factors, recognition, prevention, and treatment.* J Oral Maxillofac Surg, 2005. **63**(11): p. 1567-75.
31. Wood, J., et al., *Novel antiangiogenic effects of the bisphosphonate compound zoledronic acid.* J Pharmacol Exp Ther, 2002. **302**(3): p. 1055-61.
32. Mehrotra, B. and S. Ruggiero, *Bisphosphonate complications including osteonecrosis of the jaw.* Hematology Am Soc Hematol Educ Program, 2006: p. 356-60, 515.

33. Sonis, S.T., et al., *Bony changes in the jaws of rats treated with zoledronic acid and dexamethasone before dental extractions mimic bisphosphonate-related osteonecrosis in cancer patients.* Oral Oncol, 2009. **45**(2): p. 164-72.
34. Hoefert, S., et al., *Zoledronate but not denosumab suppresses macrophagic differentiation of THP-1 cells. An aetiologic model of bisphosphonate-related osteonecrosis of the jaw (BRONJ).* Clin Oral Investig, 2014.
35. Hoefert, S., et al., *Macrophages and bisphosphonate-related osteonecrosis of the jaw (BRONJ): evidence of local immunosuppression of macrophages in contrast to other infectious jaw diseases.* Clin Oral Investig, 2015. **19**(2): p. 497-508.
36. Hoefert, S., et al., *Altered macrophagic THP-1 cell phagocytosis and migration in bisphosphonate-related osteonecrosis of the jaw (BRONJ).* Clin Oral Investig, 2016. **20**(5): p. 1043-54.
37. Hokugo, A., et al., *Increased prevalence of bisphosphonate-related osteonecrosis of the jaw with vitamin D deficiency in rats.* J Bone Miner Res, 2010. **25**(6): p. 1337-49.
38. Carmagnola, D., et al., *Histological findings on jaw osteonecrosis associated with bisphosphonates (BONJ) or with radiotherapy (ORN) in humans.* Acta Odontol Scand, 2013. **71**(6): p. 1410-7.
39. Favia, G., G.P. Pilolli, and E. Maiorano, *Histologic and histomorphometric features of bisphosphonate-related osteonecrosis of the jaws: an analysis of 31 cases with confocal laser scanning microscopy.* Bone, 2009. **45**(3): p. 406-13.
40. Mawardi, H., et al., *A role of oral bacteria in bisphosphonate-induced osteonecrosis of the jaw.* J Dent Res, 2011. **90**(11): p. 1339-45.
41. Landesberg, R., et al., *Inhibition of oral mucosal cell wound healing by bisphosphonates.* J Oral Maxillofac Surg, 2008. **66**(5): p. 839-47.
42. Saracino, S., et al., *Exposing human epithelial cells to zoledronic acid can mediate osteonecrosis of jaw: an in vitro model.* J Oral Pathol Med, 2012. **41**(10): p. 788-92.
43. Scheper, M., et al., *A novel soft-tissue in vitro model for bisphosphonate-associated osteonecrosis.* Fibrogenesis Tissue Repair, 2010. **3**: p. 6.
44. Acil, Y., et al., *The cytotoxic effects of three different bisphosphonates in-vitro on human gingival fibroblasts, osteoblasts and osteogenic sarcoma cells.* J Craniomaxillofac Surg, 2012. **40**(8): p. e229-35.
45. Scheper, M.A., et al., *Effect of zoledronic acid on oral fibroblasts and epithelial cells: a potential mechanism of bisphosphonate-associated osteonecrosis.* Br J Haematol, 2009. **144**(5): p. 667-76.
46. Limame, R., et al., *Comparative analysis of dynamic cell viability, migration and invasion assessments by novel real-time technology and classic endpoint assays.* PLoS One, 2012. **7**(10): p. e46536.
47. Qin, Z., *The use of THP-1 cells as a model for mimicking the function and regulation of monocytes and macrophages in the vasculature.* Atherosclerosis, 2012. **221**(1): p. 2-11.

48. Chanput, W., J.J. Mes, and H.J. Wichers, *THP-1 cell line: an in vitro cell model for immune modulation approach.* Int Immunopharmacol, 2014. **23**(1): p. 37-45.
49. Baek, K.J., Y. Choi, and S. Ji, *Gingival fibroblasts from periodontitis patients exhibit inflammatory characteristics in vitro.* Arch Oral Biol, 2013. **58**(10): p. 1282-92.
50. Suthin, K., et al., *Enhanced expression of vascular endothelial growth factor by periodontal pathogens in gingival fibroblasts.* J Periodontal Res, 2003. **38**(1): p. 90-6.
51. Lacey, D.L., et al., *Osteoprotegerin ligand is a cytokine that regulates osteoclast differentiation and activation.* Cell, 1998. **93**(2): p. 165-76.
52. Kong, Y.Y., et al., *OPGL is a key regulator of osteoclastogenesis, lymphocyte development and lymph-node organogenesis.* Nature, 1999. **397**(6717): p. 315-23.
53. Hsu, H., et al., *Tumor necrosis factor receptor family member RANK mediates osteoclast differentiation and activation induced by osteoprotegerin ligand.* Proc Natl Acad Sci U S A, 1999. **96**(7): p. 3540-5.
54. Teitelbaum, S.L. and F.P. Ross, *Genetic regulation of osteoclast development and function.* Nat Rev Genet, 2003. **4**(8): p. 638-49.
55. Simonet, W.S., et al., *Osteoprotegerin: a novel secreted protein involved in the regulation of bone density.* Cell, 1997. **89**(2): p. 309-19.
56. Bostanci, N., et al., *Differential expression of receptor activator of nuclear factor-kappaB ligand and osteoprotegerin mRNA in periodontal diseases.* J Periodontal Res, 2007. **42**(4): p. 287-93.
57. Mogi, M., et al., *Differential expression of RANKL and osteoprotegerin in gingival crevicular fluid of patients with periodontitis.* J Dent Res, 2004. **83**(2): p. 166-9.
58. De Colli, M., et al., *Nitric oxide-mediated cytotoxic effect induced by zoledronic acid treatment on human gingival fibroblasts.* Clin Oral Investig, 2015. **19**(6): p. 1269-77.
59. Dinarello, C.A., *Biologic basis for interleukin-1 in disease.* Blood, 1996. **87**(6): p. 2095-147.
60. Pfizenmaier, K., H. Wajant, and M. Grell, *Tumor necrosis factors in 1996.* Cytokine Growth Factor Rev, 1996. **7**(3): p. 271-7.
61. Graves, D.T. and D. Cochran, *The contribution of interleukin-1 and tumor necrosis factor to periodontal tissue destruction.* J Periodontol, 2003. **74**(3): p. 391-401.
62. Matsumoto, A., H. Anan, and K. Maeda, *An immunohistochemical study of the behavior of cells expressing interleukin-1 alpha and interleukin-1 beta within experimentally induced periapical lesions in rats.* J Endod, 1998. **24**(12): p. 811-6.
63. Chiang, C.Y., et al., *Interleukin-1 and tumor necrosis factor activities partially account for calvarial bone resorption induced by local injection of lipopolysaccharide.* Infect Immun, 1999. **67**(8): p. 4231-6.

64. Wang, C.Y., N. Tani-Ishii, and P. Stashenko, *Bone-resorptive cytokine gene expression in periapical lesions in the rat.* Oral Microbiol Immunol, 1997. **12**(2): p. 65-71.
65. Takahashi, K., et al., *Assessment of interleukin-6 in the pathogenesis of periodontal disease.* J Periodontol, 1994. **65**(2): p. 147-53.
66. Han, Y.W., et al., *Interactions between periodontal bacteria and human oral epithelial cells: Fusobacterium nucleatum adheres to and invades epithelial cells.* Infect Immun, 2000. **68**(6): p. 3140-6.
67. Moreau, M.F., et al., *Comparative effects of five bisphosphonates on apoptosis of macrophage cells in vitro.* Biochem Pharmacol, 2007. **73**(5): p. 718-23.
68. Zhao, L., et al., *Effects of biphenyl sulfonylamino methyl bisphosphonic acids on Porphyromonas gingivalis and cytokine secretion by oral epithelial cells.* Med Chem, 2013. **9**(6): p. 855-60.
69. Soydan, S.S., et al., *Effects of alendronate and pamidronate on apoptosis and cell proliferation in cultured primary human gingival fibroblasts.* Hum Exp Toxicol, 2015. **34**(11): p. 1073-82.
70. Cozin, M., et al., *Novel therapy to reverse the cellular effects of bisphosphonates on primary human oral fibroblasts.* J Oral Maxillofac Surg, 2011. **69**(10): p. 2564-78.
71. Ziebart, T., et al., *Geranylgeraniol - a new potential therapeutic approach to bisphosphonate associated osteonecrosis of the jaw.* Oral Oncol, 2011. **47**(3): p. 195-201.
72. Walter, C., et al., *Prevalence and risk factors of bisphosphonate-associated osteonecrosis of the jaw in prostate cancer patients with advanced disease treated with zoledronate.* Eur Urol, 2008. **54**(5): p. 1066-72.
73. Cremers, S.C., G. Pillai, and S.E. Papapoulos, *Pharmacokinetics/pharmacodynamics of bisphosphonates: use for optimisation of intermittent therapy for osteoporosis.* Clin Pharmacokinet, 2005. **44**(6): p. 551-70.
74. Komatsu, Y., et al., *Zoledronic acid suppresses transforming growth factor-beta-induced fibrogenesis by human gingival fibroblasts.* Int J Mol Med, 2016. **38**(1): p. 139-47.
75. Jones, G.R., et al., *Mass or molar? Recommendations for reporting concentrations of therapeutic drugs.* Med J Aust, 2013. **198**(7): p. 368-9.
76. Hosokawa, Y., et al., *Increase of CCL20 expression by human gingival fibroblasts upon stimulation with cytokines and bacterial endotoxin.* Clin Exp Immunol, 2005. **142**(2): p. 285-91.
77. Hosokawa, Y., et al., *CXCL12 and CXCR4 expression by human gingival fibroblasts in periodontal disease.* Clin Exp Immunol, 2005. **141**(3): p. 467-74.
78. Domeij, H., T. Yucel-Lindberg, and T. Modeer, *Cell interactions between human gingival fibroblasts and monocytes stimulate the production of matrix metalloproteinase-1 in gingival fibroblasts.* J Periodontal Res, 2006. **41**(2): p. 108-17.

79. Seguier, S., et al., *Inhibition of the differentiation of monocyte-derived dendritic cells by human gingival fibroblasts.* PLoS One, 2013. **8**(8): p. e70937.
80. Allred, D.C., et al., *Prognostic and predictive factors in breast cancer by immunohistochemical analysis.* Mod Pathol, 1998. **11**(2): p. 155-68.
81. Harvey, J.M., et al., *Estrogen receptor status by immunohistochemistry is superior to the ligand-binding assay for predicting response to adjuvant endocrine therapy in breast cancer.* J Clin Oncol, 1999. **17**(5): p. 1474-81.
82. Arce, K., et al., *Imaging findings in bisphosphonate-related osteonecrosis of jaws.* J Oral Maxillofac Surg, 2009. **67**(5 Suppl): p. 75-84.
83. Bianchi, S.D., et al., *Computerized tomographic findings in bisphosphonate-associated osteonecrosis of the jaw in patients with cancer.* Oral Surg Oral Med Oral Pathol Oral Radiol Endod, 2007. **104**(2): p. 249-58.
84. Leite, A.F., et al., *Imaging findings of bisphosphonate-related osteonecrosis of the jaws: a critical review of the quantitative studies.* Int J Dent, 2014. **2014**: p. 784348.
85. Stockmann, P., et al., *Panoramic radiograph, computed tomography or magnetic resonance imaging. Which imaging technique should be preferred in bisphosphonate-associated osteonecrosis of the jaw? A prospective clinical study.* Clin Oral Investig, 2010. **14**(3): p. 311-7.
86. Reid, I.R., *Osteonecrosis of the jaw: who gets it, and why?* Bone, 2009. **44**(1): p. 4-10.
87. Reid, I.R. and J. Cornish, *Epidemiology and pathogenesis of osteonecrosis of the jaw.* Nat Rev Rheumatol, 2011. **8**(2): p. 90-6.
88. Giraudo, E., M. Inoue, and D. Hanahan, *An amino-bisphosphonate targets MMP-9-expressing macrophages and angiogenesis to impair cervical carcinogenesis.* J Clin Invest, 2004. **114**(5): p. 623-33.
89. Montague, R., et al., *Differential inhibition of invasion and proliferation by bisphosphonates: anti-metastatic potential of Zoledronic acid in prostate cancer.* Eur Urol, 2004. **46**(3): p. 389-401; discussion 401-2.
90. Twiss, I.M., et al., *The effects of nitrogen-containing bisphosphonates on human epithelial (Caco-2) cells, an in vitro model for intestinal epithelium.* J Bone Miner Res, 1999. **14**(5): p. 784-91.
91. de Groen, P.C., et al., *Esophagitis associated with the use of alendronate.* N Engl J Med, 1996. **335**(14): p. 1016-21.
92. Rubegni, P. and M. Fimiani, *Images in clinical medicine. Bisphosphonate-associated contact stomatitis.* N Engl J Med, 2006. **355**(22): p. e25.
93. Otto, S., et al., *Bisphosphonate-related osteonecrosis of the jaw: is pH the missing part in the pathogenesis puzzle?* J Oral Maxillofac Surg, 2010. **68**(5): p. 1158-61.
94. Otto, S., et al., *Bisphosphonate-related osteonecrosis of the jaws - characteristics, risk factors, clinical features, localization and impact on oncological treatment.* J Craniomaxillofac Surg, 2012. **40**(4): p. 303-9.
95. Walter, C., et al., *Influence of bisphosphonates on endothelial cells, fibroblasts, and osteogenic cells.* Clin Oral Investig, 2010. **14**(1): p. 35-41.

96. Pabst, A.M., et al., *The influence of bisphosphonates on viability, migration, and apoptosis of human oral keratinocytes--in vitro study.* Clin Oral Investig, 2012. **16**(1): p. 87-93.
97. Kim, R.H., et al., *Bisphosphonates induce senescence in normal human oral keratinocytes.* J Dent Res, 2011. **90**(6): p. 810-6.
98. Lorenzo, S.D., et al., *Histology of the Oral Mucosa in Patients With BRONJ at III Stage: A Microscopic Study Proves the Unsuitability of Local Mucosal Flaps.* J Clin Med Res, 2013. **5**(1): p. 22-5.
99. Correia Vde, F., C.L. Caldeira, and M.M. Marques, *Cytotoxicity evaluation of sodium alendronate on cultured human periodontal ligament fibroblasts.* Dent Traumatol, 2006. **22**(6): p. 312-7.
100. Agis, H., et al., *Is zoledronate toxic to human periodontal fibroblasts?* J Dent Res, 2010. **89**(1): p. 40-5.
101. Tipton, D.A., B.A. Seshul, and M. Dabbous, *Effect of bisphosphonates on human gingival fibroblast production of mediators of osteoclastogenesis: RANKL, osteoprotegerin and interleukin-6.* J Periodontal Res, 2011. **46**(1): p. 39-47.
102. Walter, C., et al., *Bisphosphonates affect migration ability and cell viability of HUVEC, fibroblasts and osteoblasts in vitro.* Oral Dis, 2011. **17**(2): p. 194-9.
103. Ravosa, M.J., et al., *Bisphosphonate effects on the behaviour of oral epithelial cells and oral fibroblasts.* Arch Oral Biol, 2011. **56**(5): p. 491-8.
104. Simon, M.J., et al., *Expression profile and synthesis of different collagen types I, II, III, and V of human gingival fibroblasts, osteoblasts, and SaOS-2 cells after bisphosphonate treatment.* Clin Oral Investig, 2010. **14**(1): p. 51-8.
105. Fu, Q., et al., *[Effect of zoledronic acid on cell proliferation and apoptosis of human periodontal fibroblasts].* Zhonghua Kou Qiang Yi Xue Za Zhi, 2015. **50**(11): p. 667-70.
106. Lim, S.S., et al., *Differential modulation of zoledronate and etidronate in osseous healing of an extracted socket and tibia defect.* Oral Surg Oral Med Oral Pathol Oral Radiol, 2017. **123**(1): p. 8-19.
107. Monkkonen, J., H.M. Koponen, and P. Ylitalo, *Comparison of the distribution of three bisphosphonates in mice.* Pharmacol Toxicol, 1990. **66**(4): p. 294-8.
108. Adamo, V., et al., *Current knowledge and future directions on bisphosphonate-related osteonecrosis of the jaw in cancer patients.* Expert Opin Pharmacother, 2008. **9**(8): p. 1351-61.
109. Burr, D.B. and M.R. Allen, *Mandibular necrosis in beagle dogs treated with bisphosphonates.* Orthod Craniofac Res, 2009. **12**(3): p. 221-8.
110. Reszka, A.A., J. Halasy-Nagy, and G.A. Rodan, *Nitrogen-bisphosphonates block retinoblastoma phosphorylation and cell growth by inhibiting the cholesterol biosynthetic pathway in a keratinocyte model for esophageal irritation.* Mol Pharmacol, 2001. **59**(2): p. 193-202.
111. Zafar, S., et al., *Zoledronic acid and geranylgeraniol regulate cellular behaviour and angiogenic gene expression in human gingival fibroblasts.* J Oral Pathol Med, 2014. **43**(9): p. 711-21.

112. Walker, K. and M.F. Olson, *Targeting Ras and Rho GTPases as opportunities for cancer therapeutics.* Curr Opin Genet Dev, 2005. **15**(1): p. 62-8.
113. Suri, S., et al., *Nitrogen-containing bisphosphonates induce apoptosis of Caco-2 cells in vitro by inhibiting the mevalonate pathway: a model of bisphosphonate-induced gastrointestinal toxicity.* Bone, 2001. **29**(4): p. 336-43.
114. Bamias, A., et al., *Osteonecrosis of the jaw in cancer after treatment with bisphosphonates: incidence and risk factors.* J Clin Oncol, 2005. **23**(34): p. 8580-7.
115. Kobayashi, Y., et al., *Zoledronic acid delays wound healing of the tooth extraction socket, inhibits oral epithelial cell migration, and promotes proliferation and adhesion to hydroxyapatite of oral bacteria, without causing osteonecrosis of the jaw, in mice.* J Bone Miner Metab, 2010. **28**(2): p. 165-75.
116. Dimopoulos, M.A., et al., *Reduction of osteonecrosis of the jaw (ONJ) after implementation of preventive measures in patients with multiple myeloma treated with zoledronic acid.* Ann Oncol, 2009. **20**(1): p. 117-20.
117. Montefusco, V., et al., *Antibiotic prophylaxis before dental procedures may reduce the incidence of osteonecrosis of the jaw in patients with multiple myeloma treated with bisphosphonates.* Leuk Lymphoma, 2008. **49**(11): p. 2156-62.
118. Ripamonti, C.I., et al., *Decreased occurrence of osteonecrosis of the jaw after implementation of dental preventive measures in solid tumour patients with bone metastases treated with bisphosphonates. The experience of the National Cancer Institute of Milan.* Ann Oncol, 2009. **20**(1): p. 137-45.
119. Kivovics, P., et al., *Frequency and location of traumatic ulcerations following placement of complete dentures.* Int J Prosthodont, 2007. **20**(4): p. 397-401.
120. Niibe, K., et al., *Osteonecrosis of the jaw in patients with dental prostheses being treated with bisphosphonates or denosumab.* J Prosthodont Res, 2015. **59**(1): p. 3-5.
121. Kuroshima, S., Z. Al-Salihi, and J. Yamashita, *Mouse anti-RANKL antibody delays oral wound healing and increases TRAP-positive mononuclear cells in bone marrow.* Clin Oral Investig, 2016. **20**(4): p. 727-36.
122. Roelofs, A.J., et al., *Peripheral blood monocytes are responsible for gammadelta T cell activation induced by zoledronic acid through accumulation of IPP/DMAPP.* Br J Haematol, 2009. **144**(2): p. 245-50.
123. Miyagawa, F., et al., *Essential requirement of antigen presentation by monocyte lineage cells for the activation of primary human gamma delta T cells by aminobisphosphonate antigen.* J Immunol, 2001. **166**(9): p. 5508-14.
124. Thompson, K. and M.J. Rogers, *Statins prevent bisphosphonate-induced gamma,delta-T-cell proliferation and activation in vitro.* J Bone Miner Res, 2004. **19**(2): p. 278-88.
125. Amgen, *Prolia (denosumab) package insert.*, in *Amgen Inc*. 2010: Thousand Oaks, CA.
126. Anastasilakis, A.D., et al., *Long-term treatment of osteoporosis: safety and efficacy appraisal of denosumab.* Ther Clin Risk Manag, 2012. **8**: p. 295-306.

127. Anderson, D.M., et al., *A homologue of the TNF receptor and its ligand enhance T-cell growth and dendritic-cell function.* Nature, 1997. **390**(6656): p. 175-9.
128. Wong, B.R., et al., *TRANCE (tumor necrosis factor [TNF]-related activation-induced cytokine), a new TNF family member predominantly expressed in T cells, is a dendritic cell-specific survival factor.* J Exp Med, 1997. **186**(12): p. 2075-80.
129. Wensel, T.M., M.M. Iranikhah, and T.W. Wilborn, *Effects of denosumab on bone mineral density and bone turnover in postmenopausal women.* Pharmacotherapy, 2011. **31**(5): p. 510-23.
130. Hoefert, S., et al., *Clinical course and therapeutic outcomes of operatively and non-operatively managed patients with denosumab-related osteonecrosis of the jaw (DRONJ).* J Craniomaxillofac Surg, 2017. **45**(4): p. 570-578.
131. Trevani, A.S., et al., *Bacterial DNA activates human neutrophils by a CpG-independent pathway.* Eur J Immunol, 2003. **33**(11): p. 3164-74.
132. Sonis, S.T., *Pathobiology of oral mucositis: novel insights and opportunities.* J Support Oncol, 2007. **5**(9 Suppl 4): p. 3-11.
133. Steffen, M.J., S.C. Holt, and J.L. Ebersole, *Porphyromonas gingivalis induction of mediator and cytokine secretion by human gingival fibroblasts.* Oral Microbiol Immunol, 2000. **15**(3): p. 172-80.
134. Ranney, R.R., *Immunologic mechanisms of pathogenesis in periodontal diseases: an assessment.* J Periodontal Res, 1991. **26**(3 Pt 2): p. 243-54.
135. Agarwal, S., et al., *Synthesis of proinflammatory cytokines by human gingival fibroblasts in response to lipopolysaccharides and interleukin-1 beta.* J Periodontal Res, 1995. **30**(6): p. 382-9.
136. Ogawa, T., H. Uchida, and K. Amino, *Immunobiological activities of chemically defined lipid A from lipopolysaccharides of Porphyromonas gingivalis.* Microbiology, 1994. **140 (Pt 5)**: p. 1209-16.
137. Yoshimura, A., et al., *Secretion of IL-1 beta, TNF-alpha, IL-8 and IL-1ra by human polymorphonuclear leukocytes in response to lipopolysaccharides from periodontopathic bacteria.* J Periodontal Res, 1997. **32**(3): p. 279-86.
138. Nishida, E., et al., *Bone resorption and local interleukin-1alpha and interleukin-1beta synthesis induced by Actinobacillus actinomycetemcomitans and Porphyromonas gingivalis lipopolysaccharide.* J Periodontal Res, 2001. **36**(1): p. 1-8.
139. Millar, S.J., et al., *Modulation of bone metabolism by two chemically distinct lipopolysaccharide fractions from Bacteroides gingivalis.* Infect Immun, 1986. **51**(1): p. 302-6.
140. Hanazawa, S., et al., *Functional role of interleukin 1 in periodontal disease: induction of interleukin 1 production by Bacteroides gingivalis lipopolysaccharide in peritoneal macrophages from C3H/HeN and C3H/HeJ mice.* Infect Immun, 1985. **50**(1): p. 262-70.
141. Sismey-Durrant, H.J. and R.M. Hopps, *Effect of lipopolysaccharide from Porphyromonas gingivalis on prostaglandin E2 and interleukin-1-beta release*

from rat periosteal and human gingival fibroblasts in vitro. Oral Microbiol Immunol, 1991. **6**(6): p. 378-80.
142. Nishihara, T., et al., *Membrane-associated interleukin-1 on macrophages stimulated with Actinobacillus actinomycetemcomitans lipopolysaccharide induces osteoclastic bone resorption in vivo.* Cytobios, 1995. **81**(327): p. 229-37.
143. Nishihara, T., et al., *Membrane IL-1 induces bone resorption in organ culture.* J Immunol, 1989. **143**(6): p. 1881-6.
144. Graves, D., *Cytokines that promote periodontal tissue destruction.* J Periodontol, 2008. **79**(8 Suppl): p. 1585-91.
145. Di Benedetto, A., et al., *Periodontal disease: linking the primary inflammation to bone loss.* Clin Dev Immunol, 2013. **2013**: p. 503754.
146. Lopez-Jornet, P., et al., *Perioperative antibiotic regimen in rats treated with pamidronate plus dexamethasone and subjected to dental extraction: a study of the changes in the jaws.* J Oral Maxillofac Surg, 2011. **69**(10): p. 2488-93.
147. Arzneimittelinformation, *If: Divertikulitis unter Denosumab (PROLIA).* Arznei-telegramm, 2014. **45**(122).
148. Watts, N.B., et al., *Infections in postmenopausal women with osteoporosis treated with denosumab or placebo: coincidence or causal association?* Osteoporos Int, 2012. **23**(1): p. 327-37.
149. Matsuki, Y., T. Yamamoto, and K. Hara, *Detection of inflammatory cytokine messenger RNA (mRNA)-expressing cells in human inflamed gingiva by combined in situ hybridization and immunohistochemistry.* Immunology, 1992. **76**(1): p. 42-7.
150. Dobrovolskaia, M.A. and S.N. Vogel, *Toll receptors, CD14, and macrophage activation and deactivation by LPS.* Microbes Infect, 2002. **4**(9): p. 903-14.
151. Kawamura, K., et al., *Detection of M2 macrophages and colony-stimulating factor 1 expression in serous and mucinous ovarian epithelial tumors.* Pathol Int, 2009. **59**(5): p. 300-5.
152. Lu, C.F., et al., *Infiltrating macrophage count: a significant predictor for the progression and prognosis of oral squamous cell carcinomas in Taiwan.* Head Neck, 2010. **32**(1): p. 18-25.
153. Wehrhan, F., et al., *Macrophage and osteoclast polarization in bisphosphonate associated necrosis and osteoradionecrosis.* J Craniomaxillofac Surg, 2017. **45**(6): p. 944-953.
154. de Barros Silva, P.G., et al., *Immune cellular profile of bisphosphonate-related osteonecrosis of the jaw.* Oral Dis, 2016. **22**(7): p. 649-57.
155. Rogers, M.J., et al., *Biochemical and molecular mechanisms of action of bisphosphonates.* Bone, 2011. **49**(1): p. 34-41.
156. Locati, M., A. Mantovani, and A. Sica, *Macrophage activation and polarization as an adaptive component of innate immunity.* Adv Immunol, 2013. **120**: p. 163-84.
157. Mantovani, A., et al., *Macrophage plasticity and polarization in tissue repair and remodelling.* J Pathol, 2013. **229**(2): p. 176-85.

158. Sica, A. and A. Mantovani, *Macrophage plasticity and polarization: in vivo veritas.* J Clin Invest, 2012. **122**(3): p. 787-95.
159. Gu, Q., H. Yang, and Q. Shi, *Macrophages and bone inflammation.* J Orthop Translat, 2017. **10**: p. 86-93.
160. Zhang, Q., et al., *IL-17-mediated M1/M2 macrophage alteration contributes to pathogenesis of bisphosphonate-related osteonecrosis of the jaws.* Clin Cancer Res, 2013. **19**(12): p. 3176-88.
161. Sindrilaru, A., et al., *An unrestrained proinflammatory M1 macrophage population induced by iron impairs wound healing in humans and mice.* J Clin Invest, 2011. **121**(3): p. 985-97.
162. Ben-Aharon, I., et al., *Bisphosphonates in the adjuvant setting of breast cancer therapy--effect on survival: a systematic review and meta-analysis.* PLoS One, 2013. **8**(8): p. e70044.
163. Jacobs, C., et al., *Are adjuvant bisphosphonates now standard of care of women with early stage breast cancer? A debate from the Canadian Bone and the Oncologist New Updates meeting.* J Bone Oncol, 2015. **4**(2): p. 54-8.
164. Wehrhan, F., et al., *Expression of Msx-1 is suppressed in bisphosphonate associated osteonecrosis related jaw tissue-etiopathology considerations respecting jaw developmental biology-related unique features.* J Transl Med, 2010. **8**: p. 96.
165. Mountzios, G., et al., *Markers of bone remodeling and skeletal morbidity in patients with solid tumors metastatic to the skeleton receiving the biphosphonate zoledronic acid.* Transl Res, 2010. **155**(5): p. 247-55.
166. Hagemann, T., et al., *"Re-educating" tumor-associated macrophages by targeting NF-kappaB.* J Exp Med, 2008. **205**(6): p. 1261-8.
167. Porta, C., et al., *Tolerance and M2 (alternative) macrophage polarization are related processes orchestrated by p50 nuclear factor kappaB.* Proc Natl Acad Sci U S A, 2009. **106**(35): p. 14978-83.
168. Weber, M., et al., *Macrophage polarisation changes within the time between diagnostic biopsy and tumour resection in oral squamous cell carcinomas--an immunohistochemical study.* Br J Cancer, 2015. **113**(3): p. 510-9.
169. Yasuda, H., et al., *Osteoclast differentiation factor is a ligand for osteoprotegerin/osteoclastogenesis-inhibitory factor and is identical to TRANCE/RANKL.* Proc Natl Acad Sci U S A, 1998. **95**(7): p. 3597-602.
170. Walsh, N.C., et al., *Activated human T cells express alternative mRNA transcripts encoding a secreted form of RANKL.* Genes Immun, 2013. **14**(5): p. 336-45.
171. Aoki, S., et al., *Function of OPG as a traffic regulator for RANKL is crucial for controlled osteoclastogenesis.* J Bone Miner Res, 2010. **25**(9): p. 1907-21.
172. Krajewski, A.C., et al., *Influence of lipopolysaccharide and interleukin-6 on RANKL and OPG expression and release in human periodontal ligament cells.* APMIS, 2009. **117**(10): p. 746-54.

173. de Vries, T.J., et al., *Gingival fibroblasts are better at inhibiting osteoclast formation than periodontal ligament fibroblasts.* J Cell Biochem, 2006. **98**(2): p. 370-82.
174. Wada, N., et al., *Lipopolysaccharide stimulates expression of osteoprotegerin and receptor activator of NF-kappa B ligand in periodontal ligament fibroblasts through the induction of interleukin-1 beta and tumor necrosis factor-alpha.* Bone, 2004. **35**(3): p. 629-35.
175. Kimachi, K., et al., *Zoledronic acid inhibits RANK expression and migration of osteoclast precursors during osteoclastogenesis.* Naunyn Schmiedebergs Arch Pharmacol, 2011. **383**(3): p. 297-308.
176. Bedogni, A., et al., *Bisphosphonate-associated jawbone osteonecrosis: a correlation between imaging techniques and histopathology.* Oral Surg Oral Med Oral Pathol Oral Radiol Endod, 2008. **105**(3): p. 358-64.
177. Altundal, H. and O. Guvener, *The effect of alendronate on resorption of the alveolar bone following tooth extraction.* Int J Oral Maxillofac Surg, 2004. **33**(3): p. 286-93.
178. Hansen, T., et al., *Increased numbers of osteoclasts expressing cysteine proteinase cathepsin K in patients with infected osteoradionecrosis and bisphosphonate-associated osteonecrosis--a paradoxical observation?* Virchows Arch, 2006. **449**(4): p. 448-54.
179. Hansen, T., et al., *Osteonecrosis of the jaws in patients treated with bisphosphonates - histomorphologic analysis in comparison with infected osteoradionecrosis.* J Oral Pathol Med, 2006. **35**(3): p. 155-60.
180. Kataoka, M., et al., *Role of multinuclear cells in granulation tissue in osteomyelitis: immunohistochemistry in 66 patients.* Acta Orthop Scand, 2000. **71**(4): p. 414-8.
181. Happonen, R.P., et al., *Actinomyces israelii in osteoradionecrosis of the jaws. Histopathologic and immunocytochemical study of five cases.* Oral Surg Oral Med Oral Pathol, 1983. **55**(6): p. 580-8.
182. Han, X., et al., *Expression of receptor activator of nuclear factor-kappaB ligand by B cells in response to oral bacteria.* Oral Microbiol Immunol, 2009. **24**(3): p. 190-6.
183. Henderson, B., et al., *Molecular pathogenicity of the oral opportunistic pathogen Actinobacillus actinomycetemcomitans.* Annu Rev Microbiol, 2003. **57**: p. 29-55.
184. Belibasakis, G.N., et al., *Regulation of RANKL and OPG gene expression in human gingival fibroblasts and periodontal ligament cells by Porphyromonas gingivalis: a putative role of the Arg-gingipains.* Microb Pathog, 2007. **43**(1): p. 46-53.
185. Gemmell, E., K. Yamazaki, and G.J. Seymour, *Destructive periodontitis lesions are determined by the nature of the lymphocytic response.* Crit Rev Oral Biol Med, 2002. **13**(1): p. 17-34.

186. Hellstein, J.W. and C.L. Marek, *Bisphosphonate osteochemonecrosis (bis-phossy jaw): is this phossy jaw of the 21st century?* J Oral Maxillofac Surg, 2005. **63**(5): p. 682-9.
187. Hansen, T., et al., *Actinomycosis of the jaws--histopathological study of 45 patients shows significant involvement in bisphosphonate-associated osteonecrosis and infected osteoradionecrosis.* Virchows Arch, 2007. **451**(6): p. 1009-17.
188. Nair, S.P., et al., *Bacterially induced bone destruction: mechanisms and misconceptions.* Infect Immun, 1996. **64**(7): p. 2371-80.
189. Pap, T., et al., *Osteoclast-independent bone resorption by fibroblast-like cells.* Arthritis Res Ther, 2003. **5**(3): p. R163-73.
190. Bertolini, D.R., et al., *Stimulation of bone resorption and inhibition of bone formation in vitro by human tumour necrosis factors.* Nature, 1986. **319**(6053): p. 516-8.
191. Hummel, K.M., et al., *Cysteine proteinase cathepsin K mRNA is expressed in synovium of patients with rheumatoid arthritis and is detected at sites of synovial bone destruction.* J Rheumatol, 1998. **25**(10): p. 1887-94.
192. Warter, A., et al., *Mandibular pseudocarcinomatous hyperplasia.* Histopathology, 2000. **37**(2): p. 115-7.
193. Zustin, J., et al., *Pseudoepitheliomatous hyperplasia associated with bisphosphonate-related osteonecrosis of the jaw.* In Vivo, 2014. **28**(1): p. 125-31.
194. Mortensen, M., W. Lawson, and A. Montazem, *Osteonecrosis of the jaw associated with bisphosphonate use: Presentation of seven cases and literature review.* Laryngoscope, 2007. **117**(1): p. 30-4.
195. Atalay, B., et al., *Bisphosphonate-related osteonecrosis: laser-assisted surgical treatment or conventional surgery?* Lasers Med Sci, 2011. **26**(6): p. 815-23.
196. Braga, T.T., J.S. Agudelo, and N.O. Camara, *Macrophages During the Fibrotic Process: M2 as Friend and Foe.* Front Immunol, 2015. **6**: p. 602.
197. Tseng, H.C., et al., *Bisphosphonate-induced differential modulation of immune cell function in gingiva and bone marrow in vivo: role in osteoclast-mediated NK cell activation.* Oncotarget, 2015. **6**(24): p. 20002-25.
198. Russell, R.G., *Bisphosphonates: mode of action and pharmacology.* Pediatrics, 2007. **119 Suppl 2**: p. S150-62.
199. Lowik, C.W., et al., *Migration and phenotypic transformation of osteoclast precursors into mature osteoclasts: the effect of a bisphosphonate.* J Bone Miner Res, 1988. **3**(2): p. 185-92.
200. Williams, D.W., et al., *Impaired bone resorption and woven bone formation are associated with development of osteonecrosis of the jaw-like lesions by bisphosphonate and anti-receptor activator of NF-kappaB ligand antibody in mice.* Am J Pathol, 2014. **184**(11): p. 3084-93.
201. Jimi, E., et al., *Osteoclast differentiation factor acts as a multifunctional regulator in murine osteoclast differentiation and function.* J Immunol, 1999. **163**(1): p. 434-42.

202. Sabokbar, A., et al., *Human arthroplasty derived macrophages differentiate into osteoclastic bone resorbing cells.* Ann Rheum Dis, 1997. **56**(7): p. 414-20.
203. Knowles, H.J., et al., *Chondroclasts are mature osteoclasts which are capable of cartilage matrix resorption.* Virchows Arch, 2012. **461**(2): p. 205-10.
204. Udagawa, N., et al., *Origin of osteoclasts: mature monocytes and macrophages are capable of differentiating into osteoclasts under a suitable microenvironment prepared by bone marrow-derived stromal cells.* Proc Natl Acad Sci U S A, 1990. **87**(18): p. 7260-4.
205. Santini, D., et al., *The antineoplastic role of bisphosphonates: from basic research to clinical evidence.* Ann Oncol, 2003. **14**(10): p. 1468-76.
206. Santini, D., et al., *Zoledronic acid induces significant and long-lasting modifications of circulating angiogenic factors in cancer patients.* Clin Cancer Res, 2003. **9**(8): p. 2893-7.
207. Migliorati, C.A., et al., *Bisphosphonate-associated osteonecrosis of mandibular and maxillary bone: an emerging oral complication of supportive cancer therapy.* Cancer, 2005. **104**(1): p. 83-93.
208. Lang, M., et al., *Influence of zoledronic acid on proliferation, migration, and apoptosis of vascular endothelial cells.* Br J Oral Maxillofac Surg, 2016. **54**(8): p. 889-893.
209. Basi, D.L., et al., *Accumulation of VEGFR2 in zoledronic acid-treated endothelial cells.* Mol Med Rep, 2010. **3**(3): p. 399-403.
210. Yamashita, J., et al., *Effect of zoledronate on oral wound healing in rats.* Clin Cancer Res, 2011. **17**(6): p. 1405-14.
211. Deckers, M.M., et al., *Dissociation of angiogenesis and osteoclastogenesis during endochondral bone formation in neonatal mice.* J Bone Miner Res, 2002. **17**(6): p. 998-1007.
212. Santini, D., et al., *Pamidronate induces modifications of circulating angiogenetic factors in cancer patients.* Clin Cancer Res, 2002. **8**(5): p. 1080-4.
213. Ohlrich, E.J., et al., *The bisphosphonate zoledronic acid regulates key angiogenesis-related genes in primary human gingival fibroblasts.* Arch Oral Biol, 2016. **63**: p. 7-14.
214. Allen, M.R. and D.B. Burr, *Mandible matrix necrosis in beagle dogs after 3 years of daily oral bisphosphonate treatment.* J Oral Maxillofac Surg, 2008. **66**(5): p. 987-94.
215. Oliveira, P.S., et al., *Influence of osteoporosis on the osteocyte density of human mandibular bone samples: a controlled histological human study.* Clin Oral Implants Res, 2016. **27**(3): p. 325-8.
216. Hesse, B., et al., *Alterations of mass density and 3D osteocyte lacunar properties in bisphosphonate-related osteonecrotic human jaw bone, a synchrotron microCT study.* PLoS One, 2014. **9**(2): p. e88481.
217. Kim, S.M., et al., *Histochemical observation of bony reversal lines in bisphosphonate-related osteonecrosis of the jaw.* Oral Surg Oral Med Oral Pathol Oral Radiol, 2017. **123**(2): p. 220-228.

218. Bone, H.G., et al., *Ten years' experience with alendronate for osteoporosis in postmenopausal women.* N Engl J Med, 2004. **350**(12): p. 1189-99.
219. Khurana, J.S., *Bone pathology*. 2nd ed. 2009, Dordrecht ; New York: Humana Press. xiii, 416 p.
220. Hesse, B., et al., *Accessing osteocyte lacunar geometrical properties in human jaw bone on the submicron length scale using synchrotron radiation muCT.* J Microsc, 2014. **255**(3): p. 158-68.
221. Bonewald, L.F., *The amazing osteocyte.* J Bone Miner Res, 2011. **26**(2): p. 229-38.
222. Robling, A.G., et al., *Mechanical stimulation of bone in vivo reduces osteocyte expression of Sost/sclerostin.* J Biol Chem, 2008. **283**(9): p. 5866-75.
223. Aguirre, J., et al., *Endothelial nitric oxide synthase gene-deficient mice demonstrate marked retardation in postnatal bone formation, reduced bone volume, and defects in osteoblast maturation and activity.* Am J Pathol, 2001. **158**(1): p. 247-57.
224. Lieberman, J.R. and G.E. Friedlaender, *Bone regeneration and repair : biology and clinical applications*. 2005, Totowa, N.J.: Humana Press. xii, 398 p.
225. Brown, J.P., et al., *Comparison of the effect of denosumab and alendronate on BMD and biochemical markers of bone turnover in postmenopausal women with low bone mass: a randomized, blinded, phase 3 trial.* J Bone Miner Res, 2009. **24**(1): p. 153-61.
226. Kendler, D.L., et al., *Effects of denosumab on bone mineral density and bone turnover in postmenopausal women transitioning from alendronate therapy.* J Bone Miner Res, 2010. **25**(1): p. 72-81.
227. Reid, I.R., et al., *Effects of denosumab on bone histomorphometry: the FREEDOM and STAND studies.* J Bone Miner Res, 2010. **25**(10): p. 2256-65.
228. Seeman, E., et al., *Microarchitectural deterioration of cortical and trabecular bone: differing effects of denosumab and alendronate.* J Bone Miner Res, 2010. **25**(8): p. 1886-94.
229. Gerstenfeld, L.C., et al., *Comparison of effects of the bisphosphonate alendronate versus the RANKL inhibitor denosumab on murine fracture healing.* J Bone Miner Res, 2009. **24**(2): p. 196-208.
230. Ristow, O., et al., *Effect of antiresorptive drugs on bony turnover in the jaw: denosumab compared with bisphosphonates.* Br J Oral Maxillofac Surg, 2014. **52**(4): p. 308-13.
231. Huja, S.S., et al., *Remodeling dynamics in the alveolar process in skeletally mature dogs.* Anat Rec A Discov Mol Cell Evol Biol, 2006. **288**(12): p. 1243-9.
232. Sobacchi, C., et al., *Osteoclast-poor human osteopetrosis due to mutations in the gene encoding RANKL.* Nat Genet, 2007. **39**(8): p. 960-2.
233. Everts, V., T.J. de Vries, and M.H. Helfrich, *Osteoclast heterogeneity: lessons from osteopetrosis and inflammatory conditions.* Biochim Biophys Acta, 2009. **1792**(8): p. 757-65.

234. Verborgt, O., G.J. Gibson, and M.B. Schaffler, *Loss of osteocyte integrity in association with microdamage and bone remodeling after fatigue in vivo.* J Bone Miner Res, 2000. **15**(1): p. 60-7.
235. Al-Dujaili, S.A., et al., *Apoptotic osteocytes regulate osteoclast precursor recruitment and differentiation in vitro.* J Cell Biochem, 2011. **112**(9): p. 2412-23.
236. Hoefert, S., et al., *Importance of microcracks in etiology of bisphosphonate-related osteonecrosis of the jaw: a possible pathogenetic model of symptomatic and non-symptomatic osteonecrosis of the jaw based on scanning electron microscopy findings.* Clin Oral Investig, 2010. **14**(3): p. 271-84.
237. Reid, I.R. and T. Cundy, *Osteonecrosis of the jaw.* Skeletal Radiol, 2009. **38**(1): p. 5-9.
238. Roelofs, A.J., et al., *Fluorescent risedronate analogues reveal bisphosphonate uptake by bone marrow monocytes and localization around osteocytes in vivo.* J Bone Miner Res, 2010. **25**(3): p. 606-16.
239. Follet, H., et al., *Risedronate and alendronate suppress osteocyte apoptosis following cyclic fatigue loading.* Bone, 2007. **40**(4): p. 1172-7.
240. Plotkin, L.I., et al., *Prevention of osteocyte and osteoblast apoptosis by bisphosphonates and calcitonin.* J Clin Invest, 1999. **104**(10): p. 1363-74.
241. Idris, A.I., et al., *Aminobisphosphonates cause osteoblast apoptosis and inhibit bone nodule formation in vitro.* Calcif Tissue Int, 2008. **82**(3): p. 191-201.
242. Rabelo, G.D., et al., *Changes in cortical bone channels network and osteocyte organization after the use of zoledronic acid.* Arch Endocrinol Metab, 2015. **59**(6): p. 507-14.
243. Goulet, G.C., et al., *Poroelastic evaluation of fluid movement through the lacunocanalicular system.* Ann Biomed Eng, 2009. **37**(7): p. 1390-402.
244. Kerschnitzki, M., et al., *Architecture of the osteocyte network correlates with bone material quality.* J Bone Miner Res, 2013. **28**(8): p. 1837-45.
245. Bonewald, L.F. and M.L. Johnson, *Osteocytes, mechanosensing and Wnt signaling.* Bone, 2008. **42**(4): p. 606-15.
246. Xiong, J. and C.A. O'Brien, *Osteocyte RANKL: new insights into the control of bone remodeling.* J Bone Miner Res, 2012. **27**(3): p. 499-505.
247. Bonewald, L.F., *Osteocyte biology: its implications for osteoporosis.* J Musculoskelet Neuronal Interact, 2004. **4**(1): p. 101-4.
248. Cheung, W.Y., et al., *Osteocyte apoptosis is mechanically regulated and induces angiogenesis in vitro.* J Orthop Res, 2011. **29**(4): p. 523-30.
249. Bakker, A.D., et al., *Tumor necrosis factor alpha and interleukin-1beta modulate calcium and nitric oxide signaling in mechanically stimulated osteocytes.* Arthritis Rheum, 2009. **60**(11): p. 3336-45.
250. Almeida, M. and C.A. O'Brien, *Basic biology of skeletal aging: role of stress response pathways.* J Gerontol A Biol Sci Med Sci, 2013. **68**(10): p. 1197-208.
251. Kogianni, G., V. Mann, and B.S. Noble, *Apoptotic bodies convey activity capable of initiating osteoclastogenesis and localized bone destruction.* J Bone Miner Res, 2008. **23**(6): p. 915-27.

252. Bae, S., et al., *Development of oral osteomucosal tissue constructs in vitro and localization of fluorescently-labeled bisphosphonates to hard and soft tissue.* Int J Mol Med, 2014. **34**(2): p. 559-63.
253. Hallmer, F., et al., *Bacterial diversity in medication-related osteonecrosis of the jaw.* Oral Surg Oral Med Oral Pathol Oral Radiol, 2017. **123**(4): p. 436-444.
254. Sedghizadeh, P.P., et al., *Identification of microbial biofilms in osteonecrosis of the jaws secondary to bisphosphonate therapy.* J Oral Maxillofac Surg, 2008. **66**(4): p. 767-75.
255. Kesavalu, L., et al., *Omega-3 fatty acid regulates inflammatory cytokine/mediator messenger RNA expression in Porphyromonas gingivalis-induced experimental periodontal disease.* Oral Microbiol Immunol, 2007. **22**(4): p. 232-9.
256. Kesavalu, L., et al., *Rat model of polymicrobial infection, immunity, and alveolar bone resorption in periodontal disease.* Infect Immun, 2007. **75**(4): p. 1704-12.
257. Yankova, Z., et al., *Bisphosphonate-related osteonecrosis of the mandible secondary to postural pressure.* J Oral Maxillofac Surg, 2012. **70**(7): p. 1584-6.
258. Hasegawa, Y., et al., *Influence of dentures in the initial occurrence site on the prognosis of bisphosphonate-related osteonecrosis of the jaws: a retrospective study.* Oral Surg Oral Med Oral Pathol Oral Radiol, 2012. **114**(3): p. 318-24.
259. Infante-Cossio, P., et al., *Osteonecrosis of the maxilla associated with cancer chemotherapy in patients wearing dentures.* J Oral Maxillofac Surg, 2012. **70**(7): p. 1587-92.
260. Levin, L., A. Laviv, and D. Schwartz-Arad, *Denture-related osteonecrosis of the maxilla associated with oral bisphosphonate treatment.* J Am Dent Assoc, 2007. **138**(9): p. 1218-20.
261. Yazdi, P.M. and M. Schiodt, *Dentoalveolar trauma and minor trauma as precipitating factors for medication-related osteonecrosis of the jaw (ONJ): a retrospective study of 149 consecutive patients from the Copenhagen ONJ Cohort.* Oral Surg Oral Med Oral Pathol Oral Radiol, 2015. **119**(4): p. 416-22.
262. Ruggiero, S.L. and N. Kohn, *Disease Stage and Mode of Therapy Are Important Determinants of Treatment Outcomes for Medication-Related Osteonecrosis of the Jaw.* J Oral Maxillofac Surg, 2015. **73**(12 Suppl): p. S94-S100.
263. Vescovi, P., et al., *Surgery-triggered and non surgery-triggered Bisphosphonate-related Osteonecrosis of the Jaws (BRONJ): A retrospective analysis of 567 cases in an Italian multicenter study.* Oral Oncol, 2011. **47**(3): p. 191-4.
264. Herbozo, P.J., et al., *Severe spontaneous cases of bisphosphonate-related osteonecrosis of the jaws.* J Oral Maxillofac Surg, 2007. **65**(8): p. 1650-4.
265. Qaisi, M., et al., *Denosumab Related Osteonecrosis of the Jaw with Spontaneous Necrosis of the Soft Palate: Report of a Life Threatening Case.* Case Rep Dent, 2016. **2016**: p. 5070187.
266. Wilde, F., et al., *Prevalence of cone beam computed tomography imaging findings according to the clinical stage of bisphosphonate-related osteonecrosis*

of the jaw. Oral Surg Oral Med Oral Pathol Oral Radiol, 2012. **114**(6): p. 804-11.
267. Elster, A.D., et al., *Cranial imaging in autosomal recessive osteopetrosis. Part I. Facial bones and calvarium.* Radiology, 1992. **183**(1): p. 129-35.
268. Scaramuzzo, L., et al., *Clinical and histological modifications in osteopetrotic bone: a review.* J Biol Regul Homeost Agents, 2009. **23**(2): p. 59-63.
269. Hutchinson, M., et al., *Radiographic findings in bisphosphonate-treated patients with stage 0 disease in the absence of bone exposure.* J Oral Maxillofac Surg, 2010. **68**(9): p. 2232-40.
270. Bisdas, S., et al., *Biphosphonate-induced osteonecrosis of the jaws: CT and MRI spectrum of findings in 32 patients.* Clin Radiol, 2008. **63**(1): p. 71-7.
271. Carlson, E.R. and J.D. Basile, *The role of surgical resection in the management of bisphosphonate-related osteonecrosis of the jaws.* J Oral Maxillofac Surg, 2009. **67**(5 Suppl): p. 85-95.
272. Graziani, F., et al., *Resective surgical approach shows a high performance in the management of advanced cases of bisphosphonate-related osteonecrosis of the jaws: a retrospective survey of 347 cases.* J Oral Maxillofac Surg, 2012. **70**(11): p. 2501-7.
273. Mucke, T., et al., *Outcome of treatment and parameters influencing recurrence in patients with bisphosphonate-related osteonecrosis of the jaws.* J Cancer Res Clin Oncol, 2011. **137**(5): p. 907-13.
274. Stanton, D.C. and E. Balasanian, *Outcome of surgical management of bisphosphonate-related osteonecrosis of the jaws: review of 33 surgical cases.* J Oral Maxillofac Surg, 2009. **67**(5): p. 943-50.
275. Chen, W., et al., *Grainyhead-like 2 enhances the human telomerase reverse transcriptase gene expression by inhibiting DNA methylation at the 5'-CpG island in normal human keratinocytes.* J Biol Chem, 2010. **285**(52): p. 40852-63.
276. Black, D.M., et al., *Once-yearly zoledronic acid for treatment of postmenopausal osteoporosis.* N Engl J Med, 2007. **356**(18): p. 1809-22.
277. De Colli, M., et al., *In vitro comparison of new bisphosphonic acids and zoledronate effects on human gingival fibroblasts viability, inflammation and matrix turnover.* Clin Oral Investig, 2016. **20**(8): p. 2013-2021.

7 German summary

Obwohl die Erstbeschreibung der Medikamenten-assoziierten Kiefernekrose (MRONJ) nun 15 Jahre vergangen ist, bleibt die Pathogenese dieser Erkrankung immer noch unklar. Dementsprechend gibt es keinen einheitlichen Konsens über die Behandlung der MRONJ sowie allgemein akzeptierte Präventionsprotokolle. Die Behandlung von einer MRONJ ist schwierig und kostspielig und die Spätkomplikationen umfassen Schmerzen, Entzündungen, mitunter eine Unfähigkeit zu essen, extraorale Fisteln, sowie die Möglichkeit von pathologischen Frakturen. Diese Erkrankung führt daher zu einer deutlichen Minderung der Lebensqualität der betroffenen Patienten.

Da die Rolle von Weichgewebe in der Pathogenese von MRONJ unzureichend erforscht ist, untersucht diese Arbeit die Auswirkungen von Bisphosphonaten (BPs) und Denosumab in der Induktion und Hemmung von einem Zelltod und der Entzündung an Hand von Expressionsmustern von humanen gingivalen Fibroblasten (HGFs), sowie den Einfluss einer antiresorptiven Therapie auf die Wundheilung und die Angiogenese. Ein In-vitro-Test von HGFs mit und ohne den Zusatz von bakteriellen Lipopolysacchariden (LPS) und einer Co-Kultur von mononuklearen Zellen wurde mittels eines xCellingence Systems durchgeführt, um den Effekt von verschiedenen Antiresorptiva (Zoledronat, Ibandronat, Alendronat, Clodronat, Denosumab und Kombinationen von Zoledronat und Denosumab) bei niedrigen, mittleren, und hohen Konzentrationen zu untersuchen. Ein Wundheilungstest (Wound Scratch Assay) wurde ebenfalls durchgeführt und eine Gen- und Proteinexpressionsanalyse für verschiedene Zytokine und Mediatoren – einschließlich Interleukin 1beta (IL-1β), Interleukin 6 (IL-6), Interleukin 8 (IL-8), vaskulärer endothelialer Wachstumsfaktor (VEGF), Tumornekrosefaktor (TNF), Osteoprotegerin (OPG) und Rezeptoraktivator von nuklearem Faktor Kappa-B-Ligand (RANKL) – angewendet.

Eine retrospektive histologische und radiologische Untersuchung wurde ebenfalls an Knochenproben durchgeführt, um die Korrelationen von der veränderten Knochenstrukturen mit verschiedenen Krankheitsstadien und mit dem Grad der antiresorptiven Exposition zu analysieren. Insgesamt wurden 158 Knochenbiopsien von Patienten mit verschiedenen infektiösen, entzündlichen und nekrotischen Kiefererkrankungen mit Hämatoxylin und Eosin (H&E), RANKL, OPG, Tartrat-resistenter saurer Phosphatase (TRAP), Toluidinblau, CD14 und CD68 angefärbt und ausgewertet. eine Mikro-Computertomographie (µ-CT) der Proben wurde zusätzlich durchgeführt. Röntgenaufnahmen von 37 MRONJ-Patienten wurden Bezug auf radiologische Befunde vor und nach einer Therapie und im Krankheitsverlauf analysiert. Radiologische Anzeichen von Nekrose wurden ausgewertet und verglichen. Insgesamt wurden 86 Röntgenuntersuchungen ausgewertet.

Unsere Ergebnisse zeigten, dass höhere Konzentrationen von Antiresorptiva zu einem Zelltod der HGF-Zellen führen (Zoledronat 50 µM bei 66 Stunden; Alendronat 50 µM bei 64 Stunden; Ibandronat 50 µM bei 66 Stunden, alle $p < 0,05$ im Vergleich zu Kontrollen bei 90,4 Stunden), sowie die Wundheilung beeinträchtigen können (Clodronat 500 µM, Ibandronat 5 µM und 50 µM, Alendronat 50 µM, Zoledronat 5 µM + Denosumab 10 µg/ml und Zoledronat 5 µM). Diese Effekte steigerten sich unter einer Exposition mit bakteriellem LPS (Alendronat 5 µM und 0,5 µM; zusätzlich beeinflusst, $p < 0,05$) und in Co-Kulturen mit einer mononukleären Zellen (THP-1) (Zoledronat 5 µM und Zoledronat 5 µM + Denosumab 40 µg/mlM; zusätzlich beeinflusst), $p < 0,05$). Es ergaben sich auch Anzeichen einer veränderten Immunantwort mit einer erhöhten Immunreaktion und einer möglichen Dysfunktion als Folge der Exposition gegenüber Antiresorptiva. Erhöhte Spiegel von TNF (443 Genkopien von Zoledronat 50 µM mit LPS und 2,66 Genkopien von Denosumab 40 µg/ml mit LPS im Vergleich zu 0 in der Kontrollgruppe), IL-8 (16,9 Genkopien von Zoledronat 50 µM mit LPS im Vergleich zu 0,007 Genkopien in der Kontrollgruppe), IL-1β (alle Konzentrationen

erhöht, $p < 0,05$) und CD14 und CD68-Expression (gemischte Osteonekrose des Kiefers (ONJ) und Bisphosphonat-assoziierte Osteonekrose des Kiefers (BRONJ) $p < 0,001$) wurden beobachtet, möglicherweise aufgrund einer anhaltenden Entzündungsreaktion, während eine IL-6-Reaktion bei hohen Konzentrationen stickstoffhaltiger BP fehlte (alle $p < 0,05$), was auf einen Defizit eines Wechsels von der angeborenen zu einer erworbenen Immunität schließen lässt.

Eine Osteoklasteninhibierung wurde durch HGFs vermutet, die eine erhöhte Expression von OPG bei Exposition gegenüber Zoledronat (773 Genkopien) und Denosumab (6.01 Genkopien) im Vergleich zu 0,28 bei der Kontrollgruppe mit niedrigen RANKL-Spiegeln zeigten. Knochenproben zeigten jedoch positive Zellen für RANKL (BRONJ $p = 0,021$) und TRAP (gemischtes ONJ $p = 0,002$; BRONJ $p < 0,001$; BP-pausiert $p = 0,017$). Es gab keinen Hinweis auf einen antiangiogenen Effekt, was durch die Spiegel von VEGF und IL-8 sowie das Auftreten von intakten Havers'schen Systemen im Knochen vermutet wurde. Die Analyse der Knochengewebe in der histologischen und radiologischen Untersuchung deutet darauf hin, dass ein begrenztes Osteozyten-Netzwerk (mittlere Anzahl von Osteozyten-Lakunen pro μm^2 in Denosumab-assoziierter Osteonekrose des Kiefers (DRONJ): 0,00026, $p < 0,05$) und eine Ossifikation von dem Knochen (erhöhtes Verhältnis von Knochen zu Markraum $p < 0,01$ für MRONJ-Varianten; erhöhte Trabekelbreite von 601,71 µm bei Mixed-ONJ; $p = 0,03$; und das Vorhandensein einer Sklerose nachgewiesen in einer Röntgenuntersuchung bei 92% der MRONJ-Patienten) eine Rolle bei der Krankheitsentwicklung spielen kann. Unsere Ergebnisse lassen darauf schließen, dass die genaue Pathogenese davon abhängen könnte, ob das Antiresorptivum ein BP oder Denosumab ist, wobei sich klinisch die Nekrosen ähneln. Aus unseren klinischen Studien geht hervor, dass Patienten, die operativ behandelt wurden, eine bessere Heilung zeigten als Patienten, die nicht operativ behandelt wurden ($p = 0,001$). Die Cone-Beam-CT-Untersuchung erlaubte eine bessere Visualisierung von knöchernen fistelähnlichen Strukturen, von Frakturen und der bei der Größe von Sequestern (in 68,2% der Fälle) im Vergleich zum CT (in 30,8% der Fälle), und zeigte 18,4%

häufiger positive Befunde als eine Panorama-Röntgenaufnahme im direktem Vergleich.

Viele dieser Ergebnisse könnten wichtige Implikationen für MRONJ-Forschung haben und eine klinische Relevanz für die Behandlung bieten. Dies war eine der ersten Untersuchungen von HGF-Zellen in Echtzeit, insbesondere mit einer breiten Variabilität von BP-Konzentrationen. Die Untersuchung der Auswirkung von Denosumab auf HGF-Zellen sowie die Anwendung einer gleichzeitigen Kombination von Zoledronat- und Denosumab zur Simulation einer realen klinischen Situation, waren ebenfalls neue Forschungsziele. Darüber hinaus zeigen diese Ergebnisse bisher nicht berichtete Details zu den Merkmalen von DRONJ, gemischtem ONJ, BP-exponierten sowie BP- und Denosumab-exponierten Knochen, insbesondere da einen Einfluss einer Denosumabtherapie auch ohne einer vorherigen BP-Therapie nachweisen konnten.

8 Publications

Parts of this dissertation have been published in the form of the following scientific articles:

Hoefert S, **Yuan A**, Munz A, Grimm M, Elayouti A, Reinert S. Clinical course and therapeutic outcomes of operatively and non-operatively managed patients with denosumab-related osteonecrosis of the jaw (DRONJ). J Craniomaxillofac Surg. 2017 Apr;45(4):570-578.

9 Declaration of contributions to the dissertation

The dissertation work was carried out at the University Hospital Tuebingen under the supervision of Professor Dr. Dr. Siegmar Reinert.

The study was designed in collaboration with Dr. Dr. Sebastian Hoefert, doctoral supervisor.

After training by laboratory member Adelheid Munz, I carried out all experiments independently.

Statistical analysis was carried out after a consultation with the Institute for Biometry and under the supervision of Dr. Dr. Sebastian Hoefert.

I confirm that I wrote the manuscript myself and that any additional sources of information have been duly cited.

Signed_____

on _____ in Tübingen

10 Acknowledgements

I am most grateful to:
Prof. Dr. Dr. Siegmar Reinert, my wonderfully supportive doctoral supervisor
PD Dr. Dorothea Alexander Friedrich, my kind and helpful laboratory director
Prof. Dr. Andreas Nüssler
Prof. Dr. Bence Sipos
Dr. Inka Montero

Special thanks to:
PD Dr. Ashraf El Ayouti
PD Dr. Christina Schraml
Dr. Liane Schuster
Felix Umrath

This PhD Dissertation would not have happened without the support of:
Adelheid Munz
Dr. Dr. Sebastian Hoefert
My husband Bohdan and our mothers Victoria and Ping

Funded by:
Forschungsgemeinschaft Dental e.V.